Stefanie Keser, BSc

DEVELOPMENT AND EVALUATION OF TASTE MASKED PEDIATRIC MINITABLET FORMULATIONS WITH BITTER MODEL DRUGS

MASTER'S THESIS

to achieve the university degree of

Master of Science

Chemical and Pharmaceutical Engineering

submitted to

Graz University of Technology

Supervisor

Univ.-Prof. Dr. Andreas Zimmer
University of Graz, Department of Pharmaceutical Technology

Dr. Carsten Timpe
F. Hoffmann-La Roche AG, Basel, Switzerland

Basel, October 2016

AFFIDAVIT

I declare that I have authored this thesis independently, that I have not used other than the declared sources/resources, and that I have explicitly indicated all material which has been quoted either literally or by content from the sources used. The text document uploaded to TUGRAZonline is identical to the present master's thesis.

Place, Date   Signature

Abstract

An important criterion in pediatric drug delivery is taste acceptance. As many drugs have a bitter taste, appropriate taste masking is a key requirement. Minitablets are a suitable dosage form for children having high dosing flexibility in combination with taste masking using standard coating technologies.

The key objective of this work was the development of efficiently taste masked minitablet formulations with two bitter model drugs at low and high drug load (cetirizine dihydrochloride, acetaminophen). The coating process using 3 different polymers and 2 technologies (Wurster & drum coater) was investigated.

Acetaminophen is known to have poor compressibility, and due to the high drug loading of the tested formulation, a fine grade of microcrystalline cellulose was required to prevent capping, although this then had a negative impact on flowability.

The minimum necessary coating level for the pH dependent polymers (Eudragit EPO®, Kollicoat® Smartseal 30D) was for the acetaminophen minitablets 4mg/cm². Critical were the amount of swellable excipients in the core and the elasticity of the coating layer.

Taste masking with the pH independent Surelease® of the acetaminophen minitablets was achieved for 60s only at 4mg/cm² coating level due to high amount of swelling excipients. A 2^3 DoE was performed with cetirizine minitablets to investigate effects of spray rate, spray time and polymer to pore former ratio on taste masking and dissolution. An optimum was found at a spray rate of 2g/min, 70min spray time and at a polymer to pore former ratio of 80:20.

In a first feasibility study coating of minitablets was also successfully performed at lab scale in a conventional drum coater process with a newly designed tailor-made polyamide insert.

Taste masked cetirizine minitablets were evaluated in a human taste panel and depicted a good correlation to in vitro taste assessments in artificial saliva with a bitterness threshold previously determined by e tongue and human taste panel.

Kurzzusammenfassung

Ein wichtiges Kriterium pädiatrischer Arzneimittel ist die Akzeptanz. Da viele Wirkstoffe einen bitteren Geschmack haben, ist eine gute Geschmacksmaskierung eine wichtige Voraussetzung. Minitabletten (MT) sind eine geeignete Arzneiform für Kinder, da sie eine hohe Dosierungsflexibilität ermöglichen und durch etablierte Coatingtechnologien geschmacksmaskiert werden können.

Das Ziel der Arbeit war geschmacksmaskierte pädiatrische Minitablettenformulierungen mit zwei Modelwirkstoffen (Cetirizin(CET)=5%, Acetaminophen(Para)=50%) zu entwickeln. Der Coatingprozess mit 3 verschiedenen Polymeren und 2 Technologien wurde untersucht.

Auf Grund des hohen Wirkstoffanteils von Para musste wegen der schlechten Tablettiereigenschaft eine feine Qualität der mikrokristallinen Celullose verwendet werden um das Deckeln zu verhindern. Der Nachteil war die Verschlechterung der Fliessfähigkeit.

Die Geschmacksmaskierung der Para MT wurde mit einer Coatingschicht von 4mg/cm^2 der pH abhängigen Polymere Eudragit EPO® und Kollicoat® Smartseal 30D erreicht. Der Anteil der quellenden Hilfsstoffe in der MT Formulierung und die Elastizität des Polymers wurden als kritisch beurteilt.

Die Geschmacksmaskierung der Para MT mit dem pH unabhängigen Polymer Surelease® wurde wegen dem hohen Anteil der schwellenden Hilfsstoffen mit einer Coatingschicht von 4 mg/cm^2 nur für 60s erreicht. Mit den CET MT wurde ein 2^3 Versuchsplan durchgeführt, um den Einfluss des Anteils Polymer zum Porenformer, der Sprührate und der Sprühzeit zu untersuchen. Das Optimum wurde bei 80:20, 2g/min und 70min gefunden.

Die erste Machbarkeitsstudie bei der Minitabletten in einem konventionellen Trommelcoater mit einem massangefertigten Innensack gecoatet wurden, war erfolgreich.

CET MT wurden in einer in vivo Geschmacksverkostung getestet und zeigen eine gute Korrelation zum in vitro Geschmackstest in künstlichen Speichel. Der Bitterkeitsschwellenwert wurde mit der künstlichen Zunge und der Geschmacksverkostung bestimmt.

Acknowledgement

Abbreviations

ACN	Acetonitrile
ADI	Acceptable daily intake
API	Active Pharmaceutical Ingredient
AS	Artificial Saliva
BATA	Brief access taste aversion
BCS	Biopharmaceutical Classification System
bw	body weight
CET	Cetirizine Dihydrochloride
conc	concentration
CTA	Conditioned Taste Aversion
DL	Drug Load
DoE	Design of Experiments
EMA	European Medicines Agency
EPO	Eudragit E PO®
ffc	Flow function coefficient
IPC	In process control
MCC	Microcrystalline cellulose
MeOH	Methanol
MFT	Minimum Film forming Temperature
MT	Minitablet
mV	millivolt
ns	not specified
Para	Paracetamol (Acetaminophen)
pBCS	pediatric Biopharmaceutical Classification System
PCA	Principle Component Analysis
pCMA	Potential Critical Material Attribute
pCPP	Potential Critical Process Parameter
pCQA	Potential Critical Quality Attributes
Ph.Eur.	European Pharmapoea
PLS	Partial Least Square
PSD	Particle Size Distribution
PVA	Polyvinylalcohol
QRA	Quality Risk Assessment
resp.	respectively
RABS	Restricted area barrier system
SEM	Scanning Electron Microscopy
SGF	Simulated Gastric Fluid
SMA	Kollicoat® Smartseal 30D
Sur	Surelease®
T_g	Glass Transition Temperature
USP	United States Pharmacopeial
X-Ray-µCT	X-Ray Micro-Computed Topography

Table of Content

1. Introduction

In the European Union between 45-60 % of medicines administered to children are off-label prescriptions and unauthorized medicines [1]. However children are not just small adults due to their difference in physiology and pharmacokinetic, e.g. metabolic capacity, organ maturation and drug clearance [2]. Therefore the European Medical Agency (EMA) published in 2014 the "Guideline on pharmaceutical development of medicines for pediatric use" [3]. After which the acceptability of tablets was considered as a function of the child's age and the tablet size. Prior tablets were considered as inappropriate for children younger than six years [4]. Since then few researchers have proven the acceptability of minitablet in children ranking from infants to school kids. As minitablets are supposed to be multiple unit dosages forms, the acceptability of multiple minitablets was recently studied [5]. The use of minitablets for the treatment of children offer key benefits compared to other dosage forms, since no or minimal manipulation before use is needed, and the dose accuracy and flexibility which is given by incrementally adjusting the number of minitablets to the children's age or body weight [6]. Dose flexibility is especially important because the magnitude of doses required through childhood can vary 100 fold [7].

The compliance of pediatric patients varies from 11 to 93 % [8]. The taste of the dosage form has a major influence on the compliance, as taste, in 75 % of the cases, the reason of the refusal of medication by children [9]. Consequently a sufficient taste masking is particularly important for pediatric medications.

Taste masking by film coating is the most common and effective method [10]. Since minitablets have a uniform size and shape, they represent an ideal coating substrate. For that reason the taste masking of minitablets via film coating should be further investigated.

The objective of this work was to develop a taste masked pediatric minitablet formulation with bitter tasting model drugs at low and respectively high drug load (DL) (Cetirizine Dihydrochloride DL=5%, Acetaminophen DL=50%). The minitablets should be effectively taste masked, where no API is released in the oral cavity, but still have an immediate release in the stomach. The focus of this work was the development and the investigation of the coating process with different polymers using a fluidized bed and a drum coater. Potential problems and problem solving during development of a taste masked minitablet formulation should be investigated as well.

2. Literature Review

2.1.   Minitablets

The traditionally used dosage forms for the pediatric population are liquid like syrup, because normal-sized tablets were considered as inappropriate for children younger than six years [4]. However, liquid dosage forms have the disadvantage that they are often chemically, physically and microbiologically instable, represent a challenge regarding controlled release properties, allow only limited number of safe excipients with regards to preservatives and are often unreliable regarding dosing because of incomplete swallowing [11]. Especially in third world countries the WHO favors that young children should be preferably treated with oral solid medicines due to the availability of clean drinking water [12]. One option for a suitable pediatric solid oral dosage form are minitablets.

Minitablets are defined in scientific literature as small sized tablets having a diameter of 3 mm or less [13]. Compared to pellets, minitablets have a uniform size, a smooth surface and a lower porosity [13] and can therefore be produced with small size and dose variability within and between batches [14]. Minitablets can be used as a single or multiple unit dosage form. As a multiple unit dosage form they can be filled into capsules, stickpacks or compressed into bigger tablets. Multiple unit dosages forms offer several advantages, such as a reduced risk of local irritation and dose dumping [15]. It is easier to achieve a modified release profile compared to liquid dosage forms. Furthermore the gastric residence time is more reproducible [16].
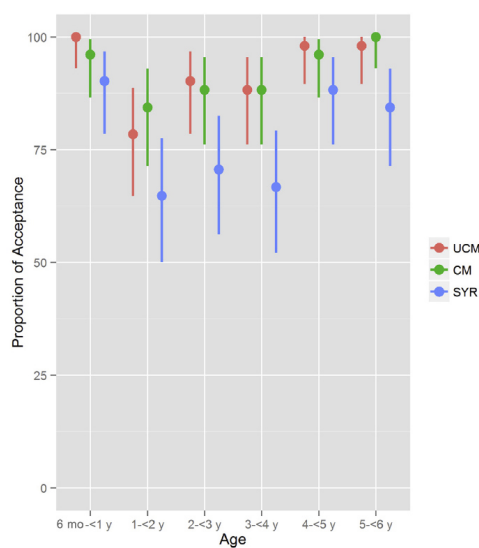
Figure 1: Acceptability of syrup (SYR), uncoated (UCM) and coated (CM) minitablets [17]
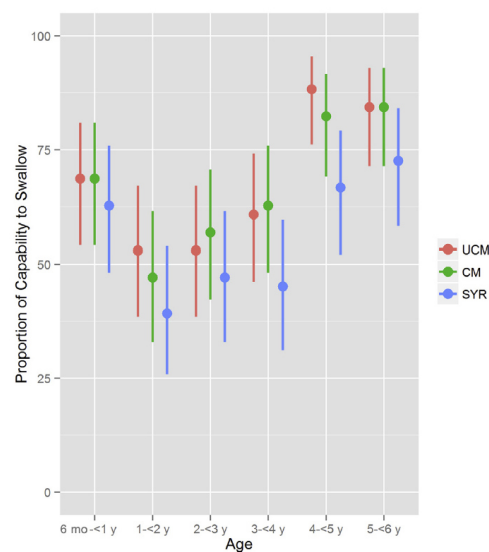
Figure 2: Capability to swallow of syrup (SYR), uncoated (UCM) and coated (CM) minitablets [17]

The acceptability of minitablets in a pediatric population has been studied by several researchers (Table 1). Klingmann showed that the acceptability of coated and uncoated minitablets was significantly superior to syrup over all studied age groups (2 days – 7 years) (Figure 1), particularly predominant in children between one and four years [6], [17], [18].

Table 1: Acceptance of minitablets in pediatric populations

Author	Year	No. of patients	Age	Type of dosage forms	Result
Thomson et al.	2009	100	2–6 years	3mm uncoated MT	62% swallowed intact 22% chewed
Van de Vijver et al.	2011	16	6-30 month	2mm enteric coated pancrelipase MT	Well tolerated, mean palatability fair to good
Spomer et al.	2012	60	0.5-7 years	2mm uncoated MT vs. syrup	67% swallowed intact 27% chewed
Klingmann et al.	2013	306	0.5-6 years	2mm uncoated & coated MT vs. syrup	47.1-88.2% swallowed intact
Van Riet-Nales et al.	2013	148	1-4 years	4mm uncoated vs 3 other dosage forms	MT superior acceptability and preference
Kluk et al.	2015	60	2-3 years	2 & 3mm coated MT, 5-10 per child	2 y: 50% swallowed intact 3y: 64% swallowed intact
Klingmann et al.	2015	151	2-28 days	2mm uncoated MT vs. syrup	81.1% swallowed intact
Klingmann	2016	374	6–23 month 2-6 years	2mm uncoated MT (25-400 per child) vs. 5-10ml syrup	73.7 resp. 80.6 % swallowed intact (100 resp. 25 MT) 16.1 resp. 31.2 % swallowed intact (400 resp. 100 MT)

The use of minitablets for the treatment of children offers key benefits compared to other dosage forms: no or minimal manipulation before use is needed, they are small sized and easy transportable. They can reduce the burden of potentially toxic excipients, as adding preservatives is not needed, they can be produced on conventional manufacturing equipment and depict often better drug stability and require less restricted storage conditions (e.g. refrigeration) [17]. Furthermore the dose could be incrementally adjusted to the age of the children simply by the number of minitablets given [6]. This is especially important because the magnitude of doses required through childhood can vary 100 fold [7].

Taste masking by film coating and chewing

For the administration of medicines to the pediatric population a sufficient taste masking is mandatory. When the taste masking approach is to put a physical layer between the API and the taste buds via a taste masking coating of the minitablets, the risk arises that children could chew the minitablet before swallowing them. That could lead to a complete loss of the taste masking and in such cases compliance would not be ensured. Klingmann [17] studied also the acceptability of coated minitablets which were layered with a hypromellose film and reported that even when the children chewed before swallowing, that the coating layer was just deformed and not destroyed. The maximum bite force of children between 4 to 6 years is 5.69 kg [19] and comparably much lower to the bite force of adults (18 kg, 18 - 20 years) [20], which could ensure the coat integrity. In the focused age group of 4 years and older, over 80 % of the children were able to swallow the minitablet intact without chewing the minitablet [17] (Figure 2). Moreover the EMA Guideline indicates that minitablets are normally swallowed intact but they can also be chewed unless it is not prohibited [21]. In chronical treatments with coated minitablets there will be probably a learning effect when a bitter taste is exhibited after chewing. Furthermore when the level of suffering is high, a child would accept and follow the instructions.

Compared to coated minitablets having a modified release or a gastric resistant coat, chewing is not critical from a pharmacokinetic point of view for an immediate release product. Nevertheless it needs to be written in the leaflet that the minitablet should not be chewed before swallowing.

Another aspect of the ability of swallowing minitablets is their number. Mostly minitablets are considered as a multiple-unit dosage form. Kluk has proven already that 2 to 3 years old children are able to swallow up to 10 minitablets (2 and 3 mm) [22]. There is an ongoing study from Klingmann about the acceptance of multiple minitablets between 25 to 400 units. They divided the children between 6 month and 6 years into two age groups (6 – 23 month and 2 – 6 years). In the younger age group the acceptability of 25, 100 MT and 5 ml syrup and in the older age group 100, 400 MT and 10 ml syrup was investigated. It has been shown that in the younger age group the suitability and swallowability of 25 and 100 MT is significantly higher compared to the syrup [23]. In the older age group the suitability and swallowability of the MT was nearly similar to the syrup and still a good alternative to the syrup.

2.2.   Manufacturing process

2.2.1.   Granulation

Granulation is the size enlargement of powder particles by agglomeration. By granulating of a powder mixture the risk of segregation is reduced, flowability and compactability are improved and dust generation in the further handling steps can be reduced which is beneficial for the handling of highly potent drugs. A granulation process is generally conducted in 4 steps: 1. Blending, 2. Aggregation (by binder or pressure) 3. Grinding or drying and 4. Fractioning. The formed agglomerates should be sufficiently strong to enable further downstream processing.

Five primary bonding mechanisms can be distinguished [24]:

1. Adhesion and cohesion forces
2. Interfacial forces in mobile liquid films
3. Solid bridges
4. Attractive forces
5. Mechanical interlocking's

The main granulation methods are wet -, dry granulation and direct compression.

2.2.1.1.   Dry granulation

The dry granulation process is conducted via roller compaction or sluggers where the powder mixture is compressed with pressure into slugs or compressed sheets. Afterwards it is milled and sieved to reach the targeted particle size. This method is beneficial for water sensitive APIs, but the drug load is generally limited compared to a wet process. While on one side flowability will be improved by a compaction process on the other side further downstream compressibility is reduced due to the first densification step [25].

2.2.1.2.   Wet granulation

Wet granulation is the mixing of a dry powder with a binder liquid. It can be conducted either in a high shear granulator or in a fluidized bed, and more recently by using a twin screw extruder.

A high shear mixer has typically a two or three bladed impeller and an auxillary chopper which breaks down the lumps. First the powder mixture is dry blended and subsequently a binder solution or water is added to moisten the particles. The primary particles bind to each

other. The endpoint of a granulation can be determined by the mixing time, the amount of added binder solution, the power consumption or other PAT technologies to produce particles with a defined size or material property (e.g. strength). Afterwards the mass is screened and dried. In general this technology can bear the risk of over-granulation and lump formation and the investment costs are typically higher as this process requires an additional drying step. Compression properties (e.g. compactability, compressibility, tablettability) are often superior compared to a dry process [25] .

In the fluidized bed the particles are fluidized in an air stream and granulation liquid is sprayed by a nozzle onto the powder bed. Agglomerates are formed when the droplets of the binder solution collide with the powder particles. The wet agglomerates are immediately dried by the hot air stream. Compared to the high shear granulator, fluid-bed granulation and drying can be conducted in one machine.

2.2.1.3.   Direct compression

For direct compaction, the components of the power mixture are simply mixed and directly compressed into tablets. Hence fewer processing steps are necessary, which increases the productivity and reduces the final costs of the tablets. Furthermore moisture and heat effects are eliminated. This method is often limited by the drug load and problematic for powder mixtures with insufficient compression properties and flowability [25]. Raw materials are often more expensive, because the use of pretreated materials is necessary, e.g. spray dried fillers.

Strategy for the selection of the most suitable granulation process for minitablets

The following factors should be considered for the selection of the granulation technology for minitabletting:

- good flowability
- maximum particle size
- absence of stickiness

For minitableting a good flowability is necessary to ensure sufficient die filling, which is often achieved by wet granulation and dry granulation.

Regarding particle size Mielck and Flamming [26] established a ratio of die diameter (D) to the maximum particle size (d), which should be larger than 3 to prevent blocking of the small dies. But as a rule of thumb the particles size of the granules should have rather not more

than 1/10 of the die diameter to ensure an easy die filling. Since dry and wet granulation lead to an enlargement of the particle sizes, direct compression can become the appropriate method for minitableting with the prerequisite that the raw materials respectively the resulting powder blend meet the criteria mentioned above [13].

2.2.2.   Compression

Minitablets can be manufactured by compression of a powder mixture or granulate using an hydraulic, eccentric or rotary tablet press. The tablet press is typically equipped with specially designed multiple toolings (multiple tip die and multiple tip punches), because single tip punches would lead to an extremely low productivity. Furthermore the tableting mixture is slowly consumed by the compression process, which results in a long residence time in the filling station and increases the risk of segregation due to vibration and shearing [27].

2.2.2.1.   Punches

Multiple tip punches have two and more tips. Most of the tableting tooling suppliers offer multiple tip punches in several diameters and arrangements of the tips. In 1965 Hershberg [28] studied the compression of miniature tablets and due to extensive tip deformation and vibration it led to tablet fragmentation and tooling aberration. He invented the rule of thumb that the length of the tips (upper and lower together) should be maximum 5 times the tip diameter. As a consequence the lower tip length is shorter and therefore also the die needs to be undercut. The punches can be divided into multiple part assembly punches (with external or internal cap fixing) or monoblocks (Figure 4 -Figure 7) [29]. The multiple part assembly punches have the advantages that the replacement of a damaged single tip is possible. On the other hand monoblock punches are easier to clean and are more resistant to tip breaking [27]. Due to the high length-to-diameter ratio non-coaxial stress could occur which could lead to tip breaking. The reason is misalignment of punch tips to die opening because of impreciseness of the tableting tool itself or by not sufficiently fixed orientation during the tableting process. Therefore

Figure 3: Technical drawing multitip punch

the tablet press should be equipped with key ways for the upper and lower punches. Minitablets usually need lower compression pressure per tip due to the smaller cross-section surface. A punch tip having a diameter between 2 – 3 mm can withstand compression pressures of 2 – 3 kN. Therefore the maximal compression pressure is multiplied by the number of tips.

Figure 4: Multiple part assembly punch (external cap fixing), side view

Figure 5: Multiple part assembly punch, 12 tips, frontal view

Figure 6: Monoblock punch, 24 tips, side view

Figure 7: Monoblock punch, 24 tips, frontal view

2.2.3.   Coating

The coating process is a well-established process in the pharmaceutical industry. Coating is the homogenous layering of tablets, pellets or granules. Due to the continuous coating layer the API has to a certain extent, been stability-protected from the potential negative influences of oxygen, moisture and light. By using special polymers, the dosage form can also be protected from gastric juice when the coating layer is insoluble at low pH. The patient compliance can also be increased, due to better acceptance by coloring, better distinction of different dosage strengths, masking of the taste, odor and improvement of swallowing. Moreover by applying a coating the release properties can be modified, e.g. to an extended release profile of the drug. Another type of coating is the active coating, when the API is dissolved or suspended in the coating suspension and then sprayed onto placebo pellets.

Prior to the introduction of polymer based coatings in the 1970s usually sugar suspensions were used. Then the tablet weight increased typically around 50 - 100 % to achieve a homogeneous layering. Nowadays polymer suspensions are used as coating material. The weight increases are less compared against the sugar coating because a thin film between 20-200µm is sufficient for a homogeneous coating. A further advantage of film coating compared to sugar coatings is that the process is less complex, more cost efficient with regards to shorter processing times. Due to the wide range of different polymers types, there are many possibilities with regards to aesthetic, extended/delayed drug release, enteric coating and taste masking.

Typically a formulation of the coating suspensions contains a polymer, a plasticizer, a colorant and a solvent which is removed during the coating. The polymer is the major ingredient and has - depending on its chemical structure, its molecular weight and distribution - a great influence on the film and its physical and chemical properties. A

plasticizer is often needed to reduce the glass transition temperature (T_g) to enable the coalescence of coating particles and increases the elasticity of the film.

Another form of coating is the hot melt coating. In the 1960s melt coating was firstly applied in pharmaceutical industry. The drug is typically fluidized in a fluidized bed coater and the molten lipid is sprayed onto the particles. The use of this technology is dependent on the coating agent selected for taste masking or controlled release as recently shown [30], but is not widely used.

The commonly used technologies used for coating are performed either in a fluidized bed or a drum coater.

2.2.3.1. Film formation

Bindschaedler has described in 1983 the process of film formation [31]. The coating liquid is atomized by the spray nozzle and the droplets make contact with the solid. There they deposited on the surface with water in the voids. When the free water or the solvent is evaporated the polymer particles come to a close packing. Further evaporation causes the generation of capillary forces. This formed pressure causes deformation of the particles. Due to viscous flow and movement of the particles across the interphases of the particles a continuous and coherent film can be built by coalescence. To enable the polymer particles to coalescence the surrounding temperature has to exceed the glass transition temperature of the polymer/plasticizer system. As a rule of thumb the product temperature should be 10 to 15 °C above the minimum film forming temperature (MFT) [32]. The process of film formation is very sensitive to the process conditions. Too fast evaporation would cause poor film formation and when the water is too slowly evaporated the water could partially dissolve excipients and/or API at the surface. API could also then migrate into the coating layer and would get trapped, modifying the release profile of the drug.

2.2.3.2. Fluidized Bed Technology

In the fluidized bed the particles are held in a fluidized state, where the particles behave more like a fluid. The fluidized state is produced by an air flow through the particle bed. A minimum velocity (minimum fluidization velocity) of the air stream is necessary to fluidize the bed. Important process parameters are the air flow (velocity), inlet air temperature, the spray rate and pressure and the resulting product temperature. Fluidized bed technology is known for high heat and mass transfer rates, which shortens the processing time. In the pharmaceutical industry it is used for granulation, drying and coating. For a granulation or

coating process, liquids are applied by a spray nozzle to the particle bed. Depending if and where the spray nozzle is mounted, the fluidized bed equipment can be used for different process operations (Figure 8):

a) No spray nozzle → Drying
b) Top spray: Granulation, Coating
c) Bottom spray: **Wurster coating**, Granulation
d) Tangential spray: Granulation, Pelletisation, Coating
e) Rotor: Coating, Pelletisation

a)　　　　　b)　　　　　c)　　　　　d)　　　　　e)
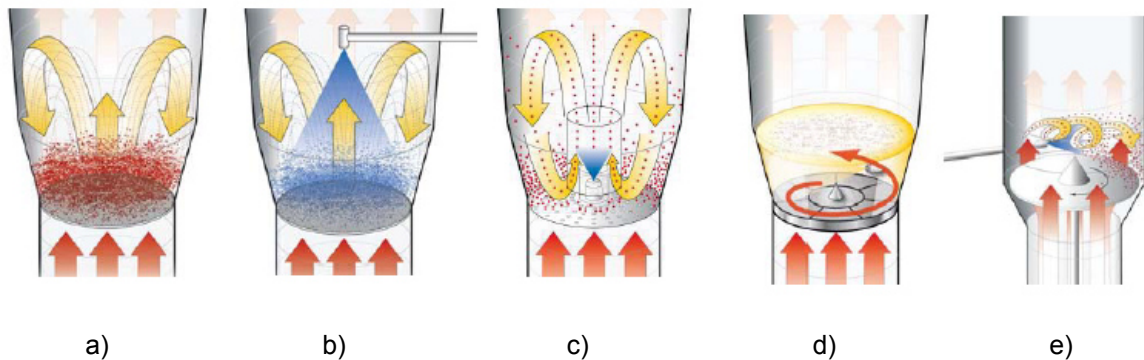
Figure 8: Fluidized bed configurations [33]

Wurster Coating

The Wurster process uses a different air distribution plate. The air distribution plate is split into two zones: an up-bed zone, which surrounds the spray nozzle; and a down-bed zone (Figure 9). The down-bed zone of the air distribution plate has less frequent and finer perforation, so that the particles in the resting zone are ventilated and still suspended, to prevent agglomeration of the particles. The up-bed zone is more perforated and has wider orifices, so that the particles entering this zone can be sufficiently accelerated into the spray zone. The Wurster column is located at a specific distance above the up-bed zone. Depending on the different air

Down   Up - bed
bed zone   zone

Figure 9: Air distribution plate Wurster [33]

velocities of the zones and the distance between Wurster column and air distribution plate (also called column height) a Venturi effect occurs. This Venturi effect transports the particles from the resting zone horizontally to the up-bed zone. The column height needs to be adjusted so that a sufficient particle circulation can occur and a specific amount of particles is then present in the spray zone. The number of particles in the spray zone also depends on

the particle size, shape, air flow and bulk density [34]. If the column gap is too small, just a few particles are drawn into the Wurster column and a lot of coating suspension will be lost, either spray dried or adhered to the inner side of the Wurster column. On the other hand, when the column gap is too big, many particles will slowly pass through the Wurster column and the risk of agglomeration will be significantly increased. In an extreme configuration (extremely large column gap) the Venturi effect will vanish and there will be no horizontal transport to the up-bed zone.

The spray nozzle is located in the center of the air distribution plate and uses pressurized air to shear the coating suspension into droplets (two-substance nozzle). The atomization pressure has an influence on the spraying angle, size of the droplets and droplet velocity. If the atomization pressure is too, high attrition of the particles can occur and very fine droplets are produced which can lead to spray drying. On the other hand low atomization pressure leads to coarse droplets. The coarse droplets dry more slowly and could penetrate the substrate. Furthermore the risk of sticking and twinning would be in such a case increased.

Above the Wurster column is the expansion area, where the container is typically conical shaped (increasing diameter).The air velocity decreases and the particles fall down in the resting zone. Wurster containers are available to coat batches from 100-500 g up to 800 kg [34]. In the production scale up to 7 Wurster columns are mounted.

Particles from 100 µm to tablet size can be coated with the Wurster process. The advantage compared to drum coating is that the high shear forces in the column prevent sticking of particles.

2.2.3.3.   Drum Coating

Drum coating is the traditional method for coating tablets. The drum coating process is typically used for large and non-fluidizable particles like tablets or capsules. The tablets are rotated in a drum to produce a cascading movement and a coating solution is applied by a spray nozzle onto the surface of the tablet bed. The coating droplets are immediately dried on the tablets by an air flow. Depending on the configuration of the coater, routed the airflow is differently through the tablet bed [32] (Figure 10). Conventional coating pans have been formerly used mainly for sugar coating. Nowadays typically the side vented coating pans are used for film coating. The side-vented pans are perforated and the air flow is introduced at the top into the drum and gets sought out beneath tablet bed. Therefore the air is forced to go through the tablet bed and dries the coating liquid on the tablet, yielding a higher drying efficiency.
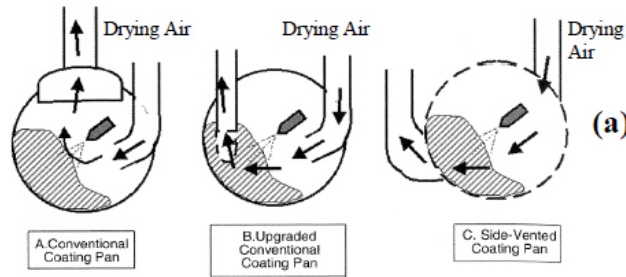
Figure 10: Configuration drum coating [32]

The exhaust temperature is an important process parameter to monitor the process. It is a function of the inlet air temperature and humidity, the spray rate, the inlet air volume and the atomizing pressure.

The spray nozzles are mounted on a spray arm which is installed in the drum above the tablet bed. The nozzles should be adjusted to a specific distance to the tablet bed in a right angle and located approximately in the upper 1/3 of the tablet bed. If more than one spray nozzle is used, overlapping of the spray pattern should be prevented due to over-wetting of the tablets. Also too high distances of the spray nozzles should be prevented because that could lead to an inhomogeneous coating distribution. For the application in drum coaters often a flat spray nozzle is used. There the spray pattern and droplet size and velocity are controlled by the atomization pressure, the fan air pressure and the needle air.

Baffles are mounted inside the drum to increase the horizontal mixing quality. With these baffles the tablets are lifted and turned from one side of the drum to the other.

2.3.   Taste masking

Many active pharmaceutical ingredients exhibit undesirable organoleptic properties such as bitter, metallic taste or burning sensation [35]. If the dosage form not gets taste masked, the patient compliance and adherence would significantly decrease. That is especially a important for the development of pediatric and veterinary medications. There are various strategies, which can lead to an improved taste perception.

2.3.1.   Taste recognition

Taste is one of the five traditional senses (sourness, saltiness, sweetness, bitterness and umami) and can be recognized on the tongue [10]. Evolutionary the taste was a protective mechanism that toxins or spoiled food not get eaten [36]. The taste is transmitted by the interaction of dissolved molecules with the different targets located in the taste buds [37]. The taste buds are onion shaped pores which include the receptor cells having G-protein coupled receptors (GPCRs) for the bitter, sweet and umami taste recognition, while for acid and salty taste sensation ion channels are responsible for the signal transduction. Until now 25 different bitter taste receptors have been discovered [38] and belong to the TAS2R family. Bitter taste can be assessed when the substance binds to the TAS2Rs receptor. Then the G-protein Gustucin is released in the cell and triggers a multistep enzymatic reaction [39]. This leads to the release of neurotransmitters and causes a nerve impulse (Figure 11).
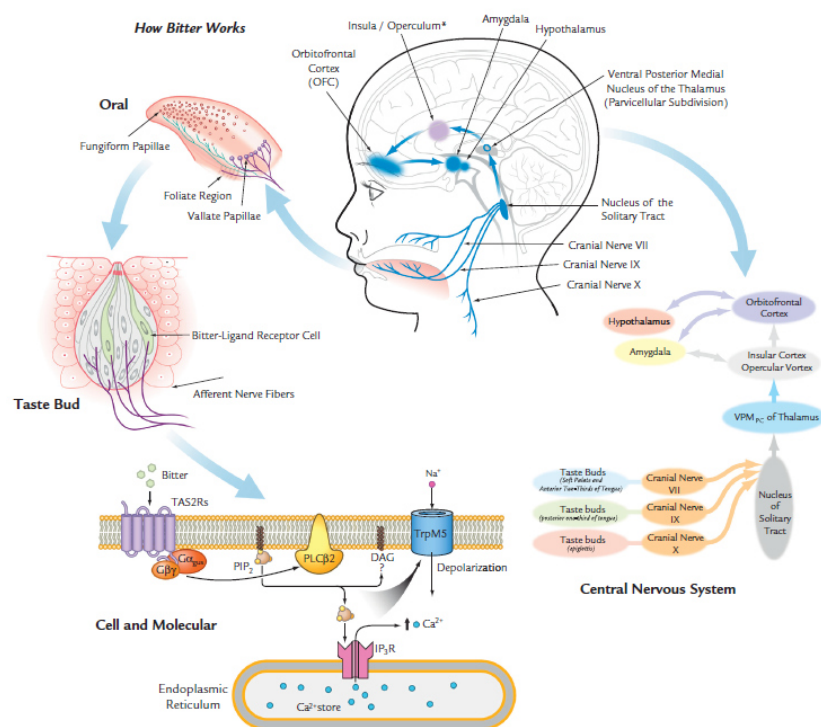
Figure 11: Bitter taste recognition [40]

In most of the cases a correlation between the taste and the chemical structure can be made. For example low molecular salts taste salty and components having nitrogen bonds exhibit often a bitter taste. In pharmaceutical development, the bitter taste is the most critical one because humans have a very low threshold for tasting bitterness, and has a major influence on the compliance and patient acceptability. This especially important for pediatric medications, since taste is in 75 % of cases the main reason medication is refused by children [9]. A correlation was made between the genotype of children and the experience of taking solid oral medication, because the homozygous PP allele determining the bitter taste receptor TAS2R38, which results in high sensitivity of bitterness and consequently refusal of bitter tasting liquid medication [41].

2.3.2.   Taste masking strategies

There are several taste masking strategies described in the literature. Taste masking strategies can by divided into the following approaches (Figure 12):
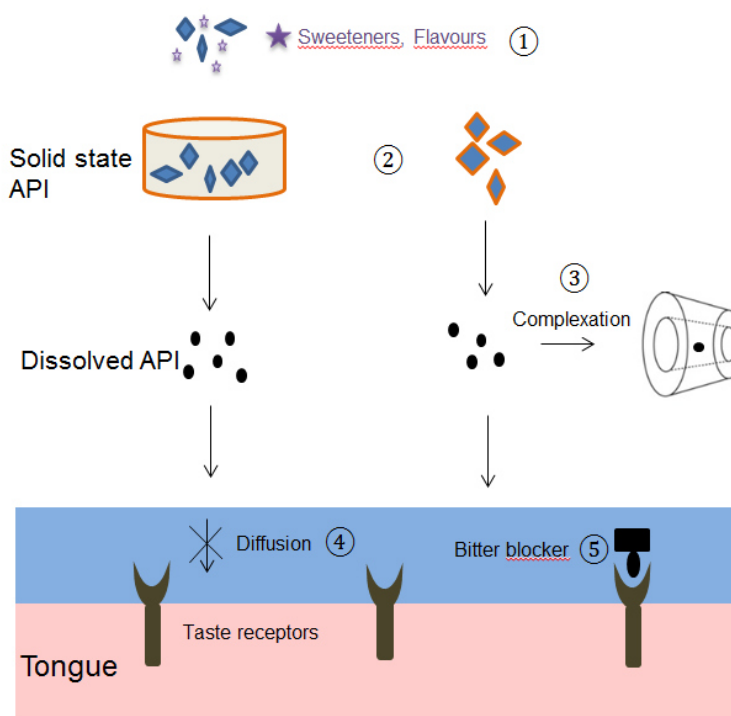
Figure 12: Taste masking approaches
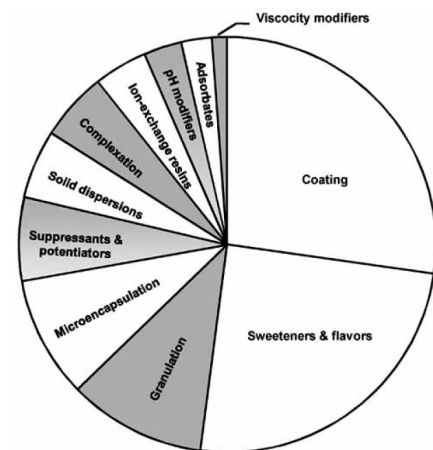
Figure 13: Taste masking technologies (1997-2007) [10]

1) sweeteners and flavours

2) applying a physical barrier between the API/dosage form and the taste receptors

3) altering the solubility of the API

4) viscosity enhancer

5) bitter blockers

Figure 13 shows the proportion of the taste masking strategies used between 1997 and 2007 based on a patent review is show. Here it shows that coating and sweeteners & flavors having the biggest share.

2.3.2.1.   Sweeteners and Flavours

The addition of sweeteners and flavors is the oldest and most simple taste masking approach because no specialized equipment is needed and bioequivalence has not affected. It can be applied both to liquid and solid dosage forms, but it is not suitable for water soluble bitter drug at a high drug load [10], since any substance which is dissolved in saliva will interact with the corresponding receptor and cause a response. Therefore sweeteners and flavors are often used in combination with other taste making technologies.

A wide range of sweeteners such as aspartame or sucralose is available. Depending on the sensory quality and on the processablility (temperature, pH stability) a specific sweetener can be chosen. The sweetness intensity of a specific sweetener changes over time and is a characteristic for the individual substance: Sweeteners can be divided into early-middle to middle-late onset of sweeteners. Therefore a combination of sweeteners is sometimes needed to provide the correct sweetness intensity over time [38]. It is difficult to determine the pervasive and extent of sweetener [38], hence the sensitivity depends on many factors.

In the literature it is reported that by addition of a physiological acceptable acid (e.g. citric acid) the taste masking efficiency of sucralose is increased [10]. By adding potentiators such as thaumatine, neohesperidine dihydrochalcone or glycyrrhizin the perception of sweeteners can be increased and this approach will also mask the unpleasant aftertaste [10].

Flavors can be extracted from a natural source or produced artificially. Natural flavors are complex mixtures, where the exact composition is mostly not known. Although they are better palatable and chemically more stable, they vary over time with regards to their composition (Batch-to-Batch variability). The flavor preferences depend on age, socio-cultural background and gender [38]. EMEA has published in their reflection paper the type of flavors as a function of the API taste and the indication [42] (Table 2 and Table 3)

Table 2: Flavors as a function of the product taste [42]

Product character	Suitable flavors
Acid	Lemon, lime, grapefruit, orange, cherry, strawberry
Alkaline	Aniseed, caramel, passion fruit, peach, banana
Bitter	Liquor ice, aniseed, coffee, chocolate, peppermint, grapefruit, cherry, peach, raspberry
Metallic	Berry fruits. Grape, peppermint
Salty	Butterscotch, caramel, hazelnut spice, maple
Sweet	Vanilla, grape, cream, caramel, banana

Table 3: Flavors as a function of the indication

Product type	Flavor often used
Anitulceratives	Lemon, fresh and balsamic blends
Laxatives	Cherry, raspberry, liquor ice, aniseed, orange/vanilla blends
Mucolytics	Orange/lemon blends, raspberry
Penicillins	Cherry, raspberry, woodberry, tutti frutti blends
Sulphonamides	Vanilla, caramel, woodberry, apricot, cherry, blackberry, banana
Tranquilisers	Aniseed/mint blends
Vasodilators	Ginger, coffee, caramel
Vitamins	Orange, lemon, tangerine, grapefruit, pineapple, tropical fruits

2.3.2.2.   Physical barrier

One approach to mask the taste is to build a physical layer between the dosage form specifically the API and the taste buds of the tongue. Therefore the interaction of the API and the taste receptors is inhibited.

Polymer and lipid coatings can be applied using conventional coating technologies, like drum coater or in the fluidized bed, though other technologies such as extrusion, spray drying or microencapsulation can be used.

Microencapsulation

Microencapsulation can be accomplished by solvent extraction or evaporation, spray drying, coacervation or spray congealing. In general microencapsulation protects the material from volatilizing, oxidation, and masks unpleasant taste [10]. Excipients used for coating are also commonly used for microencapsulation. The microencapsulated particles have typically a low particle size and are therefore suitable for preparing a taste masked suspension. Due to the

low particle sizes the suspension sediments slowly and is therefore sufficiently physically stable.

The phase separation or coacervation process is conducted in three sequential steps during continuous stirring. First three immiscible chemical phases are formed, then the coating is deposited and afterwards the coating gets solidified. The coacervation is either induced by a pH change or by the addition of a strongly hydrophilic substance [43].

For the spray drying process the API is firstly dissolved or suspended into the liquid, which is then sprayed via spray nozzle into a fluidized bed. The droplets dry due to the contact with the hot air stream and solidify. Afterwards the solid needs to be separated from the air stream to be discharged. Hoang reported the successful taste masking of acetaminophen with spray drying using a mixture of sodium caseinate and lecithin [37].

Coating

Coating is the most efficient and common taste masking strategy [10]. Drug particles, granules or tablets can be layered with a suitable coating material. The coating layer could improve stability in case of a moisture or light sensitive API and offers the ability for a controlled drug release (gastric resistance, sustained release properties) [44].

The major requirement for taste masking is that the release profile of the dosage form prior coating should not be not significantly changed to ensure the same pharmacokinetic drug product performance.

Gastric acid soluble resp. reverse enteric polymer coatings are suitable as they are insoluble in saliva (pH 6-7) but soluble at the gastric pH. With regards to excipients safety aspects, they may interact due to their ionic polymer structure with the body tissue and toxicology data should be taken into account. For example Eudragit E PO® could cause loss of weight due to food absorption effect and can influence the water and electrolyte balance. Another disadvantage of pH dependent polymers is that they cannot be suspended in liquid vehicles or food [38].

Insoluble polymers such as ethylcellulose or polyvinyl acetate with an incorporated gastro soluble pore former (e.g. calcium carbonate or magnesium oxide) can be also used for taste masking. The gastro soluble pore former is not soluble in water or saliva, but soluble in acidic gastric fluid [10]. Due to presence of such a pore former the dosage form can still have immediate release properties.

Gaber compared the suitability of minitablets to pellets for a modified release coating and found out that pellets need higher coating thicknesses for the same retardation effect. Furthermore minitablet exhibit higher stability during storage [45].

Coating with lipids is commonly used for controlled or delayed release dosage forms. Taste masking with lipids could be an alternative to the standard polymer coatings [30]. For that purpose mixture of long chain mono-, di-, and triglycerides or waxes can be used. The lipids are molten and if necessary diluted with a solvent to achieve a uniform application. Typically less excipients are required compared to the polymer coating liquids, which would simplify the formulation and might have advantages in terms of regulatory acceptance by the health authorities [38]. Furthermore lipids are more plastic compounds and there is a lower risk of cracking when compressing coated particles into tablets.

The lipids can be processed by hot melt coating resp. granulation, spray congealing or melt extrusion. Hot melt coating is an alternative to polymer coating where the molten lipid is sprayed on a fluidized particle bed. In a spray congealing process the API is dissolved in the molten lipid and sprayed into a cooling chamber. There small taste masked particles are formed. The drug load is critical, because the viscosity is typically changed during processing, with the literature suggesting a maximal drug load of 30 % [46].

Contrary heat sensitive API`s could be degraded during the melting process and often complex equipment is required. Furthermore there is a limited amount of lipid coating agents and the polymorphism of those agents should be studies due to potential change during storage [47]. Lopes showed that it is feasible to avoid the polymorphic stabilization and the resulting negative effect on the drug release during the hot melt coating process [48].

Other Technologies applying a physical barrier

There are other technologies such as extrudation, granulation and matrix formation, which can provide a physical barrier.

Extruder consists of an extrusion barrel, rotating screw and an extrusion die. The raw materials are fed into the extruder where they are mixed and kneaded by the screws. Either the powder mixture becomes molten or a binder liquid is added. The granulation mass forced through the extrusion die to form strands which can be further processed into pellets via spheronization. This process can be conducted continuously, is easily scalable and is a short process. Cationic drugs can be taste masked with polymers having high amount of anions. By the melt process the drug polymer complex is formed. Furthermore hot melt coating can prepare a solid dispersion, where the drug is molecular dispersed in the polymer matrix and the amount of free drug is reduced on the surface of the particles. Maniruzzaman has

reported a good taste masking efficiency of acetaminophen granules by hot-melt extrusion with Kollidon® VA64 [49].

Granulation is rapid and less expensive process. The granulation liquid can include polymers, flavors or waxes. Compared to the coating process the coating layer is incomplete and therefore just appropriate for API with low bitter intensity or in combination with a different taste masking approach.

When the API is included in a matrix system, the release is delayed. Therefore there is no release in the oral cavity and the dosage form can be taste masked, but also the dissolution rate is reduced.

2.3.2.3.   Alter drug solubility

The taste of a drug occurs only once the API is dissolved; otherwise it is not able to interact with the taste receptors. Therefore the physico-chemical properties of the API are an important factor taking into account for the choice of a taste masking approach. This is suitable for API having a low or medium level of bitterness. However, by altering the drug solubility the pharmacokinetic performance or bioavailability should not be negatively influenced [38].

Choice of solid form

During the development a different solid form can be chosen, when the salt, cocrystal or polymorph of the API has a different solubility profile. For taste making reasons the solid form, which has a low solubility in the liquid vehicle and a slower dissolution rate is preferred.

Complexation

Complexation is a more effective approach than the addition of sweeteners and flavors. It is technically more complex to develop and the physico-chemical properties of the API play an important role [38]. Complexation can be done by using ion exchange resin, inclusion bodies such as cyclodextrines or by creating a drug-polymer complex.

Cyclodextrines are cyclic oligosaccharides and have a cup-like shape. Taste masking can be achieved when the API-cyclodextrine complex is formed, hence the API is not able to interact with the receptor. The taste masking is effective if the amount of the free drug is low and that depends on the properties and the dose of the API. The inner cavity is relatively apolar and therefore hydrophobic. The API can be completely or a just partially incorporated. Depending on the number of glucose units, they are named differently (Table 4). The major factor for

complexation is the size of an API, e.g. an aromatic ring can be applied to a β-cyclodextrine [38].

Table 4: Nomenclature cyclodextrines

Name	Number of glucose units	Application
α – cyclodextrine	6	parenteral
β cyclodextrine	7	oral
γ cyclodextrines	8	-

Ion exchange polymers (resins) have a high MW and possess cationic and anionic groups, respectively acid and basic functional groups. Depending on the number and chemical nature of the functional group the ion exchange resins can be divided into strong and weak ion exchange resins.

The API binds to the oppositely charged resin. Therefore the concentration of free API in suspension is low and can achieve a taste masking effect. The resin is suspended in a good flavoured liquid vehicle. Consequently the API is added in excess and stirred until the equilibrium is reached. In the gastrointestinal tract the API is then replaced by a counter ion, where the API is free and can be absorbed.

It is important that the ion exchange resin is chemically stable in the pH of the vehicle and that the API does not already become desorbed in the saliva, which should occur then later under the conditions of gastric pH. Becker and Swift have proven the ability to bind 13 different APIs to two strong acid cation exchange resins (Amberlite[TM]) [50].

2.3.2.4.   Viscosity enhancer

Viscosity enhancers can be used to increase the taste masking efficiency by decreasing the diffusion rate of the dissolved API in the mouth to the taste receptors. This approach is typically used for liquid oral suspensions. Furthermore the migration of the API from the solid particles in the case of suspended API to the suspending media is retarded [10]. Excipients like hypromellose, xanthan gum, microcrystalline cellulose and sodium carboxylmethylcelluolose are often included in the suspending vehicle.

pH modifiers can be used to maintain the pH of the liquid vehicle to enhance the in situ precipitation in saliva, limit the solubility or reduce the dissolution rate. This approach can be used when the API is ionizable and has a pH dependent solubility. For example Ondansteron has relative low water solubility at a higher pH. Therefore a taste masking could be achieved by adding an alkaline agent to increase the pH of a rapidly disintegrating formulation [28].

2.3.2.5.   Bitter blockers

Bitter blockers such as adenosine monophosphate, lipoproteins or phospholipids bind competitively and antagonistic to the bitter receptor, hence inhibit the release of the G-protein gustducin. Bitter blockers have a structural analogous but are often taste less. Lipoproteins are universal bitter taste blockers [29].

Successful taste masking can be achieved when the API binds to the same bitter receptor as the bitter blocker. Until now the mechanism is not fully understood, and the development is still a "trial and error" approach [38].

Taste transduction cascade blockers can lead to a taste masking effect. The taste transduction pathway can be blocked at any stage (Figure 14). The ion channel Transient Receptor Potential Channel subfamily m 5 (TRPM5) is one component of the cascade and current research is
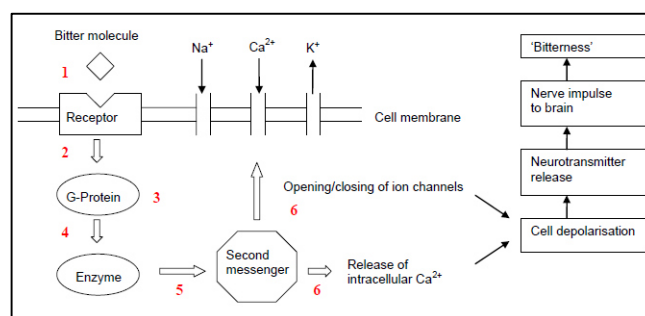
Figure 14: Taste transduction [51]

ongoing to block or enhance this ion channel [38]. But even when a suitable molecule could be found, the application in pharmaceuticals formulations will be limited due to toxicological and regulatory concerns [38].

By adding cooling (e.g. menthol, eucalyptol) and warming agents (methyl salicylate) an extreme situation can be provoked and cause an "overpower" of the bitter taste, which confuses brain [52] and then the taste is not recognized as bitter.

Selection of the taste masking technology

The most important factor, which needs to be considered for the decision of the most suitable taste masking strategy are [10]:

- intensity of bitterness
- dose of API
- properties of API (physicochemical, particle size)
- dosage form

The bitterness intensity of the API is a major factor for the decision. If the API exhibits a high bitterness intensity, which means the perception concentration is very low, taste masking approaches like sweeteners, viscosity enhancers, cyclodextrines and granulation are not sufficient [38], [10]. With these approaches the amount of the free drug is at best just lowered, so that the API can still bind to the bitter receptors. Then coating or microencapsulation, where no API can be released in the saliva, are more suitable approaches. On the contrary, when the bitterness intensity and the dose is low sweeteners and flavours could eventually mask the taste, offering the advantage that no additional process step or equipment would be needed.

The properties of an API can also limit the choice of the taste masking strategies depending on the drug particle shape and size distribution, chemical structure and physico-chemical properties:

If the particles are irregularly shaped and exhibit a wide distribution, particle coating is difficult. In that case enormous amounts of coating agents and large coating thicknesses are needed, so that the layer is sufficiently intact.

If the API has ionizable groups, it can be bound to ion exchange resins. Depending of the chemical structure and the polarity of the API taste masking can be achieved by complexation with cyclodextrines.

The theoretical option to use a modification of the API exhibiting lower solubility in saliva (e.g.by using another polymorphic form, cocrystal or salt form) should be carefully assessed with regards to not changing PK properties of the dosage form.

Depending on the selected dosage form the following taste masking strategies are suitable:

- Tablets, capsules: film coating
- Dispersible tablet: particle coating, sweeteners and flavors, viscosity enhancer
- Liquid oral formulations: sweeteners, particle coating, microencapsulation, pH modifiers, viscosity enhancers

Another factor taken into account is the chemical incompatibility of the taste masking excipients with the API (e.g. protonated cationic API and pH dependent polymers [53].

Bitter blockers are a relatively new taste masking technology. First of all the bitter blocker has to bind to the same receptor as the API and due to their mode of action bitter blockers must be administered prior to the administration of the medication [38]. That is especially crucial for the pediatric population due to the potential decrease of the compliance. Furthermore safety and toxicology data for those new types of bitter blockers in children are not available.

For the commercial implementation, it needs to be considered whether the technology can be executed on the available standard equipment or if special equipment is needed. For example for a microencapsulation process specialized equipment and know-how is needed and therefore typically conducted by contract manufacturing organizations.

2.3.3.   Taste assessment

There are several approaches to evaluate the taste during the development of an oral drug product. The human taste panel is still the most recently used method and typically conducted towards the end of the development [54]. Due to ethical and toxicology concerns in the early stages of the development especially regarding application in pediatric populations also non-human in vivo or in vitro taste assessments are becoming more relevant [54].

2.3.3.1.   In vivo taste assessment

The in vivo taste assessment can be done by human taste panel studies with either adult healthy volunteers, pediatric patients or by an animal model.

Human test panel

In vivo evaluation of taste masking is conducted with 4 to 30 healthy volunteers [55], which are either trained or not. The drug formulation is commonly placed directly on the tongue or the drug product is pretreated and then administered as a suspension or solution. After a specific time of exposure (10-30 s) the panelists rate the intensity of the taste by numbered scores. Since the residence time of the formulation in the oral cavity is even for children with ADHS and autistic disorder not longer than 30s, the exposure of the formulation should therefore not exceed the 30 s [55]. The procedure should be well controlled and equal for each panelist to deliver comparable results. Nevertheless taste perception differs based on nationality, eating habit and age [56].
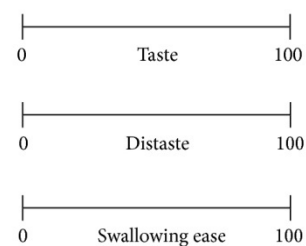

Figure 15: Facial hedonic scale [57]

Figure 16: Visual Analogue Scale [58]

The bitterness threshold can be determined by a human taste panel, where 5 to 7 API solutions with defined concentration are given to the panelists. After a specific procedure (exposure time, time of water rinse) the panelists score with predefined declaration the taste (e.g. no bitterness to strongly bitter).

The transfer of the results gained from the adult taste panel to the taste impression of children cannot be done. This would lead to dramatically false results, as the taste impression changes extremely with age [55]. The EMA recommends [3] to study the patient acceptability for pediatric medication in children as a part of the clinical studies. The taste assessment should be conducted like a game; hence children have a shorter concentration span and problems with taste fatigue. Therefore the EMA also recommends not more than 4 tests. Since very young children (≤ 3 years) cannot express themselves clearly a facial hedonic scale is used for the evaluation of the bitterness (Figure 15). For children, which are older than 6 years a Visual Analogue Scale is commonly used (Figure 16). More than half of the pediatric taste studies are done with sick children and while the taste study would be more significant when assessing the taste with healthy children, it is ethically forbidden to expose a child to a potential toxic substance [59].

Animal model

Animal models can be applied for the estimation of the taste of a compound using mice, rats, cats or dogs. They can be divided into taste discrimination and taste guided experiments. At the conditioned taste aversive (CTA) test rats are negatively conditioned to the taste of a reference substance. The rat would avoid any new compound, when it would exhibit a similar taste to the unpleasant reference taste. The operant taste discrimination model uses rats which are trained to perform a specific task depending on the similarity to the reference taste. With this model only a pairwise comparison can be done and a long training period is necessary. After that experiments can also be conducted in a high throughput mode: The rats are then sampling from a 96 well plate and performing afterward the operant discrimination taste. Before executing such an experiment training periods up to 7 weeks are necessary [54].

For the Brief-Access Taste Aversion (BATA) model rodents are deprived of water for a time period of 16 – 24 h. When they afterwards again have access to water or an aqueous solution the lickometer counts the licks the rodent makes depending on the concentration [54]. A high number of licks is an evidence for a pleasant taste. The number of licks depending on the concentration of the compound until the full aversion is computed. Therefore the palatability and not the taste quality is measure compared to the operant discrimination tests.

Another animal model was developed using the Amoeba dictyostelium cells [60]. When these cells get in contact to bitter compounds the morphology change to a round shape and the movement is inhibited depending of the concentration of the bitter compound. Cocorocchio

has proven good correlation between the bitterness responses of the Amoeba dictyostelium and the BATA model [60] using six bitter compounds.

2.3.3.2.   In vitro taste assessment

Biomimetic taste assessment

Biomimetic taste sensing systems are also called electronic tongues, e-tongues or taste sensors. They determine the taste in a similar manner to the biological taste perception in humans [61]. The electrochemical sensors coupled with chemometric methodologies can give a qualitative and quantitative analysis of organoleptic and chemical properties of substances and products. In the pharmaceutical industry the apparatuses Insent (Atsugi – Chi, Japan) and Astree sensor (Alpha M.O.S., Toulouse, France) are used. They measure with polymeric sensors using a chemical modified field effect technology. The sensor response is delivered in milliVolt (mV). Small variations in temperature, pH and age can have a large impact on the sensor response [54].

The taste masking efficiency of a drug product can be measured by the comparison of the sensor response of the taste masked formulation, the pure API and a placebo formulation. Via Principle Component Analysis (PCA) map the Euclidian distance can then be measured. The smaller the distance between the placebo and the taste masked formulation, the better the taste making approach [54].

A bitterness prediction model can be built by comparing sensor responses of a compound with known bitterness threshold resp. human taste panel data with the sensors responses of the compound. When it exhibits a linear relationship between the concentration and the sensor response a correlation can be done. Poor correlation to human taste panel data was achieved when comparing compounds with a different chemical nature [54].

Drug release studies

The amount of the drug released in simulated oral cavity condition can be measured via drug release studies as only dissolved drug in the oral cavity will interact with taste receptors [54]. Important is that only the API exhibits the bitter taste and not excipients. This measurement is commonly used to measure the effectiveness of taste-masked coating and/or complexation [61]. The composition of the dissolution media and the apparatus are adapted to simulate the physiological conditions in the oral cavity. Pein reported realistic conditions in the human mouth [55], which are listed in Table 5.

Table 5: Condition in human mouth [55]

Saliva	Tongue
• Residual volume : 1-2 ml • Flow rate: 0.5 – 1 ml/min • Osmolarity : 50 – 100 mosmol/kg • pH depending on age: 5.7 - 7.5 • Buffer capacity: 6.1 mol/l • Temperature: 35 – 36 °C	• Force: 0.135 N

Many drug release studies use phosphate puffer pH 6.8 as described in USP/NF pharmacopeia. To create more realistic conditions viscosity enhancers, inorganic salts (e.g. K+, Cl-, Na+) or enzymes (e.g. Alpha amylase, mucin) are added. An overview of the published artificial and simulated saliva is shown in Appendix I.

To mimic the hydrodynamic conditions in the mouth several approaches are described in the literature (Table 6). Yajima reported with the mini column method good correlation between in vitro and sensory analysis [62].

Table 6: Simulation approaches of oral cavity

Author	Media	Volume or – rate	Apparatus	Movement or speed	Time
Guhlman 2012	Simulated saliva	50 ml	Baker	Stirrer , 50 rpm	5 min
Shulka 2009, Sheshala 2011	Phosphate buffer pH 6.8	5 ml	25 ml Vessel	No movement	60 s – 120 s
Patra 2010	Simulated saliva	10 ml	ns	shaking	60 s
Shirai 1994 & Kondo 2011	Water	10 ml	Syringe	5 – 10 revolvings of syringe per 30s	ns
Yajima et al 2002	Phosphate buffer pH 6.5	0.3, 0.5 and 0.7 ml/min	Mini column	Flow through	ns
Thia et al. 2012	Phosphate buffer pH 7.4	1 ml/min	Mini column	Flow through	ns
Becker et al. 2016	1% Brij 30 aq. solution	100 ml	Baker	Magnetic stirrer	3 min

FIP/AAPS guidelines recommend for coated particles or granules and ODT drug release studies in a neutral pH medium, the acceptance criterion is that less than 10 % of the drug dissolved within 5 min [63]. Taste strongly depends on the taste intensity of an individual drug, so when taking that aspect into account, taste masking is achieved if the API is not

released at early time-points (0 to 5 min) or if the concentration is below the human perception threshold for identifying the taste [61].

Another acceptance criterion of sufficient taste masking is when the dissolution profile exhibits a delayed onset of the dissolution profile (resp. lag time). Guffon reported about an sufficient taste masking having a lag time of 10s [64]. In case of a sour tasting API, the taste masking efficiency can be measured by the drop of the pH, if the sour taste is related to the deprotonation of the carboxyl group of the API [65].

Selection of the taste assessment method

There are several methods available to assess the taste, but the selection of the most suitable method depends on the phase of the development and the required information (efficiency of the taste masking approach or overall taste quality).

In the early phase of the development when no toxicology data are available, human taste panels are not appropriate due to ethical and toxicological concerns. To get a first impression of the taste an animal model (e.g. BATA test) can be suitable [54]. Also e-tongues have shown good correlation in the early screening of the pure API, but should be validated by in vivo data [54]. Human taste panels are still the golden standard method. Trained panelists should be used to evaluate the overall gustatory impression [47], but this approach has disadvantages like subjectivity of panelists, potential toxicology and liability issues [61]. Since results from adult human taste panel cannot be transferred and e tongues or animals models are not specialized to reflect the taste of children, EMA recommends to include taste studies in clinical studies for the evaluation of pediatric medications [3]. The screening and optimization of taste masked formulation can be done by e tongue or in vitro drug release methods. Using the e-tongue the taste masked formulations can be compared to the placebo formulation. In vitro drug release studies cannot determine the taste itself and is just suitable if the bitterness threshold is known. This method is typically used for measuring the taste masking efficiency of coated solid dosage forms [61] and gives an estimation of the taste intensity.

Each of the taste assessment methods has its advantages and disadvantages, therefore more than one method should be applied during development.

2.4.   Summary Literature review

The literature was reviewed with the focus on manufacturing of minitablets and their acceptability in children, taste masking strategies and taste assessment approaches.

As proven in several studies minitablets are appropriate for the treatment of young children (Table 1). Due to the limited particle size, direct compression is suitable for minitableting, if the powder mixture exhibits sufficient flow and compression properties.

As shown in the previous section, many taste masking approaches are described in the literature. However coating is often the first choice for commercial applications, since it is a well-established technology (Figure 13). Nevertheless on the market there are only two minitablets for pediatric use commercially available which are taste masked via film coating. These products are Lamisil[®] (oral granules) from Novartis coated with Eudragit E PO[®] and Orfiril long[®] 150mg from Desitin coated with Ethylcellulose. This is an indication for a knowledge gap with regards to the commercial implementation of taste masked minitablets.

Despite the increasing number of scientific publications there are still areas which require further investigation such that minitablets become a fully understood technology in terms of processing and administration of minitablets. Researchers have predominately studied the coating of minitablets to achieve an extended or pulsatile drug release [27]. However the comparison of taste masking agents and the use of different coating technologies is not demonstrated. Therefore it is the aim of this thesis to fill this knowledge gap from an industrial perspective.

3. Objectives

Objective of the thesis was to develop an efficient taste masked dosage form for pediatric population having an age between two to six years in relation to production in an industrial environment.. Minitablets – a type of multiparticulate dosage form - offers the advantages of dosing flexibility; dose accuracy and can be manufactured by a conventional tablet press. Furthermore they are well tolerated by young children, which was recently proven by several researchers (Table 1).

Acetaminophen and Cetirizine dihydrochloride were used as well-known bitter model drugs. To cover a spectrum of different drug loads, the cetirizine minitablet formulation should represent a model formulation having a low drug load of 5 % and acetaminophen a high drug load of 50%. The key objective of the work was to identify the correct formulation composition using potentially tolerable and safe excipients for pediatric use and evaluate the performance of the minitablets during manufacturing and downstream processing using modified standard in-process control (IPC) testing.

Film coating is the most effective taste masking approach independent of the bitterness intensity of the API [10]. Since minitablets have a uniform size and shape, they represent an ideal coating substrate. In addition, the coating process can be performed by well-established equipment e.g. fluidized bed. For these reasons, this work investigates the suitablility of film coating of minitablets as a taste masking approach.

The focus of this work was the development and the investigation of the coating process with different commercially available polymers (both pH-dependent and -independent) with regards to their technical applicability and feasibility for the two different model drugsA secondary objective of the present work was the development of a approach to enable minitablet coating in a conventional drum coater.

The development was conducted using a Quality by Design (QbD) approach. A team-based quality risk assessment was performed to identify the potential critical process parameters (pCPPs) and the potential critical material attributes (pCMAs). A Design of Experiments approach (DoE) should be utilized to evaluate the impacts of the pCPPs and the pCMAs on the critical quality attribute (CQA) "Efficient taste masked" and "immediate release" to develop better process understanding.

The final objective of this thesis is to evaluate suitable methods to test the taste masking efficiency of coated minitablets prepared from the earlier objectives.

4. Materials and Equipment
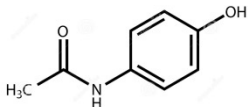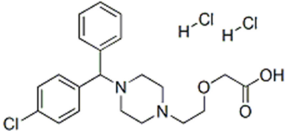
4.1. List of Materials, Equipment and Software

The used materials, equipment and software are listed in Appendix II, III, IV.

4.2. Active Pharmaceutical Ingredient (API)

4.2.1. API Overview

Table 7: Overview APIs

API	Acetaminophen	Cetirizine dihydrochloride
Synonyms	Paracetamol	
Structure		
IUPAC	N-(4-hydroxy-phenyl)acetamide	2-[2-[4-[(4-chlorophenyl)-phenylmethyl]piperazin-1-yl]ethoxy]acetic acid dihydrochloride
CAS-no.	103-90-2	83881-52-1
Molecular Formula	$C_8H_9NO_2$	$C_{21}H_{27}Cl_3N_2O_3$
Supplier	Sigma Aldrich	Sigma Aldrich
Material no.	A5000-1KG	89126-1KGF
Pharmacology	Analgesic and antipyretic activities	2nd generation histamine H1 receptor antagonist
Treatment	pain, fever	allergies, hay fever, Angioedema, urticaria
Appearance	white crystalline powder	white powder
Molecular weight [g/mol]	151.16	461.81
Melting range [°C]	168-172	100-115
Solubility (25°C, water) [mg/l]	$14*10^3$	$6.96*10^4$
Particle size d50 [µm]	58.7	76.3
LogP	0.46	1.7
Dissociation constants	pKa=9.38	$pKa_1=2.7$; $pKa_2=3.57$, $pKa_3=7.56$
Use in Children	infants	>2 years

4.2.2.   Acetaminophen

Acetaminophen is also known as Paracetamol and shows analgesic and antipyretic activities with weak anti-inflammatory properties [66] (Figure 17). It is used to temporarily reduce fever and pains which are caused due to common cold, e.g. minor sore throat, headache, flu or toothache [67]. Acetaminophen is approved to treat children
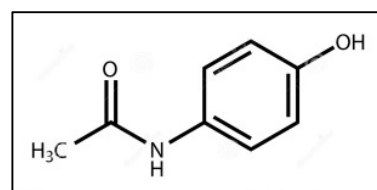
Figure 17: Acetaminophen chemical structure

from birth on [68], with the maximum daily dose of 50 mg/kg and has a minimal toxic dose of 150 mg/kg [69]. FDA has reported on overdoses of children due to dosing errors of liquid preparation [70], and these overdoses can lead to death or liver injury. Acetaminophen is classified as a BCS class I, but for a pediatric dosage forms it is classified as a pBCS III [71].

The mechanism of action is not fully understood. Boutaud states that acetaminophen is a prostaglandin H Synthase inhibitor, but the inhibitory effect depends on the redox state [72], the surrounding enzymes and the substrate concentration [73]. The pain threshold was measured by the response of transcutaneous electrical stimulation, where the threshold could be raised by intravenous injection of 1000 mg acetaminophen [74]. A fever is reduced by acetaminophen due to the blocking of the formation and release of prostaglandins and the hypothalamic thermoregulatory centers [75]. The hypothesis is that cyclooxygenase-3 in the brain is the target of acetaminophen ([76], [77]). This could explain the action of the proportion peroxidease on cyclooxigenases. Therefore is has analgesic and antipyretic effects in the brain and not anti-inflammatory because of the low levels of peroxide in peripheral tissues.

Acetaminophen binds to the bitter receptor TAS2R39 and is listed in the BitterDB database [78]. The effective concentration is 3000 µM.

Acetaminophen is mainly metabolized in the liver by three major pathways (Figure 18) [73].

- 47-62%   Glucuronidation (First order kinetic)
- 25-36%   sulfation (Michaelis Menten kinetic)
- 5-8%   Oxidation (First order kinetic)
- < 9%   Excreted unchanged via urine
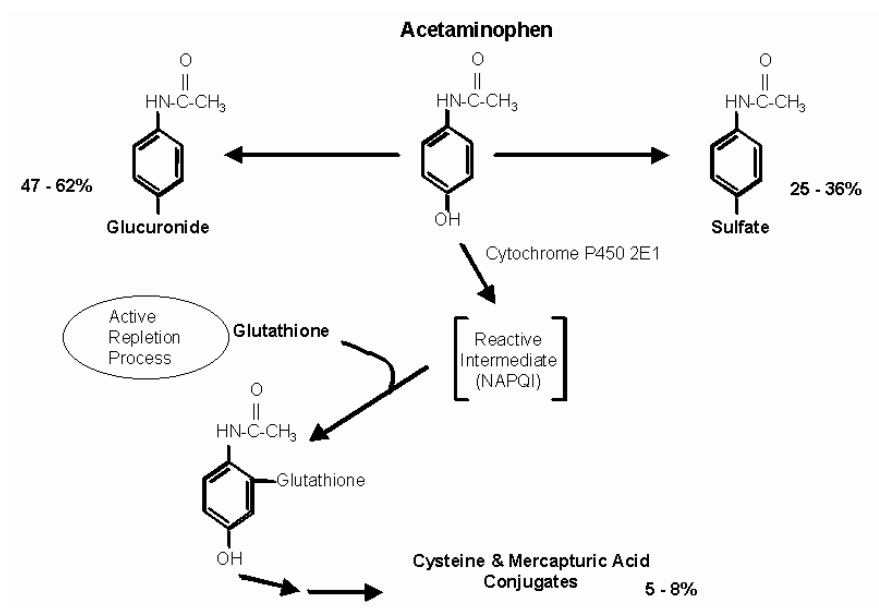
Figure 18: Acetaminophen metabolism [73]

4.2.3.   Cetirizine Dihydrochloride

Cetirizine dihydrochoride is a metabolite of the human antihistamine hydroxyzine and a second generation histamine H1 receptor antagonist. It is used for the treatment of allergies, angioedema and urticaria [79]. Cetirizine dihydrochloride selectively inhibits the peripheral H_1 receptor. Compared to traditional antihistamines

Figure 19: Chemical structure cetirizine dihydrochloride

cetirizine dihydrochloride is more lipophobic and crosses less the blood brain barrier. Therefore it has fewer side effects and does not cause drowsiness or sedation [80]. In vivo animal models have shown that the anticholinergic and antiserotonergic activity is negligible [81]. Common side effects are dizziness, sore throat, cough, nausea, constipation or headache. In children, stomach pain and vomiting may occur [82]. The safety of cetirizine dihydrochloride is proven in pediatric patients aged from 6 month to 11 years. They received doses between 0.2 to 0.4 mg/kg [81]. The dosing recommendation of children between 2 to 5 years is 2.5 mg once daily [83]. The half-life of cetirizine dihydrochloride was 5 hours in children between 2 - 6 years [84]. Around 2/3 of cetirizine dihydrochloride is excreted unchanged via the urine [84].

4.3.   Polymers

4.3.1.   Polymer Overview

Table 8: Overview polymers

	Eudragit E PO[®]	Kollicoat[®] Smartseal	Surelease[®]
Structure			
Name	Amino dimethyl methacrylate copolymer	Amino diethyl methacrylate copolymer	Ethylcellulose
Commercially available as	Powder	Aqueous Dispersion	Aqueous Dispersion
Average molar mass [g/mol]	47 000	200 000	
Composition	Polymer	Polymer with 0.6 % macrogol cetostearyl and 0.8 % sodium lauryl sulfate (30 % solid content)	Polymer plasticized with fractionated coconut oil and stabilized with Oleic acid and Ammonium Hydroxide (25 % solid content)
MFT [°C]	27 [85]	≈57	23 [86]
Glass transition temperature T_G [°C]	48	63	53.8 [87]
Solubility	< pH 5	< pH 5.5	insoluble , pH-independent
Particle size d_{50}	11 µm	150 nm	nano sized
ADI [mg/kg bw]	13.3	10	n.s.
Children	n.s	n.s.	2 years and older, precedence of use

4.3.2.   Eudragit E PO[®]

Eudragit E PO[®] is a cationic copolymer based on dimethylaminoethyl methacrylate, butyl methacrylate, and methyl methacrylate with a ratio of 2:1:1. It has an average molar mass of 47 000 g/mol. Eudragit E PO[®] is the micronized grade of Eudragit E100. Due to the dimethyl aminoethyl groups the polymer is acid soluble. In an environment having a pH higher than 5

Figure 20: Eudragit E PO

the polymer film is swellable and permeable, but in an acidic pH it forms a salt and dissolves rapidly.

The particle size distribution of Eudragit E PO[®] Powder ranges from 2 to 200 µm. But when the coating suspension is prepared with 15 % of stearic acid and 10 % of sodium lauryl sulfate a colloidal solution is build having a particle size distribution range between 60 - 80 nm. Eudragit E PO[®] is not dissolved in water [88] and forms a colloidal solution. Eudragit E PO builds out a very elastic film and as the MFT is already very low the addition of a plasticizer is not necessary. The manufacturer recommends a coating layer thickness between 1-2 mg/cm^2 for tablets and for particles a weight gain between 5 - 10 %.

It was mentioned in the literature that the anionic Polymer Eudragit E PO[®] could interact with cationic APIs [89]. A possible Interaction is that either the carboxylic group or the hydrochloride of the cetirizine dihydrochloride could protonate the tertiary amine of the polymer. Then the polymer would form a soluble salt and the taste masking functionality could be negatively affected.

Based on toxicology data the Acceptable Daily Intake (ADI) of Eudragit E PO[®] is 20mg/kg per body weight (bw). For chronical treatment and daily exposure in children this value is reduced to 13.3 mg/kg bw [90]. Due to the ionic structure the polymer may lead to food absorptions effects and could influence the water electrolyte balance [38]

4.3.3.   Kollicoat® Smartseal 30D

Kollicoat® Smartseal 30 D is a methyl methacrylate and diethylaminoethyl methacrylate in a ratio of 7:3 copolymer. It is delivered as a milky white to yellowish aqueous dispersion having a solid content of approximately 30 %. The dispersion is stabilized with 0.6 % macrogol cetostearyl ether and 0.8 % sodium lauryl sulfate. Kollicoat® Smartseal 30 D is miscible with water and retains its appearance. The mean particle size
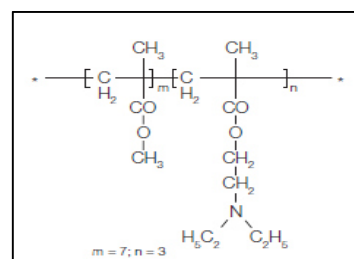
Figure 21: Kollicoat Smartseal 30D

is around 150 nm and was determined by laser scattering. The glass transition temperature is approximately 63 °C and the MFT at 57 °C. Due to the high minimum film forming temperature and the brittleness of the formed film, addition of a plasticizer is necessary. With the addition of lipophilic plasticizers, e.g. Tributyl citrate, Triethyl citrate etc. the MFT strongly decreases and the elongation of break increases (Figure 23 and Figure 22).

The recommended coating level for taste masking is between 2 – 6mg/cm². When the necessary coating layer thickness is reached, then this coat is insoluble in saliva (pH 6.8 – 7.2) for more than 2 hours. In acidic media having a pH below 5.5 the tertiary amines become protonated and the coating layer dissolves immediately. The manufacturer recommends the addition of an antioxidant for tablet formulation, because the moiety of aminoesters can be decreased by oxidation when exposed to light or stored at elevated temperatures. The coating layer could turn yellow and the dissolution could be delayed.

Figure 22: Influence of plasticizer on Elongation of break [91]
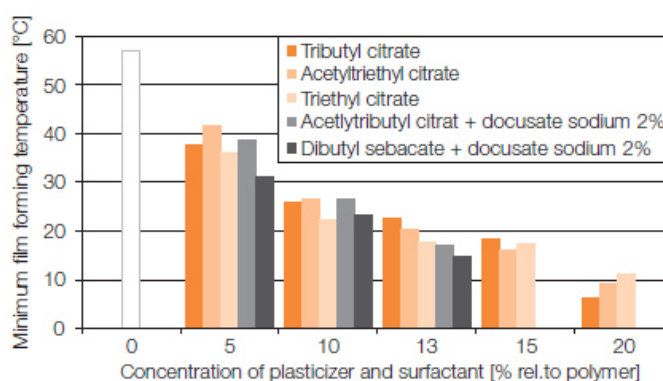
Figure 23: Influence of plasticizer on MFT [91]

According the toxicology data provided by BASF the ADI of Kollicoat Smartseal 30D is 10 mg/kg bw [92].

4.3.4.   Surelease[®]

Ethylcellulose is a non-ionic and not water-soluble cellulose ether. The solubility depends on the substitution degree (DS). In the pharmaceutical industry ethylcellulose derivates with a DS between 2.3 and 2.6 are used [94], and has molecular masses between 150 000 and 300 000. Due to their
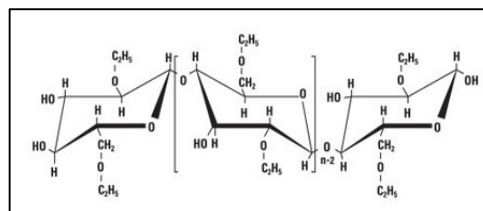
Figure 24: Ethylcellulose [93]

water-insolubility ethylcellulose is typically used as a coating polymer for extended release dosage form, where the API is released by diffusion [95]. For taste masking applications typically a pore former (e.g. HPMC, PVA) is incorporated into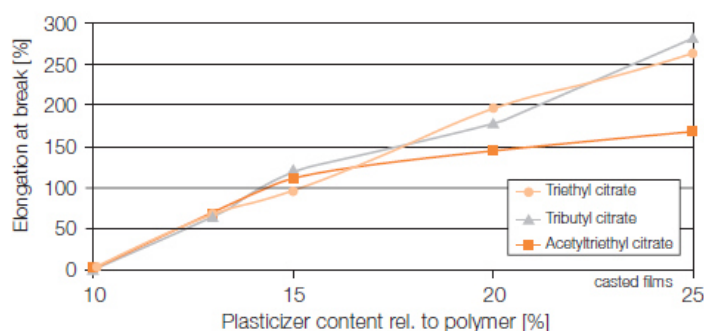 the ethylcellulose film. Surelease is used in the drug product Isentress[®] (Raltegravir) as a taste masking agent. As this product is approved for children between 2 to 12 years, Surelease can be considered as safe due to this precedence of use [96].

Ethyl cellulose is blended with oleic acid and fractionated coconut oil. Afterwards the mixture is extruded and melted. It is directly emulsified under pressure in ammoniated water with a high shear mixer. Ammonium oleate is formed to stabilize and form the plasticized ethyl cellulose particles. The additional water is added to achieve the final solid content [97].

Surelease is delivered as a stable aqueous dispersion. In the dispersion are solid nano-sized ethylcellulose spheres which are stabilized by oleic acid (Figure 25). Oleic acid is deprotonated due to the presence of ammonia. During the coating process the ammonia is evaporated and becomes protonated again. Therefore, the particles loss their charge and can adhere to each other (Figure 26). When more water is evaporated at a temperature which is higher than the minimum film forming temperature coalescence of the film will happen (Figure 27).
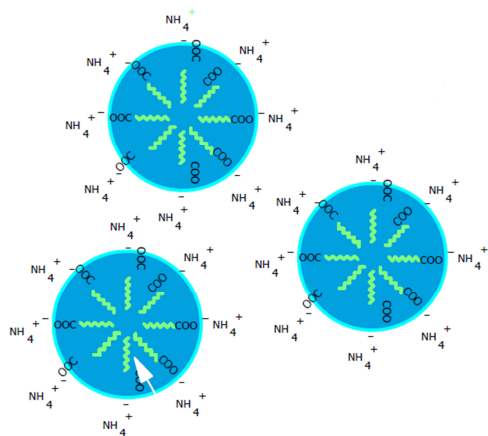
Figure 25: Surelease in dispersion [98]   **Figure 26: After Evaporation [98]**   **Figure 27: Coalescence of film [98]**
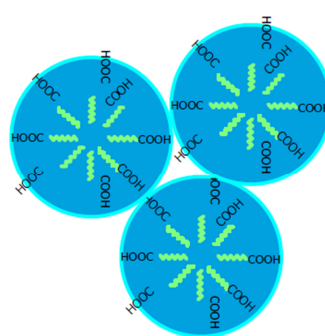
5. Methods

5.1.   Manufacturing

5.1.1.   Preparation of the powder mixture

All excipients of the internal phase were weighed on a lab balance and mixed with a Turbula T2C (Willy A. Bachofen, Switzerland) for 5 minutes at 32 rpm. Subsequently the mixture was sieved with a 900 µm screen and mixed again for 5 minutes. The external phase was dispensed and sieved with a 500 µm screen, added to the powder mixture and mixed for 2 minutes.

5.1.2.   Compression

The compression of the powder blend was performed on a Korsch XL-100 (Korsch AG, Germany) rotary tablet press. The tablet press was equipped with four sets of 2.5 mm 24 multi-tip punches (Notter GmbH, Germany). The tableting speed and the speed of the rotary feeder were set to 20 rpm. The dosing and compression depths were adjusted so that the desired weight and an average minitablet hardness of 30 N was reached.

5.1.3.   Preparation of the coating suspensions

The coating suspensions were prepared according to the suppliers recommendations.

Eudragit E PO®:

The necessary amount of Eudragit E PO®, Stearic acid and SLS was weighed on a lab balance. Then stearic acid and the SLS were added to a previous tared beaker with a part of the water while stirring. Afterwards the Eudragit E PO was added and was stirred for 1 - 1.5 h until it turned slightly yellowish. Talc and iron oxide were homogenized separately using an Ultra Turrax Polytron (PT10-5GT, Kinematica, Switzerland) for 10 min at 6000 rpm. Subsequently the pigment suspension was poured into the polymer solution while stirring. The missing amount of water was adjusted and passed through a 0.5 mm sieve to prevent blocking of the spray nozzle.

Kollicoat® Smartseal 30D:

The pigment and the talc were added to water and homogenized for 10 minutes at 6000 rpm using an Ultra Turrax Polytron (PT10-5GT, Kinematica, Switzerland) Subsequently

triethylcitrate and Kollicoat Smartseal were added and stirred for 2 h. Then the coating suspension was passed through a 300 μm sieve and flushed with the missing amount of water.

Surelease®:

Firstly the pore former suspension was prepared by adding Opadry II to deionized water. After 45 min of stirring with a Eurostar power b (IKA Werke GmbH & Co. KG, Germany), Surelease was added in the required ratio. Water and iron oxide were homogenized separately by an Ultra Turrax Polytron (PT10-5GT, Kinematica, Switzerland) for 10 min at 6000 rpm and add to the polymer suspension. Then the suspension was additionally stirred for 15 min.

5.1.4. Fluidized bed coating (Wurster coating)

For the fluidized bed coating of the minitablets the Mini-Glatt (Glatt GmbH Process Technology, Germany) equipped with the Wurster container was used (Figure 28). The Wurster tube has a diameter of 35 mm and was mounted having a distance of 14mm to the bottom plate (Figure 30). The whole fluidized bed coater was placed in a restricted area barrier system (RABS) and the auxiliary equipment was located outside. The coating suspension was placed on a balance and continuously stirred with a laboratory mixer Eurostar Power B (IKA®-Werke GmbH & CO. KG, Germany) (Figure 29). The coating suspension was pumped with a peristaltic pump (Flocon 1003, Flocon Products Inc., USA) through a 1.6 mm silicon tube to the spray nozzle. The spray nozzle is a two way nozzle from Schlick (Düsen-Schlick GmbH, Germany) having an orifice of 0.5 mm and is mounted on the bottom plate (Figure 31). The fluidized bed coater is equipped with two online temperature sensors to measure the product and the exhaust air temperature and an exhaust air humidity sensor. For granulation processes a 5 μm cartridge filter is installed, due to fast blocking of the filters during coating later a 500 μm filter mesh was then mounted for the coating experiments (Figure 32).

Figure 28: Mini-Glatt (Glatt GmbH Process Technolgy, Germany)

Figure 29: Experimental setup Fluidized bed coating Mini-Glatt

Figure 30: Wurster tube
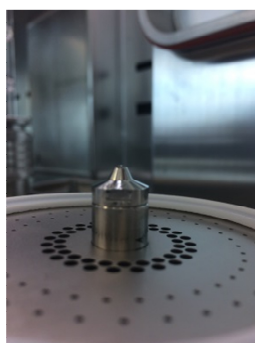
Figure 31: Spray nozzle (Düsen Schlick GmbH, Germany)

Figure 32: 500µm filter mesh

5.1.4.1.   Coating process Wurster

Before starting a coating process, the fluidized bed coater was preheated for 15 min. Then 300 g of minitablets were loaded into the Wurster container and the distance between the top of the Wurster tube and the minitablet bed was measured. Subsequently the inlet air volume was set to 89 m³/h and the atomization pressure to 0.25 bar, so that nozzle blockage was prevented. While heating, the tubing was filled with the coating suspension and the lab balance was set to zero to determine the accurate amount of sprayed suspension. When the desired product temperature was reached, the inlet air volume was increased to 99 m³/h and the atomization spray pressure was set to 1.25 bar. Then the peristaltic pump was turned on. The inlet air temperature was adjusted to ensure coating at a constant product temperature. During the coating process the process parameters were as follows (Table 9):

Table 9: Process parameter Wurster coating

Process parameters	Unit	E PO®	Smartseal 30D®	Surelease®
Inlet air temperature	°C	37-45	40-50	57-65
Product temperature	°C	28-29	27-29	42-43
Exhaust air temperature	°C	26-29	26-29	39-43
Exhaust air humidity	%rH	10.0-17.0	25-27	5.5-13.0
Air volume	bar	0.35	0.35	0.35
Air volume	m3/h	99	99	99
Atomizing air pressure	bar	1.25	1.25	1.25
Spray rate	g/min	2.0-2.5	2.0-4.0	1.0-3.0

When either the spraying time was complete or the full amount of coating suspension was applied, the peristaltic pump was turned off and inlet air volume and the atomization pressure were decreased to the previous values to reduce the mechanical stress. The inlet temperature was kept constant for further 10 min to ensure that film formation was complete. Afterwards the coated minitablets were discharged.

5.1.5.   Drum coating

The drum coating was performed on a GMPC1 (Glatt GmbH Process Technology, Germany) and was equipped with the 1.6 l perforated drum (Figure 33). The baffles were removed to integrate the tailor-made inlet bag. The perforation of the drum was covered with a 700µm polyamide mesh (Figure 34). The coating suspension was placed on a balance and continuously stirred with a laboratory mixer RzR2041 (Heidolph Instruments GmbH & Co.KG 2016). The coating suspension was pumped with a peristaltic pump (Sci 323, Watson-Marlow Ltd.) through a 1.6mm silicon tube to the spray nozzle. The spray nozzle is a two way nozzle from Schlick (Düsen-Schlick GmbH, Germany) having an orifice of 0.8 m (Figure 35). The product temperature is measured with an infrared pistol (830-T2, Testo AG, Switzerland,).
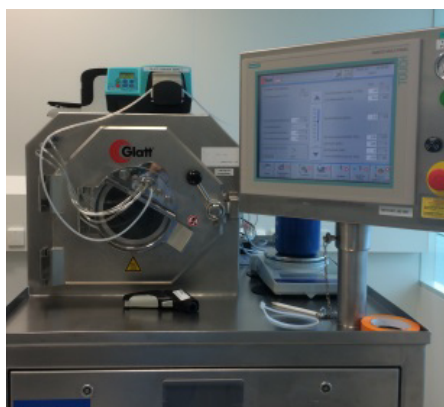
Figure 33: GMPC-1 (Glatt GmbH Process Technology, Germany)
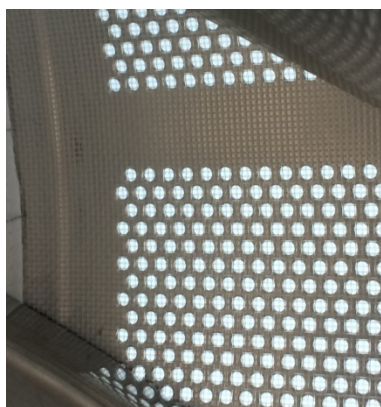
Figure 34: 700µm polyamid mesh

Figure 35: Spray nozzle (Düsen Schick GmbH, Germany)

5.1.5.1.   Coating process Drum

First the drum coater was preheated for 30 min. Then the minitablets were loaded and the distance between the spray nozzle and the minitablet bed was measured. During the heat up of the minitablets the drum speed was set to 5 rpm until the product temperature was reached. The drum speed was then increased to 10 rpm. The spray rate, the air volume and air temperature was adjusted so that the required product temperature was reached. The process parameters are shown in Table 10. Samples were taken periodically to measure the LOD. When the full amount of coating suspension was applied the peristaltic pump was turned off and the drum speed was decreased again to 5 rpm.

Table 10: Process parameter Drum coating

Process parameters	Unit	Para2.3.VI	CET1.2.XIII - XV
Polymer	Type	Eudragit E PO®	Surelease® (80%)
Batch size	g	1000	700
Distance Nozzle Tablet bed	cm	11.5	12
Nozzle bore	mm	0.8	0.8
Drum speed	rpm	10-12	10-12
Inlet air temperature	°C	37 - 50	54 - 64
Exhaust air temperature	°C	32 - 39	42 - 45
Exhaust air humidity	%rH	31 - 39	23 - 26
Air volume	m^3/h	60	70 - 80
Atomizing air pressure	bar	0.8	0.8
Pattern air pressure	bar	0.7	0.7 – 0.9
Spray rate	g/min	2.0 - 4.0	1.45 – 5.3
Spray time	min	432	70 - 148

Using a thermodynamic approach for scaling and process transfers

One approach for scaling up a coating process is to keep the thermodynamic conditions constant. That means the same amount of energy should be available to evaporate the sprayed coating liquid. In practice the product temperature and the relative humidity should be kept equal. The influencing parameters are the inlet air volume, the coating liquid amount and the heat losses (Figure 36).

Am Ende modeled the following equation based upon the first law of thermodynamics and the conservation of mass and included both in an energy and mass balance [99]. This modeling approach assumes a well-mixed system and can be used for closed non isolated systems. It includes a Heat Loss Factor (HLF) which is specific for an apparatus and can be determined by at least two trials. This value can be calculated using the published equations (1) and (2).

By varying the process parameters, e.g. inlet air volume, inlet air temperature and spray rate, the coating process can be modelled to reach the same exhaust temperature and exhaust relative humidity.
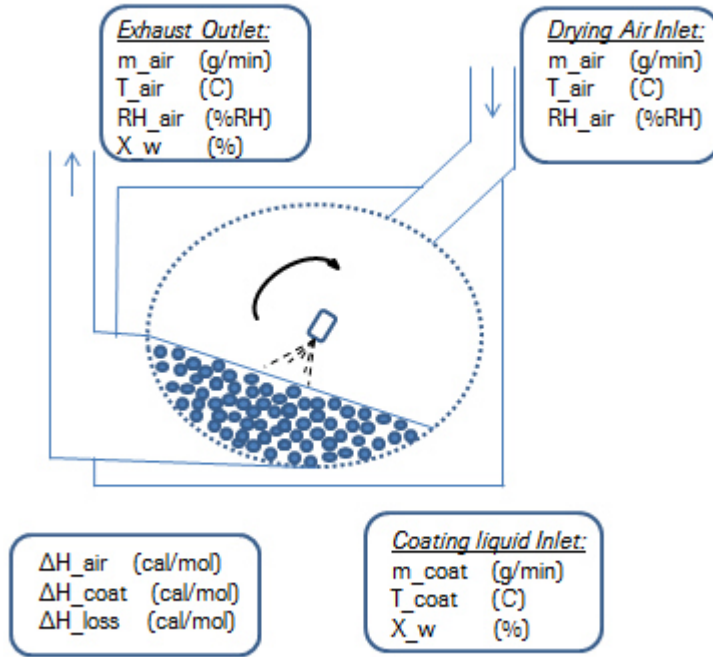
Figure 36: Thermodynamic model, Parameter

$$T_{air,out} = \frac{m_{air,in}c_{p,air}T_{air,in} + x_w m_{coat}c_{p,w}T_{coat} - x_w m_{coat}\Delta H_{vap,w} + HLF * T_{RT}}{m_{air,in}c_{p,air} + x_w m_{coat}c_{p,w} + HLF} \tag{1}$$

$$RH = \frac{8.314472 * x_w m_{coat}T_{air,out}}{18 * P_{sat} * Q_{air,out}} \tag{2}$$

m   mass (air,in =inlet air; coat= coating) [kg/s]]

c_p specific heat capacity (w=water; air= air) [KJ/Kg*K]

x_w water fraction [%]

T   temperature (air,in = inlet air, RT=room temperature, coat=coating liquid) [K]

HLF   heat loss factor [KJ/s*K]

$Q_{air,out}$ energy of the exhausted air [J/s]

P_{sat} saturation pressure [Pa]

5.2.   API characterization

5.2.1.   Particle size distribution (PSD)

At first a microscopic picture of the particles was made to obtain an impression of the PSD for the development of the laser diffraction methode using the microscope Imager Z1 (Zeiss, Germany). Therefore approximately 20 mg of the API was placed into a test tube and 2 ml of paraffin oil was added. The suspension was dispersed using a Vortex Genie (Scientific Industries Inc., USA) at level 8 for 30 s. A droplet was placed on a (microscope) slide and a representative picture was made with the microscope.

The particle size distribution was measured with the laser diffraction spectrometer Mastersizer 3000 (Malvern Instruments LtD. UK). The Frauenhofer approach was used to calculate the particle sizeses between 0.02 and 3000 µm. The powder was fed and dispersed by the AeroS dispersion unit. The laser diffraction method was developed by conducting three measurements using a pressure gradient between 0 and 1 bar. The following parameters have been chosen:

Table 11: Parameter PSD measurement with Mastersizer 3000

Parameter	Value
Sample mass [g]	0.5 ± 0.05
Hopper gap [mm]	2
Feed rate [%]	20
Venturi [°]	180
Laser obscuration [%]	0.1 – 6

Based on the resulting PSD a suitable pressure was chosen having a compromise between deagglomeration and no damage of particles.

5.2.2.   Mechanical properties

The API was stored for at least 24 h in the desiccator. 2 g of the API was weighed and placed in the punch. Using different compression forces, compacts with different solid fractions were produced. After the storage of the compacts for at least 12 h in the desiccator to enable the elastic recovery, the mass and the volume can be measured to calculate the solid fraction.

5.2.2.1.   Pendulum Impact Device
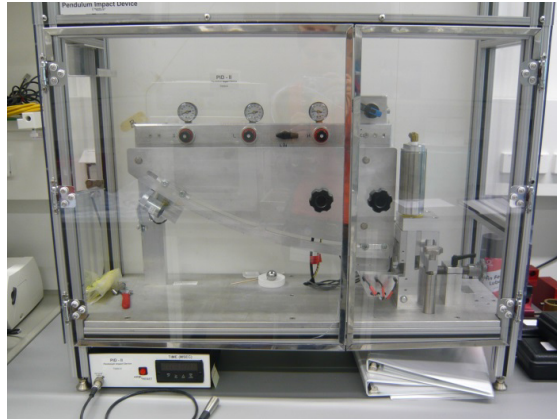
Figure 37: Indenter   **Figure 38: Pendulum Impact Device (PID)**

The Pendulum Impact Device was used to characterize the compacts (Figure 37 and Figure 38). The spherical indenter has a diameter of 2.54 cm and a mass of 66.48 g. The length of the pendulum is 93.2 cm and it is released from an angle of 30°. The compacts were bombarded with a metal ball and afterwards the dimension of dent is measured using a 3D microscope. From the dimensions of the dent the dynamic hardness H_d, the strain index SI and the Module of elasticity E' was calculated according the following equations:

Dynamic hardness

The dynamic hardness H_d is a measure of a materials resistance to high speed impact. By evaluating the deformation the plasticity can be calculated. Dynamic hardness is calculated according Equation (3) using the mass of indenter (m), gravitational acceleration constant (g), radius of indenter (r), radius of the dent (a), initial height of indenter (h_i) and rebound height of indenter (h_r) [100], [101], [102].

$$H_d = \frac{4 \cdot m \cdot g \cdot r \cdot h_r}{\pi \cdot a^4} \cdot \left(\frac{h_i}{h_r} - \frac{3}{8}\right) \tag{3}$$

Reduced modulus of elasticity

The reduced modulus of elasticity is a measure of the immediate recovery of the deformation after the applied stress is removed. A high reduced modulus of elasticity reflects greater stiffness and less dimensional change [100] and is calculated according to the following Equation (4).

$$E' = \frac{4 \cdot m \cdot g \cdot r^2 \cdot h}{\pi \cdot a^5} \cdot \left(\frac{h_i}{h_r} - \frac{3}{8}\right) \tag{4}$$

Young's modulus of elasticity

Young's modulus of elasticity is an index for the stiffness of an elastic material. It is the ratio of the applied stress (σ) to the strain ($\varepsilon = \Delta l / l$) [103], [104]. (Equation (5))

$$E_f = \frac{\sigma}{\varepsilon} \tag{5}$$

Strain index

The strain index is an indication of the relative strain during the decompression, when plastic deformation occurred. Very elastic materials have a high strain index. It is calculated by dividing the dynamic hardness H_d with the reduced elastic modulus (E') [102] (Equation (6)).

$$SI = \frac{H_d}{E'} \tag{6}$$

5.2.2.2. Texture Analyzer

To measure the quasi static properties of the compacts, the Texture Analyser (TA.HD.plus; Stable Micro Systems, UK) was used (Figure 39). It was a spherical ball having the same diameter than the PID attached. The compacts were compressed with a designated force for 10 minutes. Then the dent diameter can be measured and the quasi static hardness H_s and the viscoelastic index VI can be calculated according the following equation:
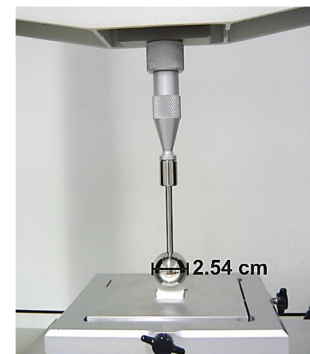

Figure 39: Textrue Analyser, spherical ball attachment

Quasi static hardness

The quasi static hardness H_s determines the relative hardness of a material. It is calculated using the applied force (F) and the area of the dent (A) (see Equation (7))

$$H_s = \frac{F}{A} \tag{7}$$

Viscoelastic Index

The viscoelastic index (VI) is a ratio of the irreversible (viscous) and reversible (elastic) deformation. A low index (1-10) implies that the hardness is independent of the stress duration and a high index (<30), that the hardness is dependent on the duration of the applied stress. For pharmaceutical applications a high viscoelastic index is undesirable because the tablet performance would depend on the speed of the tablet press. It is calculated by dividing the dynamic hardness (H_d) by the quasi static hardness (H_s), as shown in Equation (8).

$$VI = \frac{H_d}{H_s} \tag{8}$$

The texture analyser can also be used to define the tensile strength, Brittle Fracture Index and the Bonding Index. For that measurement a rectangular attachment was installed in the texture analyser and the force required to break the compact is measured. This measurement was done as well with compacts having a central hole to calculate the compromised tensile strength.
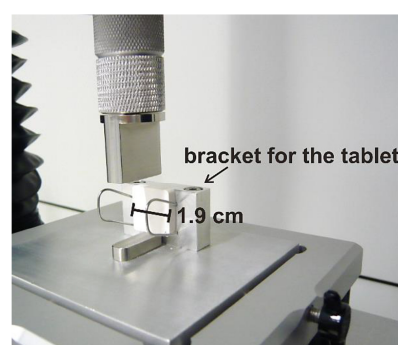
Figure 40: Texture Analyser, rectangular attachment

Tensile strength

Tensile strength is the greatest longitudinal stress that the material can withstand without breaking apart. The compromised tensile strength σ_{To} is the tensile strength measured with a compact having a centered hole. This centered hole is the predetermined breaking point. Both tensile strength (σ_T) are calculated using the compact pressure (σ_C), see Equation (9).

$$\sigma_T = 0.16 \cdot \sigma_c \tag{9}$$

Brittle fracture index

The brittle fracture index (BFI) is an index for the brittleness of a material. It is calculated with the tensile strength (σ_T) and the compromised tensile strength (σ_{To}) computed from a compact with a hole (see Equation (10)). If a material can release stress the compromised tensile strength can approach the tensile strength. A BFI of 1 indicates a very brittle material and a value of 0 for very non-brittle materials. Materials having a BFI lower than 0.2 have a tendency to cap and laminate during compression [105].

$$BFI = 0.5 \cdot \left(\frac{\sigma_T}{\sigma_{To}} - 1 \right) \tag{10}$$

Bonding index

The bonding index (BI) gives an insight into of the material strength after decompression and recovery. It indicates the extent of particle bondings after decompression and characterizes if the material remains intact after the compression. When tablets are produced from material with a low BI (BI<0.005), they might be fragile after compression. In comparison with materials having a high BI (0.005 < BI < 0.04) it is likely that strong tablets will be formed due to a high level of bondings [106] [100]. Con the contrary, a high BI could also indicate sticking and picking tendency of the tableting process [105]. The BI is calculated by dividing the tensile strength (σ_T) by the dynamic hardness (H_d) (Equation (11))

$$BI = \frac{\sigma_T}{H_d}$$

(11)

5.3. Determination of the Bitterness Threshold

5.3.1. E – Tongue

Taste-sensing-system Insent TS5000-Z (Intelligent Sensor Technology, Inc., Atsugi-chi, Japan) equipped with Ag/AgCl reference electron and membrane electrodes in following types were used:

- Umami Sensor AAE
- Saltiness sensor CT0
- Sourness sensor CA0
- Bitterness sensor C00 (for acidic bitter materials)
- Astingency sensor AE1
- Bitterness sensor BT0 (for bitter hydrochloride salts)
- Bitterness sensor AN0 (for basic bitter materials)
- Sweetness sensor GL0 (prototype)

Each sample was measured five times, where the first two were not used for any calculation. First the probe was dipped for each between 90-120 s in three different wash solutions. Subsequently a sensor check was performed in a conditioning solution. Then the sample was measured for 30 s. The responses of the sensor were measured as electrical potentials [mV] due to the adsorption of the molecules to the membrane sensors. Afterwards the probe was dipped for each 3 s in two wash solutions. The sensor responses were analyzed with Microsoft Excel 2007.

5.3.2.   In vivo human taste panel

A single center, blind and randomized human taste panel with untrained panelists was performed. The participants were not allowed to smoke or eat before the taste panel.

Determination of the bitterness threshold

Seven aqueous cetirizine dihydrochloride solutions having the concentration 0.5, 1, 10, 50, 100, 200 µg/ml were prepared. The panelist took 5 ml of the solution for 10 s in the mouth. Afterwards the solution was spit out and the mouth was rinsed with water at least three times. Subsequently the panelist was asked to evaluate the taste according the following bitterness scores (Table 12). The evaluation sheet is shown in the Appendix XIII. The results were analyzed using the software JMP (Version 12,SAS Institute, Cary, NC, USA).

Table 12: Bitterness scores

Bitterness score	Classification	Description
1	No taste	„I cannot detect a difference to water"
2	Perception	"I detect some difference but was not able to be specific about taste"
3	Slightly bitter	"I detect a bitter taste, but I is fairly okay"
4	Moderate bitter	"I detect a bitter taste and it is unpleasant"
5	Strongly bitter	"It is awful"

Evaluation of the taste masking efficiency

For the evaluation of the taste masking efficiency the panelist was asked to put three coated cetirizine dihydrochloride minitablets, which is equal to one pediatric dose, on the tongue and not move the tongue or mouth during the test. The time was measured until the panelist first perceives a taste. Then the minitablets were spat out. The maximum duration of the test is 5 minutes. The panelist was asked to rinse the mouth with water for at least three times.

5.4.   Powder mixture and Minitablet Characterization

5.4.1.   Bulk- and tapped density

The bulk (ρ_B) and tapped density (ρ_T) were determined according Ph.Eur. 8.2.. On a lab balance 100 g of the powder mixture was weighed and transferred into a 250 ml graduated cylinder. Then the bulk volume was recorded. On the tapping volumeter STAV2003 (J. Engelsmann AG, Germany) the necessary amount of taps were conducted and the tapped volume was recorded.

The Hausner ratio (H) gives an indication of the flow properties [107] and is calculated by the following formula (12) as described in USP <616> (Bulk Density and Tapped Densty of Powders).

$$H = \frac{\rho_T}{\rho_B} = \frac{V_B}{V_T}$$
(12)

The Carr's Index C is calculated from the bulk volume V_B and the tapped volume V_T [108] and is a measure of the compressibility (Equation (13)). The lower the percentage, the lower is potentially the weight variability of the tablets due to the improved flowability of the blend.

$$C = \frac{(V_B - V_T)}{V_B} \cdot 100\%$$
(13)

For a directly compressible powder mixture, a Hausner factor lower than 1.3 and a Carr's Index lower than 30 % are desirable.

5.4.2.   Flowability

The flowability was measured using the ring shear tester RST XS (Schulze, Germany). The ring shear cell was filled with the powder mixture and the excess powder was scraped off so that it results in an even surface. Then the filled shear cell was weighed and placed on the ring shear tester. Afterwards the lid, the loading rod and tie rods are assembled. The weight of the filled shear cell is typed into the software so that it can calculate the bulk density of the sample. First, normal force is applied and then the shearing takes place until the shear stress does not increase any further and the powder is sheared again under reduced normal stress. This measurement cycle is repeated 4 times and the software determines the yield locus and the ff_c value is calculated by the division of the consolidation stress σ_1 by the unconfined yield

strength σ_c. The characterization of the flow behavior by the ff_c (flow function coefficient) values to the according Jenike [109] is shown in Figure 41.
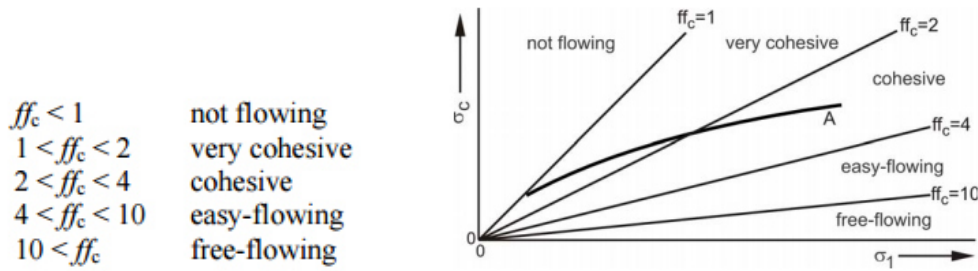

$$ff_c < 1 \quad\quad \text{not flowing}$$
$$1 < ff_c < 2 \quad \text{very cohesive}$$
$$2 < ff_c < 4 \quad \text{cohesive}$$
$$4 < ff_c < 10 \quad \text{easy-flowing}$$
$$10 < ff_c \quad\quad \text{free-flowing}$$

Figure 41: Characterization of the flowability by the ffc value

5.4.3.   Pycnometric density of the powder blend

According Ph.Eur. 2.2.42 the pycnometric density is the volume occupied by a known mass of powder which is equivalent to the volume of gas displaced by the powder using a gas displacement pycnometer [110]. This volume includes the volume of the open pores which are accessible to the gas, but not the sealed pores. The pycnometric density was measured using a helium pycnometer AccuPyc 1330. The weight of the sample was 3.5±0.1 mg and all measurements were conducted twice.

The pycnometer purges the sample container five times per measurement with helium. The gas occupies all voids except of the sealed voids and the voids which are inaccessible for helium. The helium volume is measured which is necessary to reach the pressure equilibrium. Consequently the gas volume enters into the reference container and the resulting pressure is measured. From the given sample and reference container volume V_c resp. V_r and the resulting pressures the volume of the sample can be calculated via Equation (14), where P_1 is the pressure in the sample chamber and P_2 is the pressure in the reference chamber is. By having the sample weight, the solid fraction and the gas pycnometric density can be calculated.
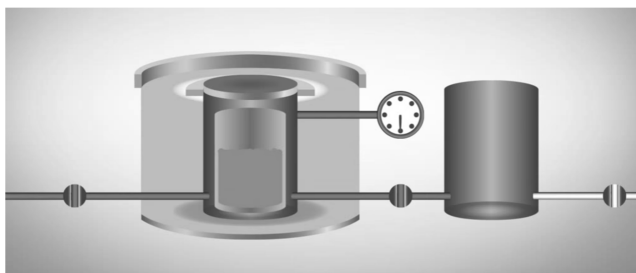

$$V_s = V_c + \frac{V_r}{1 - \frac{P_1}{P_2}} \tag{14}$$

Figure 42: Gas pycnometric density measurement [111]

5.4.4.   Tablet height

The heights of the minitablets were determined using a digital caliper TESA ShopCal 150 mm or by the Multitest 50 (Dr. Schleuniger, Germany). Ten minitablets were examined and the mean was calculated.

5.4.5.   Porosity and solid fraction

The porosity of the tablet is the ratio of the volume of the voids to the volume of the tablet. It can be calculated according the following Equations (15) and (16)

$$Porosity \ [\quad] = \frac{V_{Void}}{V_{Tablet}} = \frac{V_{Tablet} - {m_{Tablet}}/{\rho_{Powder}}}{V_{Tablet}} \tag{15}$$

$$V_{Tablet}[mm^3] = r^2 \cdot \pi \cdot H_{Band} + 2 \cdot V_{cap} \tag{16}$$

The solid fraction of a tablet is the volume of solids divided by the volume of the tablet. It can be calculated using the porosity according the following Equation (17). Due to prior knowledge the solid fraction of a tablet should have a value in the range of 0.8 to 0.9.

$$SF \ [\quad] = 1 - Porosity = \frac{{m_{Tablet}}/{\rho_{Powder}}}{V_{Tablet}} \tag{17}$$

5.4.6.   Tablet hardness and tensile strength

The diametrical crushing strength was determined using the Sotax hardness tester HT1 (Sotax AG, Switzerland). The crushing strength in this work is used as an indication for the tablet hardness. For each measurement 10 tablets were tested and the mean was calculated.
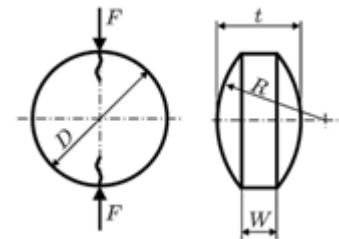
Figure 43: Tablet dimensions

The breaking force depends on the fractured surface. Therefore tensile strength is more suitable for comparison reasons. According to the author [112] the tensile strength can be empirically calculated from the diameter D, band height W, the total height t of the minitablet and the breaking force according the following equation (18).

$$\sigma_T = \frac{10 \cdot F}{\pi D^2 \left[\left(\frac{t}{D}\right) - 0.126 \left(\frac{t}{W}\right) + 3.15 \left(\frac{W}{D}\right) + 0.01 \right]} \tag{18}$$

5.4.7. Disintegration

The disintegration test was performed in a Sotax DT3 (Sotax AG, Switzerland). The vessel was filled with 900 ml deionized water and was heated up to 37±0.5 °C. The amount of minitablets for one dose was used. The disintegration test was performed according Ph.Eur. 2.9.1. The test was performed with six dose units.

5.5. Characterization of the taste masked Minitablets

5.5.1. Loss on drying (LOD)

To determine the LOD value, minitablets were grinded with universal laboratory mill M20 (IKA Werke GmbH & Co. KG, Germany). Subsequently 5±0.5 g of the powder was measured in the Halogen Moisture Analyzer HR83-P (Mettler Toledo AG, Switzerland) at 90 °C. The measurement is complete when the weight of the sample is decreasing less than 2 mg within 30 s.

5.5.2. Weight gain

After the coating process, 100 minitablets were weighed. The Weight Gain (WG) was calculated having the LOD values for the uncoated and coated minitablets according the following equation (19). Where $m_{i,w}$ represents the initial average mass of the uncoated and $m_{f,w}$ the final average mass of the coated minitablets. The index d represents the dry masses of the minitablet which are corrected with the respective LOD values.

$$WG\ [\%]\ =\frac{m_{i,d}}{m_{f,d}}\cdot 100\% = \frac{m_{i,w}\cdot \left(\frac{100-LOD}{100}\right)}{m_{f,w}\cdot \left(\frac{100-LOD}{100}\right)}\cdot 100\% \tag{19}$$

5.5.3. Coating Uniformity

The Coating Uniformity (CU) is the variation in weight gain of the individual coated minitablets of one coating experiment. The CU is calculated by the following equation (20) where $m_{f,d,j}$ and $m_{i,d}$ are the initial and final dry masses and WG is the average weight gain of the minitablets.

$$CU\ [mg] = \sqrt{\sum_{j=1}^{n=100}\frac{1}{n-1}(m_{f,d,j}-m_{i,d}-WG)^2} \tag{20}$$

5.5.4.   Coating Process Efficiency

The Coating Process Efficiency (CPE) is the yield of the coating process. It is the ratio between the actual amount applied to the minitablets to the theoretical applied amount. Coating losses of up to 10 % is a typical value in industry. If the coating loss is larger than 10%, it is an indication that either over wetting or spray drying occured. When the process is to wet the coating material could be transferred from the minitablets to the equipment wall. On the other hand when the process is too dry, the coating droplets dry before they reach the minitablets and are sought out by the exhausted air. The CPE is calculated by the following equation (21), where WG_{real} is the actual measured weight gain and WG_{theor} is the theoretical weight gain.

$$CPE \ [\%] = \frac{WG_{real}}{WG_{theor}} \cdot 100\% \qquad\qquad\qquad \textbf{(21)}$$

5.5.5.   Coating film thickness and morphology

5.5.5.1.   Scanning Electron Microscopy

Scanning Electron Microscopy (SEM) uses a focused electron beam hitting the sample surface. The electrons from the beam can extract electrons from the sample surface resp. from the inner shell of the atoms on the surface. These electrons are called secondary electrons and are detected by the secondary electron detector which is located at a 45° angle to the electron beam. Due to that geometrical arrangement shadowing effects are generated to enable the high topographic resolution.

The SEM images were acquired using a ∑igma VP (Zeiss, Oberkochen, Germany) system. The full acquisition of the image takes 444.6 s having a line averaging of 17 scans per frame to reduce the noise. The sample was prepared by gold sputtering to allow a good conductivity. The gold sputtering was conducted on a Cressington 108 Auto sputter having a current intensity of 30 mA under a flow of Argon at 0.1 bar. Each sample was exposed to 120 s of sputtering.

5.5.5.2.   X-Ray Micro-Computed Topography (μCT)

For the X-Ray μCT imaging the sample is placed between the X-ray source and the detector. Due to different densities and elementary composition, the material shields more or less X–rays, which results in different X-ray extinction coefficients. The X-ray μCT acquires a series of X-ray shadow images of the sample at different angles. From those 2D images, the

computer calculates via an algorithm virtual cuts cross sections and 3D reconstructions. The internal and external structure of the sample can be investigated without damage the sample.

The minitablet was fixed with modelling clay on the sample holder and placed in the apparatus. The acquisition of the shadow images was performed on the Skyscan 1172 , S/N 08E01109, (Bruker microCT, Kontich, Be) with a pixel resolution of ca. 2 µm, rotation step of 0.380 deg over 180 deg, with an integration time of 400 ms with the X-ray source tuned to 60 kV, 167 µA. The processing of the images was executed with the NRecon software. The 2-dimensional images were displayed with the DataViewer 1.4 software and the 3-dimensional images with the CTVox 2.4 software.

5.6.   *Dissolution*

The dissolution was measured in simulated gastric fluid (SGF) with a pH of 1.6. The SGF is produced by dissolving sodium chloride in deionized water to obtain a concentration of 34.2 mM. The pH was adjusted to a pH of 1.6 by using 1 M HCl. The criterion for immediate release of solid oral dosage forms for pediatric population was investigated by Batchelor [113]. The result of the survey was that 85 % of the drug should be released within 15 minutes using a dissolution volume between 250 and 500 ml (Children between 2-5 years) Therefore the dose to volume ratio set to a nominal concentration of 0.125 mg/ml and 0.0417 mg/ml for acetaminophen and cetirizine dihydrochloride. One minitablet was used and the dissolution volume was scaled down to the dose to volume ratio. For cetirizine dihydrochloride a volume of 166 ml would be needed as a dissolution volume to apply the same dose to volume ratio. Hence the solubility of cetirizine dihydrochloride is larger than 350 mg/ml, the maximal volume of the µDiss Profiler™ is 20 ml used while the sink condition kept (solubility 8 fold larger than nominal concentration).

The drug release kinetic was measured in a miniaturized dissolution apparatus µDiss Profiler™ (PION Inc., USA) with attached online UV vis probes. The UV vis probes were equipped with tips having 1 mm measuring length resp. 10 mm for acetaminophen and for cetirizine dihydrochloride and measured simultaneously the drug concentration in the vessel. The hydrodynamic kinetic was imitated with a cross-shaped magnetic stirrer at a rotational speed of 50 rpm. The data was collected and processed by AuPro Software (Version 5.1.6.0, PION Inc., USA). The dissolution experiments were performed in triplicate (n=3)

5.7.   In vitro Taste Assessment

To evaluate the efficiency of the taste masking the initial drug release in artificial saliva was tested. The mean stimulated salivary flow of healthy children (mean age 7.94 years) is between 0.82-0.93 ml/min. For a dissolution duration of 5 minutes, 5 ml of artificial saliva would be appropriate as a dissolution volume [114]. The following composition of artificial saliva was used [115] (Table 13)

Table 13: Composition artificial saliva [115]

Component	Composition	Concentration [g/l]
Potassium dihdydrogenphosphate	25 mM	3.402
Sodium chloride	6.88 mM	0.402
Calcium chloride dihydrate	1.42 mM	0.209
Potassiom chloride	9.55 mM	0.712
Sodium azide	0.08 mM	0.005
porcine gastric mucin	1.80 g/l	1.800
alpha amylase	1.00 g/l	1.000
Xanthan gum 200 mesh	0.75 g/l	0.750
pH	*7.1*	*7.1*

The components of the artificial saliva were mixed with a magnetic stirrer and the pH was adjusted to 7.1 using 1 M KOH solution. According to the review article of Kaye [116], the pH in the oral cavity of children between 2 and 5 years is approx. 7.1. The dissolution was conducted in a 7 ml screw cap vial, which is rotated by an orbital shaker (10 rpm) in a heating chamber (37±0.5 °C). The number of minitablets equal to one dose were counted and weighed before the dissolution experiment. After 1, 3 and 5 minutes a 200 µL sample was removed and centrifuged at 13'000 rpm for 60 s. Supernatant was diluted with acetonitrile to precipitate the proteins and centrifuged again (13'000 rpm, 20 s). Then a sample was withdrawn and diluted with the mobile phase. The released drug concentration was measured with a HPLC. The parameters used are shown in the table below (Table 14). The resulting data were processed using Empower[®]3 Software (Waters Corporation, Milford, USA). The in vitro taste assessment experiments were conducted in triplicate (n=3).

Table 14: Parameter HPLC Analysis

Method	Acetaminophen	Cetirizine Dihydrochloride
HPLC	Separation Module 2795, Photodiode Array Detector 2996; Waters Corporation, Milford, USA	Separation Module 2690, Dual λ Absorbance Detector 2487; Waters Corporation, Milford, USA
Mobile phase	0.01M KH_2PO_4:MeOH: ACN 84:4:12 (v/v), isocratic	$2.9*10^{-3}$ % Phosphoric acid: ACN 60:40(v/v), pH 1.85, isocratic
Rinsing solution	H_2O:ACN ; 1:1	H_2O:ACN ; 1:1 (v/v)
Column	Reverse phase C8 (XTerra® 4.6x50 mm, 3.5 µm, Waters Corporation, Milford, USA)	Reverse phase C18 (XBridge®; 4.6x75 mm, 2.5 µm, Waters Corporation, Milford, USA)
Injection Volume	10 µl	100 µl
Flow rate	1 ml/min	0.8 ml/min
Temperature	25 °C	25 °C
Wavelength	215 nm	230 nm

The taste masking was achieved when the drug release was zero or below the bitterness threshold. In the literature several bitterness thresholds of acetaminophen were reported. As acceptance criterion the concentration of 1080 µg/ml was used for acetaminophen [117]. The bitterness threshold of cetirizine had to be investigated.

5.8.   Excipient Incompatibility Study

The excipient compatibility was tested by an accelerated stability study. Physical mixtures of the Cetirizine (CET), CET:Polymer (1:1) and MT Formulation:Coating Formulation (1:1). The 1:1 Mixture of CET and the polymer should represent the worst case condition and the mixture of the minitablet formulation with the formulation of the coating should represent the composition of the interface. The compositions of the physical mixtures are shown in Table 15.

The components were weighed into a 100 ml screw cap glass container and mixed for 5 min in a Turbula shaker. The open glass container were stored in a climatic chamber for 4 weeks at 50 °C and 75 % rH.

The equivalent amount of 10 mg cetirizine was weighed into a 100 ml volumetric flask. Approximately 50 ml water was added into the volumetric flask and sonificated for 15 min to dissolve the API. Subsequently the volumetric flask was filled with water until the mark. If the powder mixture build a suspension, the volumetric flask was shaken and 100 µl was centrifuged for 60s at 13 000 rpm. Then 100 µl was removed and diluted with the mobile

phase as described in Table 14 (Mobile phase Cetirizine Dihydrochloride). The Cetirizine content of the samples was quantified using the HPLC method described in the method 5.7 in Table 14. The content measurement was performed in quintuplicate (n=5).

Table 15: Composition physical mixtures

No.	1	2	3	4	5
Desciption	CET	CET + EPO	CET + SMA	MT formulation + EPO formulation	MT formulation + SMA formulation
Cetirizin	10.0	5.0	5.0	0.25	0.25
FlowLac 100	-	-	-	2.95	2.95
Avicel PH 102	-	-	-	1.7	1.7
Aerosil	-	-	-	0.05	0.05
Magnesium Stearate	-	-	-	0.05	0.05
Eudragit E PO	-	5.0	-	2.85	-
Stearic acid	-	-	-	0.43	-
SLS	-	-	-	0.29	-
Colorant	-	-	-	0.01	0.05
Kollicoat Smartseal	-	-	5.0	-	3.85
TEC	-	-	-	-	0.18
Talc	-	-	-	1.43	0.93
Sum	10.0	10.0	10.0	10.0	10.0

5.9.   *Quality Risk Assessment (QRA)*

The potential factors were divided into properties of API, excipient properties and process parameters of the fluidized bed coating. The potential Critical Quality Attributes (pCQAs) were determined. The influence of the potential factor on each pCQA was evaluated by rating by scoring them between 1 and 3. The scores of severity and probability are defined as shown in Table 16. From the score the risk of the particular factor can be distinguished as shown in Table 17.

Table 16: Scores of severity and probability, QRA

Severity	3	*Robustness:* process not reliable and not acceptable, changes lead to process failures *Quality*: batch has to be destroyed/replaced; likely "out-of-specification"
	2	*Robustness*: batch-to-batch variation possible, process runs within narrow parameters, stricter process control required, changes to be carefully considered *Quality*: occasional failures likely, cosmetic defects
	1	*Robustness:* reliable, reproducible, consistent processability; process tolerates variability; changes have no effect *Quality:* product is always/likely within specification or acceptance Criteria
Probability	3	is expected based on experiences; frequently/ most likely to occur
	2	no experience so far (e.g. new technology); occasionally to occur
	1	is not expected based on experiences; never to occur

Table 17: Risk based on severity and probability

		Probability		
		low (1)	medium (2)	high (3)
Severity	high (3)	medium risk	high risk	high risk
	medium (2)	medium risk	medium risk	high risk
	low (1)	low risk	low risk	medium risk

6. Results and Discussion

6.1.   API Characterization

6.1.1.   Particle size distribution (PSD)

6.1.1.1.   Acetaminophen

The microscopic picture of acetaminophen shows irregularly formed crystals having mainly diameters of approximately 10 µm and 100 µm. This result was confirmed by the laser diffraction measurements. The hopper gap had to be increased to 3 mm and a pressure of 0 bar was chosen. The particle size distribution is displayed in Figure 45 and Table 18. The density distribution of one measurement shows a peak at 1100 µm (blue curve, Figure 45). This peak is caused by loose agglomerates and can be neglected because the mean peak is still similar to the other two measurements.
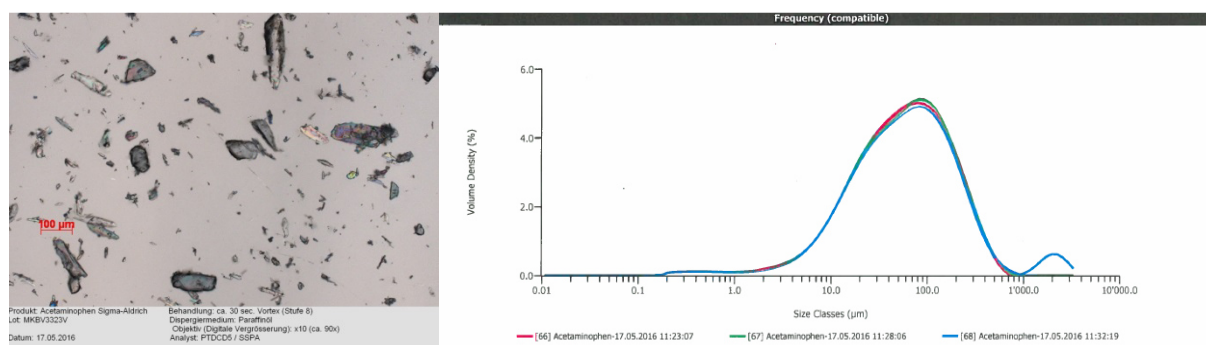

Figure 44: PSD Acetaminophen, Microscope

Figure 45: Density distribution Acetaminophen, Laser diffraction

	D_{10} [µm]	D_{50} [µm]	D_{90} [µm]
Mean	11.1	58.7	232
Standard deviation	0.186	1.61	21.9
Srel [%]	1.67	2.75	9.42

Table 18: PSD Acetaminophen, Laser diffraction

6.1.1.2.   Cetirizine Dihydrochloride

The microscopic picture of cetirizine dihydrochloride shows a few particles having a diameter of around 100 µm and a lot of very small particles (Figure 46). Some particles show needle-shape morphology.

During method development it was shown that at a pressure of 1 bar breakdown of bigger particles was observed, also indicated by a shift of the density curve to smaller particles (see Appendix V). Out of these findings a pressure of 0.5bar was chosen for regular measurements. The particle size distribution is displayed in Figure 47 and Table 19. The particle size distribution varies above a diameter of 500 µm as a result of undispersed loose agglomerates.

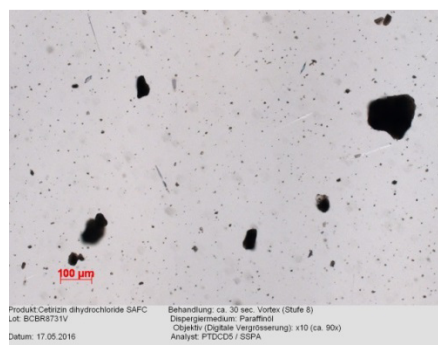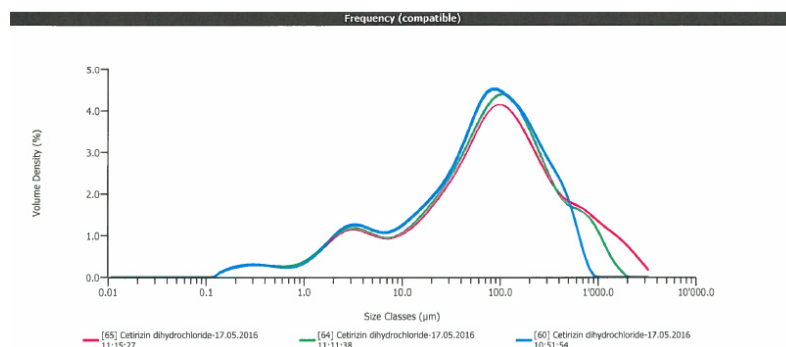**Figure 46: PSD Cetirizine Microscope**

Figure 47: Density distribution Cetirizine, Laser diffraction

	D$_{10}$ [µm]	D$_{50}$ [µm]	D$_{90}$ [µm]
Mean	3.29	76.3	487
Standard deviation	0.121	7.98	185
Srel [%]	3.69	10.5	37.9

Table 19: PSD Cetirizine, Laser diffraction

6.1.2.   Mechanical Properties

The compression of pure acetaminophen into compacts was difficult. With increased compaction pressure the compacts tend to cap and stick to the punches. Typical measurements are performed with compacts having a solid fraction of 0.85; however, due to the low compressibility of acetaminophen just a solid fraction between 0.79 and 0.81 could only be reached. For comparison the resulting values need to be extrapolated to a solid fraction of 0.85. These uncertainties led to errors. After the measurement with the PID for the calculation of the dynamic hardness all compacts had cracks. For the measurement of the quasi static hardness a force of only 20 N could be applied with the texture analyser so that compacts did not break. The resulting dent diameter was only 2.5 mm which is too small in regards to the accuracy and the resulting measuring error.

The preparation of the cetirizine compacts was also difficult. The compacts stuck to the punches and could not be removed without breakage. After layering the punches with magnesium stearate, compacts with a solid fraction between 0.67 and 0.71 could be produced. Pre-compression was necessary to manufacture those compacts. After the

measurement with the PID for the calculation of the dynamic hardness cracks were visible on the compacts. The quasi static hardness could be measured with a force of 200 N.

In the following Table 20 the mechanical property and the calculated tableting indices of acetaminophen and cetirizine are shown.

Table 20: Overview mechanical properties

Property	Limit value	Desired value	Acetaminophen			Cetirizine		
			Mean	Error [%]	Interpre-tation	Mean	Error [%]	Interpre-tation
True density [g/cm^3]			**1.297**			**1.3706**		
Mechanical Properties								
Solid Fraction SF		0.85	**0.85**		good	**0.85**		good
Compaction Pressure Cp [MPa]	20-40 100-150	40-100	**101.4**	3.9	marginal	**181.4**	2.2	poor
Tensile Strength σ_T [MPa]	0.5 -1	>1	**0.43**	4.1	poor	**6.76**	8.4	good
Dynamic Hardness H_d [MPa]	70-100 200-400	100-200	**19.69**	4.6	poor	**475.24**	6.1	poor
Quasi-static Indentation Hardness H_{qs} [MPa]			**5.3**	6.7		**116.1**	6.0	
Reduced Elastic Modulus E' [GPa]			**1.45**	5.3		**29.68**	8.3	
Compromised Tensile Strength σ_{To} [MPa]			**0.22**	6.0		**1.32**	9.7	
Tableting indices								
Brittle Fracture Index (BFI)	0.3-0.5	< 0.3	**0.478**	7.3	marginal	**2.054**	12.8	poor
Dynamic Bonding Index (BI$_w$)	0.005 -0.01	>0.01	**0.022**	6.2	good	**0.014**	10.4	good
Quasistatic Bonding Index (BI$_B$)			**0.081**	7.8		**0.058**	10.3	
Strain Index (SI)			**0.014**	2.7		**0.016**	4.7	
Degree of Viscoelasticity (DOV)	10-30	1-10	**3.7**	8.1	good	**4.1**	8.6	good

Interpretation of results

The Amidon prediction model uses the Hiestand simulation [118]. According to this model the properties of a powder mixture can be modeled with regards to the tableting indices with six components. The relative amount of the placebo mixture had to be entered and the mechanical properties and tableting indices were visualized as a function of the drug load. The effect of speed and lubrication is neglected and it is only valid for direct compression blends.

The acetaminophen formulation needs a large amount of microcrystalline cellulose to reach acceptable tensile strength. In Figure 48 the modeled tensile strength is shown for an API/placebo mixture comprising of 100 % microcrystalline cellulose (MCC) at different drug loads and different solid fractions. For comparison reasons in Figure 49 the same diagram is shown for an API/ placebo mixture comprising of 50 % MCC and 50 % mannitol. A tensile strength below 1 represents poor (red colored area), between 1 and 2 only marginal and above 2 good compressibility (green colored). Just with a high solid fraction of 0.9 and 100 % MCC a good tensile strength can be reached with a drug load of 50 %.

The cetirizine formulation has a drug load of 5% therefore there is only a small influence on the tabletability.
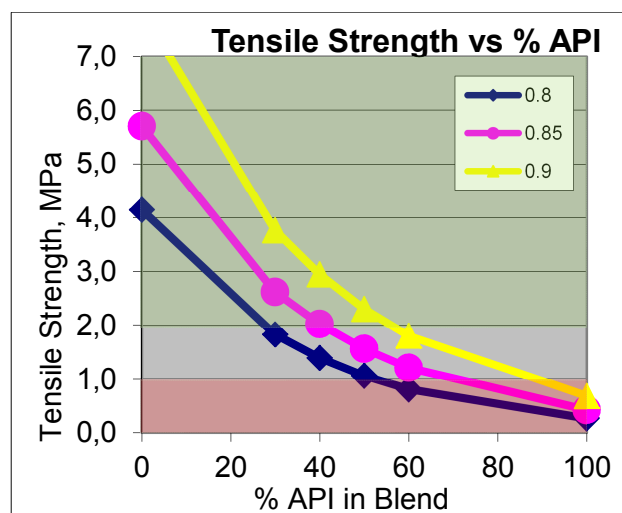

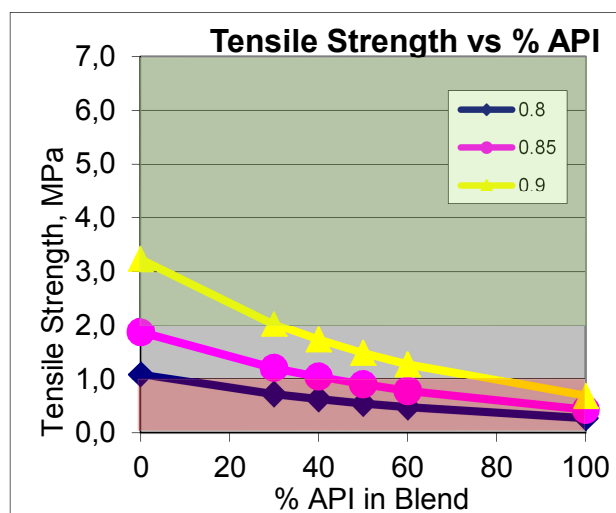Figure 48: Tensile strength vs drug load acetaminophen, 100 % MCC

Figure 49: Tensile strength vs. drug load acetaminophen, 50 % MCC & 50 % mannitol

6.2.   Development of a direct compressible minitablet formulation

6.2.1.   Acetaminophen

The formulation with acetaminophen should represent a model minitablet formulation with a high drug load of 50 %. The minitablets should have a sufficient hardness that they can withstand the mechanical stress during the coating process; a hardness of 30 N was set as a target value. To enable more a sphereical-like shape for the minitablets their aspect ratio (d:h) should be between 1:1 and 1:1.5. For the first formulation screening multi tip punches with 12 tips and a tip diameter of 2 mm was chosen.

Strategy

The starting point of the formulation development was the paper "Minitabletting: Improving the compactability of paracetamol" [13]. It states that the capping tendency of acetaminophen formulations could be reduced with minitabletting. The following formulation **P1** (see Table 21) was prepared according to section 5.1.1. In contrast to the paper FlowLac 100 was used instead of Pharmatose DCL11. Both excipients are spray dried lactose monohydrates, but they exhibit a different particle size. According to manufacturer information, Pharmatose DCL11 has a typical particle size of 34 µm [119] and FlowLac100 a mean particle size of around 100 µm [120].

For the formulations P2-5 the amount of Aerosil was increased from 0.5 to 1 % to improve the flowability of the powder mixture.

The approach for formulation **P2** and **P3** was to increase mechanical strength of the tablet, so that the compression pressure can be reduced and consequently the elastic recovery will decrease. Therefore microcrystalline cellulose was used, as it exhibit good dry binding properties. Two grades of microcrystalline cellulose were used. In formulation P2 Avicel PH 101 with a nominal particle size of 50 µm and in formulation P3 Avicel PH 102 with a nominal particle size of 100 µm was used [121].

In formulation **P4** 50% of the filler was replaced by spray dried mannitol (Parteck M100), which has excellent flow properties to improve the flowability of the powder mixture. This should enable a faster filling of the die and the reduction of entrapped air, which could also be a reason for capping.

Magnesium stearate could reduce the binding strength of the powder mixture in case of long mixing time [122]. The tablet press is equipped with only 4 punches and approximately 390 mg is transported out of the filling shoe per revolution; consequently the powder mixture has

a long residence time in the feeder. Therefore the magnesium stearate is replaced with Polyethylenglycol 6000 in formulation **P5**.

Results

The formulation **P1** at high compression pressures led to capping of the minitablets and with reduced compression pressure the minitablets were too fragile. The reason could be the use of the different filler grade compared to the one used in literature [13]. Furthermore the formulation described in the paper was compressed with an eccentric tablet press with 24 ±1 strokes per minute, thus the powder mixture has more time to fill the die and the risk of entrapped air is reduced. Additionally the dwell time was longer.

Due to the fine Avicel particles in formulation **P2** the flowability (ffc = 6.7) was reduced, but according to Jenike the powder mixture is still easily flowing [109] and also the Hausner and Carr's index were increased. The formulation was compressible without capping.

Formulation **P3** resulted in higher values for the flowability (ffc = 8.1) compared to P2 due to the larger particle size of the microcrystalline cellulose particles. The Carr's index and Hausner factor remained similar to the P2 formulation. However, formulation P3 exhibited a capping tendency.

By the use of Parteck M100 in formulation **P4,** the Hausner factor and the ffc were improved slightly compared to P2. However, the formulation was not compressible since nearly all MTs capped and also a sticking tendency was present. The compression of formulation P4 led to high ejection forces (>1000 N), which is an indication for high elastic recovery.

Formulation **P5** showed similar powder properties to P3, but the formulation was also not compressible due to extensive capping.
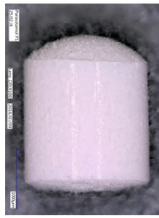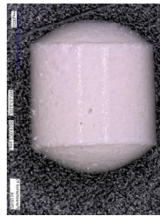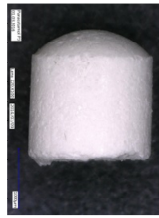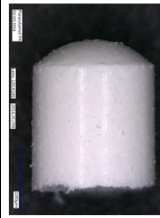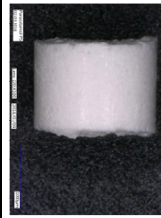
Conclusion

The poor compression property of acetaminophen is well described in the literature ([123], [124], [125], [126]). Acetaminophen is typically used as a reference substance to investigate the capacity of direct compression excipients. The elastic components of the mainly brittle material lead to stress inside the tablet after the compression [13]. This stress is then released by elastic recovery which destroys many of the formed bonds and capping could occur. Furthermore acetaminophen exhibits anisotropic properties, that results in stress and could weaken the tablet as well [127]. The tableting properties of acetaminophen could be improved by granulation, the selection of a different polymorphic form or a different crystal habit [13], e.g. the orthorhombic form [128].

Due to the large amount of crystalline acetaminophen the formulations exhibit poor compression properties and all formulation except of P2 led to capping. Therefore only

formulation P2 was compressible with the use of 3 kN pre-compression force. The moderate flowability of the powder mixture led to a relatively high weight variation of 4.09 % per single minitablet, though as a single dose is administered by multiple minitablets dose accuracy is increased.

Table 21: Formulations Acetaminophen MT

Batch	P1	P2	P3	P4	P5
Formulation					
Acetaminophen	50.00	50.00	50.00	50.00	50.00
FlowLac 100	49.00	0.00	-	-	-
Avicel PH 101	-	48.50	-	-	-
Avicel PH 102	-	-	48.50	24.25	47.00
Parteck M100	-	-	-	24.25	-
Aerosil	0.50	1.00	1.00	1.00	1.00
Magnesium Stearate	0.50	0.50	0.50	0.50	-
Polyethylenglycol 6000	-	-	-	-	2.00
Sum	*100.00*	*100.00*	*100*	*100.00*	*100.00*
IPC powder mixture					
Bulk density [g/cm³]	0.556	0.365	0.39	0.417	0.393
Tapped density [g/cm³]	0.774	0.527	0.56	0.579	0.557
Hausner factor	1.39	1.44	1.44	1.39	1.42
Carr's Index [%]	28.30	30.59	30.58	27.92	29.41
ffc	8.90	6.70	8.10	7.10	8.10
IPC tablets					
Mean weight [mg]	9.855	8.435	8.290	n.a.	n.a.
Srel weight [%] (n=1)	4.30	4.09	3.76	n.a.	n.a.
Heigth [mm]	2.778	2.454	2.462	n.a.	n.a.
Aspect ratio	1.389	1.227	1.231	n.a.	n.a.
Breaking force [N]	8	18	12.2	n.a.	n.a.
Capping	yes	no	tendency	yes	yes
Compression force [kN]	9.30	7.50	6.60	n.a.	n.a.
Dosing [mm]	4.4	5.8	4.7	n.a.	n.a.
Band height [mm]	1.7	1.4	1.4	n.a.	n.a.
comments	capping	-	capping tendency	capping and sticking	capping

Problem observed during Formulation screening

It was observed that minitablets experience defects during ejection at the scraper. The tips of the punch are circularly arranged (Figure 50). At the ejection position the tips emerge ca. 1.2 mm out of the die. After the first minitablets are stripped by the scraper they fall in the center and are surrounded by the emerging tips. Subsequently they jam between the emerging tips and the scraper (Figure 51). The resulting broken minitablets are shown in Figure 52 and Figure 53.
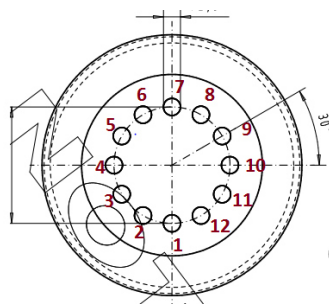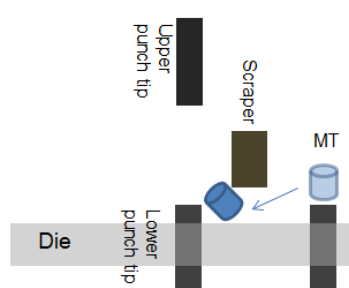

Figure 50: Tip arrangement, 2mm Punch

Figure 51: MT destroyed by scraper

Figure 52: Destroyed MT (i)

Figure 53: Destroyed MT (ii)

Possible Solution

The first approach was to fix a foam cushion with double sided tape on the scraper. The elastic material released the stress when a minitablet is jammed between the emerging tip and the scraper. However a significant number of the minitablets were catapulted away against the housing of the tablet press and caused a low yield. This solution was therefore just a short term solution. After a few rotations powder accumulated between the foam cushion and the tape causing the minitablets to stick under the foam and become abraded. Furthermore this solution would clearly not be applicable for any GMP or commercial manufacturing.

Another possible solution is to remove every 2nd tip from the multi tip punch, so that the minitablets could leave the circle of tips. But the maximum compression pressure would need to be reduced to 6 kN and this set-up would be critical with regards to the mechanical stability of the punches.

The amount of destroyed MTs could be reduced by decreasing the emerging height of the tips out of die. But the available ejection rail is not adjustable and a new rail needed to be ordered and grinded down by approximately 1 mm.

Punches with a different tip arrangement, e.g. centered or in rectangular arrangement, could possibly also solve this technical problem; hence the minitablet cannot be trapped in the center of the punch.

Therefore it was decided to use punches with a more centered tip arrangement for the following trials. These punches have a 2.5 mm tip diameter and possess 24 tips on one punch.

With this new tooling it was feasible to compress formulation P2 with the 2.5 mm punches without any breakage of MTs at the scraper. The dosing height was adjusted to a minitablet weight of 14.3 mg, which results in 28 MTs per a dose of 200 mg of acetaminophen, which is a common dose for children between 2 and 6 years. The relative weight variation of the single tablet could be significantly reduced to 3.9% due to larger die openings. The relative weight variation of the targeted dose of 200 mg was 0.8%. The aspect ratio of 1:1.1 (height 2.7 mm) led to a hardness of 31.3 N.

Discussion

Capping:

The hypothesis that the magnesium stearate covered the particles due to the long mixing time in the filling chamber, which would cause a loss of binding strength and result in capping, was proven wrong. According to this theory the formulation P5 (without magnesium stearate) should have no evidence of capping but instead also led to extensive capping. Again the high amount of crystalline acetaminophen was the root cause due to its poor compression properties [129].

Even formulation P3 with the coarser Avicel PH 102 showed a capping tendency. Compared to formulation P2 the microcrystalline cellulose has twofold larger particles. Therefore the numbers of formed bondings during the compression is smaller with regards to a reduced surface area when compared against the finer Avicel PH101. Due to the general large elastic recovery of acetaminophen crystals and less previously formed bondings stayed intact after decompression and also with this formulation capping occurred for this formulation.

The other fillers (mannitol, lactose) did not provide enough binding strength, which is shown the mechanical properties of the fillers in Table 22. The ability to provide a high binding strength is represented by a high value of the value tensile strength (σ_T) and bonding index (BI).

Table 22: Mechanical properties pure fillers

Excipient	Lactose Monohydrate	Mannitol (Parteck M200)	Microcrystalline cellulose (Avicel PH101)	Microcrystalline cellulose (Avicel PH102)
C_p	132	116	109	99.7
σ_T	0.590	3.940	6.146	5.550
σ_{To}	0.480	1.860	5.775	5.320
H_d	183.0	385.0	157.9	155.7
H_{qs}	41	51.8	49.8	46.2
BI	0.0032	0.0102	0.0389	0.0356
BFI	0.11	0.56	0.03	0.02
VI	4.5	7.4	3.2	3.4

Flowability:

A large amount of fine microcrystalline cellulose (Avicel PH 101) was necessary to get acceptable hardness without capping. The nominal particle size of Avicel PH 101 is 50 µm, which caused poor flowability compared to the other formulations. Due to the poor flowability the dies were insufficiently filled, which resulted in high relative MT weight
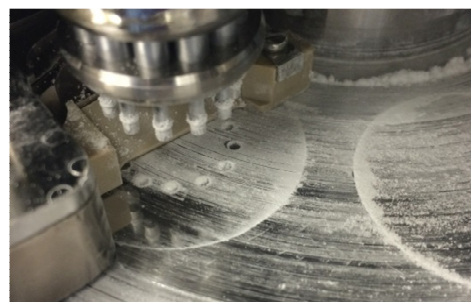

Figure 54: Insufficient die filling

variation of 4.1 %. The insufficient die filling occurred mostly close to the rotation axis of the tablet press. That could be reduced by arranging the tips of the punches in a rectangular manner or if the tips are centered and the outer radius of the tips is reduced.

By using the 2.5 mm punches with a more centered tip arrangement, the relative variability of the single minitablet could be decreased to 3.9 % and the relative variation of the dose (n=28 MT) to 0.8 % (Table 25). The variation of weight was acceptable due to the high number of given minitablets per dose. But the insufficient die filling caused also a high absolute standard deviation of 8 N in the hardness of the MTs (Srel= 25.57 %). As the compression volume is for each die the same and if the die is not completely filled, then the porosity resp. hardness gets lower. This of course could become critical for the following coating process.

A Hausner factor of 1.44 and a Carr's index of 30.6 % are quite high (Table 23) and are rather critical for the direct compression. After the setting of the process parameters, the compaction pressure increased due to densification of the powder mixture. Subsequently the dosing height needed to be adjusted until the compression pressure stayed constant.

Granulation would improve flowability into the dies; however, care must be taken in regards to the granule diameter and the die diameter so that adequate filling take place.

The disintegration time of the compressed P2 formulation was just 18 s, which can be problematic for the coating process due to the fast water uptake.

Table 23: Final formulation and properties acetaminophen MT

Formulation	Acetaminophen (P2)	
	Composition [%]	Mass per MT [mg]
Acetaminophen	50.0	7.19
Avicel PH 101	48.5	6.97
Aerosil	1.0	0.14
Magnesium Stearate	0.5	0.07
Sum	*100.0*	*14.37*
IPC powder mixture		
Bulk density [g/cm³]	0.37	
Tapped density [g/cm³]	0.53	
Hausner factor	1.44	
Carr's Index [%]	30.6	
Ffc	6.7	
IPC tablets		
Mean weight [mg]	14.22	
Srel weight [%] (n=28)	0.80	
Height [mm]	2.70	
Aspect ratio	1:1.1	
Breaking force [N]	31.3	
Tensile strength [MPa]	1.61	
Disintegration [s]	18	

6.2.2.   Cetirizine Dihydrochloride

The formulation with cetirizine should represent a model minitablet formulation having a low drug load of 5%. The physical requirements of the minitablets are equal to the acetaminophen minitablets (hardness 30N, aspect ratio 1:1 – 1:1.5). For the first formulation screening multitip punches with 24 tips and a tip diameter of 2.5 mm were used.

Strategy

The typical dose of cetirizine for children between 2 to 6 years is 2.5 mg. That would result in a target minitablet weight of either (Low) 12.5 mg (n=4) or (High) 16.67 mg (n=3) for a drug load of 5 %. For each formulation 500g of the powder mixture was prepared according Method 5.1.1 (Table 24).

Formulation **CET1** contained the fillers microcrystalline cellulose and spray dried lactose in a ratio of 1:2 (Avicel PH 102 : Flowlac 100). Furthermore it contains Aerosil and Magnesium stearate each at 1 % content.

Formulation **CET2** contained the fillers spray dried mannitol and microcrystalline cellulose in a ratio of 1:2 (Parteck M100 : Avicel PH 102). Additionally crosscarmelose sodium was used as a superdisintegrant and talc as glidant each at a concentration of 5 %. In this formulation sodium stearyl fumarate was used instead of magnesium stearate.

Formulation **CET3** contained the fillers microcrystalline cellulose and agglomerated isomalt in a ratio of 1:1.3 (Avicel PH 102 : GalenIQ 721). Furthermore sodium stearyl fumarate (3 %) and crosscarmellose sodium (5 %) were used.

Results

All formulation showed a good compressability without tableting defects. All results are shown in Table 24.

The powder mixture of formulation **CET1** had an excellent flowability (ffc = 20) and the Hausner factor had an acceptable value of 1.29 (Table 24). To stay in the limit of the aspect ratio the minimal tablet height had to be at least 2.5 mm. With the lower target weight of 12.5 mg the minitablets reached a hardness of 11 N, which is not sufficient. The minitablets having a target weight of 16.67 mg had a glossy appearance and a hardness of 30 N. The disintegration time was 57 s.

Formulation **CET2** had good powder characteristics with regards to the flowability (ffc=12.4: free flowing) and Hausner factor (1.27) (Table 24). The minitablets having the lower target

weight had a hardness of 18 N. The minitablets were not fragile, but did not have the required hardness of 30 N. With the high minitablet target weight all requirements could be fulfilled. The disintegration time of both target weights were below 20 s.

Formulation **CET3** had the worst powder properties compared to the other formulations. The Hausner factor was larger than 1.30 (Table 24), which is an indication for a high compressiblilty that may result in high weight variation during the tableting process. The ffc value was 9.4 which is classified according to Jenike as "easy flowing". It was feasible to produce minitablets with both target weight, but the lower target weight exhibited an insufficient hardness of 14 N. The disintegration time of the minitablets having the higher target weight was 109 s.

Discussion

All formulations were compressible and no tableting defects were observed. None of the formulations could fulfill the requirements with the lower target weight, due to the minimum height of 2.5 mm and the required hardness of 30 N. At the higher target weight a good compromise could be reached regarding hardness and aspect ratio with all formulations.

The weight variability of the minitablet formulations was in an acceptable range between 0.65 – 1.09 %. For the higher target weight three minitablets and for the lower target weight four minitablets were weighed. The process variability may even be reduced in the steady state to avoing frequent stopping and adjustment of the parameters during the formulation screening.

The formulations had acceptable powder properties with regards to flowability and Carr's Index. Formulation CET 1 and 2 were superior compared to CET3. CET3 had the highest Hausner factor and Carr's index and the lowest ffc value. Despite the included superdisintegrant the observed disintegration time of 109 s was comparably long. The high solid fraction of 0.9 could be the reason for this long disintegration time.

The disintegration time of the CET2 formulations were extremely short and could not be determined exactly with the disintegration tester. This could be critical for a subsequent coating process due to the water sensitivity of the minitablets. If the coating liquid cannot be immediately evaporated it may dissolve partially the surface. This could be problematic especially for aqueous based coating processes. For that reason formulation CET1 having the higher target weight was chosen instead of formulation CET2 for the coating experiments (see Table 25).

Table 24: Formulations Cetirizine MT

Batch	CET1		CET2		CET3	
Formulation						
Cetirizine	5.0		5.0		5.0	
FlowLac 100	59.0		-		-	
Avicel PH 102	34.0		52.0		37.0	
Parteck M100	-		31.0		-	
Agglomerated Isomalt	-		-		49.0	
Crosscarmellose Sodium	-		5.0		5.0	
Talc	-		5.0		-	
Aerosil	1.0		1.0		1.0	
Magnesium Stearate	1.0		-		-	
Sodium stearyl fumerate	-		1.0		3.0	
Sum	*100.0*		*100.0*		*100.0*	
IPC powder mixture						
True density [g/cm^3]	1.540		1.561		1.514	
Bulk density [g/cm^3]	0.475		0.442		0.407	
Tapped density [g/cm^3]	0.611		0.562		0.538	
Hausner factor	1.287		1.270		1.323	
Carr's Index [%]	22.3		21.2		24.4	
Ffc	20.0		12.4		9.40	
IPC tablets	CET1_L	CET1_H	CET2_L	CET2_H	CET3_L	CET3_H
Mean weight [mg]	12.45	16.6	12.58	16.63	12.53	16.6
Srel weight [%]	0.65	0.76	0.75	0.94	1.09	0.85
Heigth [mm]	2.52	2.95	2.51	3.11	2.52	2.97
Aspect ratio	1:1.01	1:1.18	1:1.00	1:1.24	1:1.01	1:1.12
Breaking force [N]	11	30	18	28	14	30
Tensile strength [MPa]	0.53	1.70	0.86	1.67	0.67	1.71
Compression force [kN]	9.80	18.20	10.70	12.00	10.30	16.30
Band height [mm]	1.14	1.30	1.10	1.70	1.14	1.44
Dosing [mm]	4.25	5.94	4.71	6.45	4.92	6.6
Solid fraction	0.81	0.89	0.81	0.83	0.83	0.90
Disintegration [s]	-	57	<20	<20	-	109

Table 25: Final formulation and properties Cetirizine

Formulation	Cetirizine dihydrochloride (CET1_H)	
	Composition [%]	Mass per minitablet [mg]
Cetirizin dihydrochloride	5.0	0.83
Avicel PH 102	34.0	5.67
FlowLac 100	59.0	9.84
Aerosil	1.0	0.17
Magnesium Stearate	1.0	0.17
Sum	100	16.67
IPC powder mixture		
True density [g/cm^3]	1.54	
Bulk density [g/cm³]	0.48	
Tapped density [g/cm³]	0.61	
Hausner factor	1.29	
Carr's Index [%]	22.28	
ffc	20.0	
IPC tablets		
Mean weight [mg]	16.60	
Srel weight [%]	0.76	
Heigth [mm]	2.95	
Aspect ratio	1.18	
Breaking force [N]	30.0	
Tensile strength [MPa]	1.70	
Solid fraction [ ]	0.89	
Disintegration [s]	57	

6.3.   Quality risk assessment

The goal of the QRA was to identify potential critical material attributes (pCMAs) and process parameters (pCPPs) and subsequently to evaluate their impact on the critical drug product quality attributes (CQAs) by performing Design of Experiment (DoE) based trials. This should also help to gain better process understanding and to develop an appropriate drug product process control strategy.

The Quality Risk Assessment (QRA) was conducted in a cross functional team approach. Scientists from different R&D functions (formulation development, process development, analytical development and operations) participated.

The pCQAs of the minitablets based drug product were determined by the team as follows:

- Appearance
- Efficient taste masking
- Content Uniformity
- Dissolution (immediate release)

The Quality Risk Assessment was performed based on prior knowledge and initial experimental data. The potential critical factors which were evaluated with a high risk (red colored) are shown in Table 26 (Appendix VI).

Discussion

In this case study only the factors, which might exhibit a high risk for the pCQAs "Efficient taste masking" and "dissolution" were taken into account:

Further information and assessments regarding pCMAs and pCPPs are mentioned below:

Polymer choice: The manufacturer of the pH dependent polymer Eudragit E PO® states that the polymer can interact with APIs having anionic activities [130]. Therefore excipient compatibility studies with cetirizine, Eudragit E PO® and Kollicoat® Smartseal 30D were performed (Chapter 6.8 Excipient Incompatibility Study).

Plasticizer concentration: The plasticizer concentration in the coating liquid has an influence of the film formation by reducing the minimum film formation temperature (MFFT). Therefore it is critical for the pCQA "Efficient taste masking". The use of a plasticizer is only necessary for the polymer Kollicoat® Smartseal 30D. The effect of the plasticizer was not further investigated, hence the manufacturer delivered valuable information about the plasticizer concentration dependent on the minimum film forming temperature [91].

Antioxidant - Kollicoat® Smartseal: The oxidation of the aminoesters of the polymer Kollicoat® Smartseal 30D could cause a delay in the dissolution profile. Therefore the manufacturer recommends the addition of an antioxidant to the coating formulation. According the manufacture it is just required for normal sized tablets and not for pellets or particle coatings like minitablets [91].

Ratio polymer/pore former: The ratio of Surelease® to the pore former was evaluated as being potentially critical for the pCQA "efficient taste masked", since the pore former influences the drug release at the early dissolution testing time-points. It was decided that this should be investigated in a DoE. For the Surelease coating formulation no talc is needed and the plasticizer is already been incorporated. The manufacturer recommends a product temperature between 40 and 45 °C. Therefore the product temperature was set to a fixed value of 43±0.5 °C to reduce the number of needed experiments.

Product temperature: The product temperature is a response of the inlet air temperature, the spray rate and inlet air volume. It has an influence on the film formation process. The product temperature should be at least 10 to 15 °C higher than the minimum film forming temperature (MFT) to ensure the film formation. The manufacturer of the polymers recommended either a product temperature or published the MFT as a function of the plasticizer concentration.

Spraying rate and spraying time: The coating thickness is a result of the spraying rate and the spraying time, which has an influence of the functionality of the coat. Both factors were evaluated as potentially critical for "efficient taste masked" and "dissolution". A high spray rate will also produce larger droplets, which need more time to evaporate. This could cause several coating defects, like partial dissolving of the surface or sticking together of wetted tablets.

Volumetric flow rate: Number minitablets in spraying zone (controlled by distance Wurster column/bottom plate, inlet air volume, atomization pressure): The number of minitablets, which are present at a specific time point in the Wurster column is important for the process efficiency. The number is a function of the distance between Wurster column and bottom plate, the volumetric flow rate and the atomization pressure of the spray nozzle. Due to the preliminary experiments a good setting of those parameters could be found at 14 mm, 99 m³/h and 1.5 bar and were not further investigated.

Table 26: Results QRA

pCPPs / pCMA	pCQAs	Risk control strategy	Comments
Cetirizine Dihydrochloride (Interaction with pH dependent polymers)	efficient taste masked	Excipient compatibility study	Paper: Dionysios et al. 2010 [131]
Plasticizer concentration Kollicoat® Smartseal 30D	efficient taste masked	Manufacturer recommendation	
Talc concentration	Appearance	Manufacturer recommendation	Sticking, intact film
Antioxidance – Kollicoat® Smartseal 30D	Dissolution	Manufacturer recommendation: Tablets, not Pellets	
Ratio Surelease:Pore Former	efficient taste masked	DoE	pH independent Polymer
Product temperature	efficient taste masked	DoE	Film formation
Spray rate	efficient taste masked Dissolution	DoE	Coating thickness
Spray time	efficient taste masked Dissolution	DoE	Coating thickness
Volumetric flow rate	efficient taste masked	DoE	

6.4.   *Wurster Coating Trials*

Overview of all coating trials is shown in the Appendix VII and VIII.

During the development of the coating process the following problems were observed.

Layering of the Wurster column

During the coating process the coating suspension adhered to the inner side of the Wurster column. This layer was further building up until fluidization was inhibited and consequently the spraying process had to be stopped (Figure 55). Since minitablets got stuck to the wet surface and tripped off again, this caused damage of the film-coat.

The reason for this problem was a too large spray cone or a too low number of minitablets being present in the spray zone to take up the coating suspension. The spray cone

Figure 55: Layering of the Wurster column

can be influenced by the atomization pressure, the nozzle bore diameter resp. nozzle cap. The amount of minitablets in the spray zone can be influenced by the distance of the baseplate to the Wurster column, the volumetric flow rate and the perforation of the base plate.

By the reduction of the volume flow rate an increased atomization pressure could not prevent the layering of the Wurster column. However, the use of a reduced nozzle bore of 0.5 mm led to a narrower spray cone which then prevented the layering of the Wurster column.

Filter clogging

During the coating process the fluidization of the minitablet decreased, despite corrective adjustment of the volumetric flow rate. The reason for the insufficient fluidization was the clogging of the installed 5 µm filters (Figure 56). The periodical filter blow off could not remove the particles resp. plates from the filter. However that would not have been the best solution, because at each filter blow off API particle could fall on the coat and would be present at the minitablet surface, which could lower the taste masking efficiency. By decreasing the atomization

Figure 56: Clogged filter

pressure larger droplets were produced and spray drying became less probable, but it still led to clogging of the filters.

The problem could finally be solved by installing a 500 µm metal mesh instead of the 5 µm filter candles (Figure 57). That change could have led to a decrease of the coating process efficiency, since liquid coating droplets could have removed via the exhaust air, though after the installation of this new filter coating process efficiency was still high (over 90%).

Figure 57: 500 µm mesh filter

Coating defects

All coated batches of the acetaminophen minitablets showed approximately 1% of minitablets having coating defects. These minitablets had dissolved surfaces and the coating layer was partially flaked off (Figure 58). These coating defects occurred independently whether the spray rate was set to low or high level.

Figure 58: Coating defects

One explanation could be the larger variation of the minitablet hardness across the batch. It was observed that minitablets having a low weight had also a low hardness between 13 to 20 N. These minitablets also have a significantly lower solid fraction. Generally a lower solid fraction of a tablet leads to a lower disintegration time [132]. Therefore the outliers in hardness are then more sensitive to wetting and the minitablet surface is then rapidly dissolved even when exposing them with a very low spray rate. Once the tablet surface is partially dissolved by the coating liquid the incooperated MCC of the formulation can start to swell and flake off a part of the coat.

To proof this hypothesis, outliers were sorted out by their lower weight using an automatic weight sorter (SADE SP 100; CI precision, UK). The resulting minitablets had no outliers in hardness and were then coated with the same process parameters. This batch did not contain any coating defects and therefore it can be concluded that the outlier in hardness caused the coating defects.

The high variation of the hardness could be reduced by improving the compressibility or the flowability. The compressibility could be improved by granulation or by using the orthorhombic crystal form of acetaminophen [133]. When the compressibility properties are enhanced, the use of fillers for direct compression with excellent flow properties is possible.

6.4.1.   Acetaminophen

6.4.1.1.   pH dependent Polymers

The coating trials were performed with the following coating suspension compositions (Table 27). The acetaminophen minitablets were coated with different coating levels of Eudragit E PO® (EPO) and Kollicoat® Smartseal 30D (SMA), which is shown in Table 28 and Table 29. The polymer EPO was applied having coating levels of 2, 4, 6 and 8 g/cm² and SMA having 1, 1.5, 2, 4, and 7 g/cm².

Table 27: Composition pH dependent coating suspensions

Formulation	Kollicoat® Smartseal 30D (SMA)	Eudragit E PO® (EPO)
	Composition [%]	Composition [%]
Kollicoat Smartseal	33.33	-
Eudragit E PO	-	11.40
TEC	1.51	-
Stearic acid	-	1.71
SLS	-	1.14
Talc	8.00	5.70
Colorant	0.40	0.06
Water	56.76	80.00
Sum	*100.00*	*100.00*

A minimum coating level of 4 mg/cm² was necessary for an efficient taste masking in artificial saliva (AS) for both polymers (Figure 59). At this coating level the coating layer of the EPO coated minitablet stayed intact for 5 minutes when testing the dissolution in artificial saliva, however the SMA coated minitablets had cracks where small amounts of the API were then released. Despite this finding the resulting concentration was below the bitterness threshold and therefore classified as taste masked. But Kollicoat® Smartseal had a lower taste masking efficiency compared to Eudragit E PO® in that particular case.
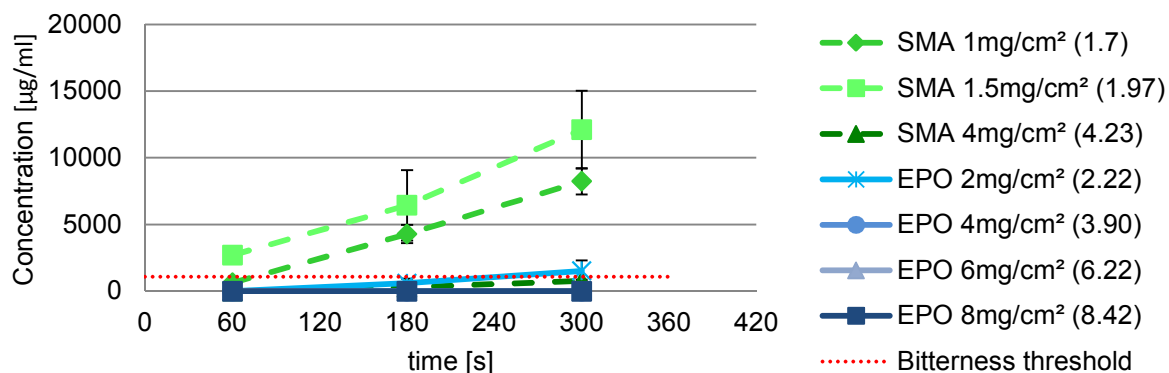
Figure 59: In vitro taste assessment in AS: acetaminophen MT coated with pH dependent polymers

Also at lower coating levels below 4 mg/cm² the minitablets still exhibited an intact and homogeneous coating layer, which is shown in Figure 60. When the minitablets came into contact with water a bursting effect was observed and sufficient taste masking could not be achieved.

When testing the minitablets in simulated gastric fluid even at a high coating level of approximately 7 mg/cm² the coated acetaminophen minitablets still exhibited immediate release characteristics (Figure 61).
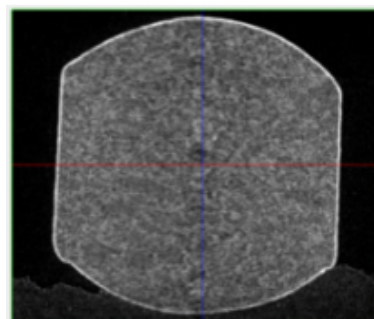
Figure 60: X-ray µCT: SMA 1.5mg/cm²
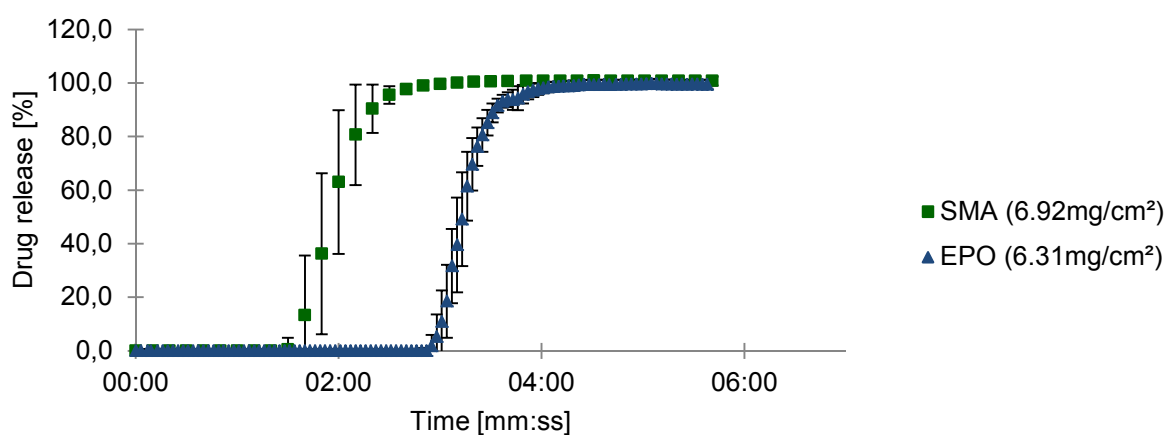
Figure 61: Dissolution in SGF: acetaminophen MT coated with EPO and SMA

Table 28: Results acetaminophen MT coating trails with Eudragit E PO®

Batch	Para2.2.III	Para2.3.VI			
Polymer	EPO; 7mg/cm²	EPO; 2mg/cm²	EPO; 4mg/cm²	EPO; 6mg/cm²	EPO; 8mg/cm²
Process evaluation					
LOD before [%]	2.04	2.02	2.02	2.02	2.02
LOD after [%]	1.83	2.07	1.98	1.86	1.92
Initial MT weight [mg]	14.37	14.22	14.22	14.22	14.22
Final MT weight [mg]	17.11	15.192	15.912	16.899	17.869
Srel weight [%]	5.14	6.05	6.58	7.46	7.04
Weight gain [%]	19.32	6.78	11.94	19.03	25.79
Polymer applied [mg/cm²]	6.31	2.22	3.90	6.22	8.42
Coating Uniformity [ ]	0.86	0.9	1.027	1.237	0.984
Coating Process Efficiency [%]	78.90	100.8	87.5	93.6	95.3
Problems	Blockage of Filter	-	-	-	-
IPC coated MT					
Appearance	good	inhomogeneous in color	rough surface	rough surface	rough surface
Hardness [N]	53.10	44.8	39.4	50.2	52
Height [mm]	2.88	2.77	2.8	2.88	2.92
Coating Thickness [µm] µCT (n>600)	80.6±1.2	-	-	-	-
Coating Thickness [µm] SEM (n=4)	79.25±5.3	-	-	-	-
Dissolution SGF immediate release [mm:ss]	02:15	-	-	-	-

Table 29: Results acetaminophen MT coating trails with Kollicoat® Smartseal

Batch	Para2.2.V	Para2.3.IV		Para2.3.V	
Polymer	SMA; 7mg/cm²	SMA; 1mg/cm²	SMA; 1.5mg/cm²	SMA; 2mg/cm²	SMA; 4mg/cm²
Process evaluation					
LOD before [%]	2.04	2.06	2.06	2.03	2.03
LOD after [%]	1.78	1.76	1.95	1.93	1.94
Initial MT weight [mg]	14.37	14.22	14.22	14.22	14.22
Final MT weight [mg]	17.46	14.703	14.907	15.021	16.246
Srel weight [%]	5.60	5.74	5.50	5.39	14.66
Weight gain [%]	21.85	3.74	4.98	5.71	14.32
Polymer applied [mg/cm²]	6.92	1.70	1.97	1.97	4.23
Coating Uniformity []	0.961	0.829	0.804	0.794	0.473
Coating Process Efficiency [%]	86.49	160.34	121.51	88.63	95.79
Problems	Blockage of Filter				
IPC coated MT					
Appearance	small amount of broken MT	rough surface, broken MT, inhomogeneous in color	rough surface, broken MT, inhomogeneous in color	rough surface, broken MT	rough surface, broken MT
Hardness [N]	53.30	29	33.3	36.6	42.2
Height [mm]	2.91	2.73	2.79	2.89	2.83
Coating Thickness [µm] µCT (n>600)	78.3±2.2	13.3±0.3	18.7±0.4	22.8±0.3	37.1±0.7
Coating Thickness [µm] SEM (n=4)	85.8±5.7	10±0.8	20.3±3.3	23±1.4	39±4.2
Dissolution SGF immediate release [mm:ss]	03:37	-	-	-	-
Comments	-	too wet process → dissolving surface		still dissolved surface despite reduction of spray rate from 4 to 2 g/ min	

Discussion

For the taste masking with pH dependent polymers the minimal necessary coating level was investigated. In the case of acetaminophen minitablets a coating level of 4 mg/cm² was fully sufficient for taste masking.

At lower coating levels e.g. 1.5 mg/cm² the taste masking was not sufficient due to bursting of the minitablets. The coating layer is insoluble at high pH but still permeable to water. When the minitablets come into contact with water, it permeates through the coating layer into the core of the minitablets. Then the MCC of the core starts to swell. Subsequently the internal pressure increases until it exceeds the mechanical strength of the coating layer. The

rupture of the coating layer starts at the edges, which could be due to a thinner coating layer at the edge. However, it was found that the layer thickness was homogeneous even at the edges, as shown in Figure 62. The coating layer is color-coded based on thickness. On the lower side of the minitablet in Figure 62 is an artefact present due to fixing material used in the X-ray µCT measurement. Overall the coating thickness seems to be very homogeneous and not thinner at the edges of the minitablets.
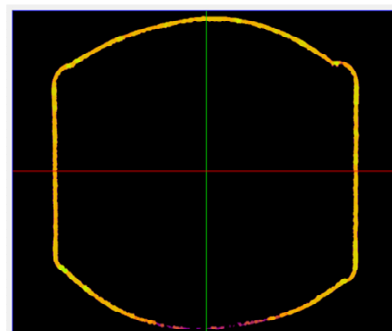
Figure 62: X-ray µCT (color –coded): SMA 1.5mg/cm²

The rupture observed at these edges could be explained by a stress concentration effect. The pressure is higher at the edges due to the geometry of the minitablet. After rupture of the coating layer, API is released and taste masking is no longer given. The amounts of minimum required coating levels can be probably further reduced, when the amount of swellable excipients is decreased. In this particular case also the elastic deformation capability of the film has an influence on the minimal required coating level: when the coating layer has a higher elasticity the core can swell more without bursting effects.

According Bürki Eudragit E® shows a higher maximum elongation to break compared to Kollicoat® Smartseal having the same plasticizer concentration, which could be due to the lower molecular weight and lower glass transition temperature [134]. The maximum elongation to break is an indication for the elasticity of the film and could the reason for the lower taste masking efficiency of Kollicoat® Smartseal compared to Eudragit E PO® at a coating level of 4 mg/cm².

6.4.1.2. pH independent Polymer

The pH independent polymer Surelease® can extend the release. Therefore the water soluble PVA – based pore former Opadry II was in cooperated. The compositions of the coating suspensions are shown in Table 30.

Table 30: Coating suspension composition Surelease®, acetaminophen minitablets

Formulation	Surelease 80:Opadry20	Surelease 85:Opadry15
	Composition [%]	Composition [%]
Surelease	48	51
Opadry II clear	20	15
Water	32	34
Sum	*100*	*100*

Coating trials with different polymer to pore former ratios (85:15; 80:20) and coating levels (2 – 6 % coating weight gain) were performed. The results are shown in Table 31. Further the effect of curing for 24 hours at 40°C and 60°C was investigated.

Figure 63 shows the taste masking efficiencies of the Surelease® coated minitablets. Taste masking was reached for 60s in artificial saliva of all batches except for Para2.3.I having the highest amount of pore former and the lowest coating weight gain. All batches met the immediate release requirement (85% drug release within 15 min) (Figure 64). The dissolution curves of the coating batches Para2.2.VII (Sur85 4%), Para2.3.II (Sur80 4%) and Para2.3.III (Sur80 6%) show a stepwise increase due to the different lag times of the individual dissolution curves.
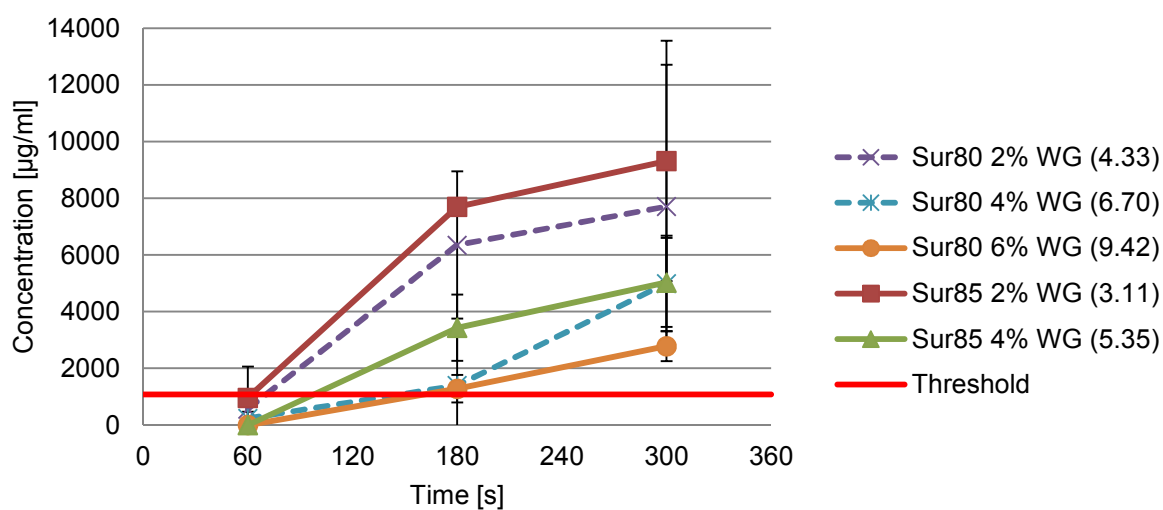
Figure 63: In vitro taste assessment in AS: acetaminophen MT coated with Surelease®
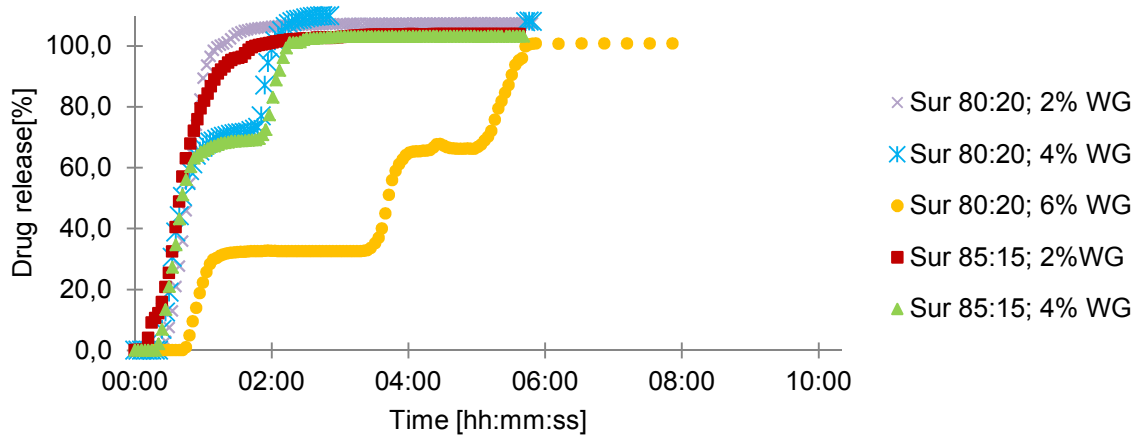
Figure 64: Dissolution in SGF: acetaminophen MT coated with Surelease®

Table 31: Results acetaminophen MT coating trials with Surelease®

Batch	Para2.2.VI	Para2.2.VII	Para2.3.I	Para2.3.II	Para2.3.III
Polymer	Surelease (85:15), 2%WG	Surelease (85:15); 4%WG	Surelease (80:20), 2%WG	Surelease (80:20), 4%WG	Surelease (80:20), 6%WG
Process evaluation					
LOD before [%]	2.04	2.04	1.99	1.99	1.99
LOD after [%]	2.19	2.08	2.2	2.05	1.99
Initial MT weight [mg]	14.37	14.37	14.30	14.22	14.22
Final MT weight [mg]	14.54	15.07	14.69	15.11	15.15
Srel weight [%]	5.18	11.42	5.19	5.02	5.63
Weight gain [%]	1.03	4.79	2.45	6.25	6.59
Polymer applied [mg/cm²]	1.33	2.30	1.86	2.84	3.20
Coating Uniformity []	0.736	1.685	0.745	0.743	0.836
Coating Process Efficiency [%]	51.40	119.84	122.43	156.29	109.85
IPC coated MT					
Appearance	rough Surface and broken	rough Surface	rough Surface	good	good
Hardness [N]	27.70	28.30	30.00	30.10	31.30
Height [mm]	2.75	2.75	2.76	2.77	2.78
Dissolution SGF immediate release [m:ss]	1:05	2:03	0:59	1:52	5:26
Taste masking [µg/ml] Conc. after 60;180;300	961; 7697; 9315	134; 1165; 1569	1446;8122; 10684	847; 5661; 7189	809; 4982; 6481

Discussion

The taste masking with the pH independent polymer Surelease® was achieved for 60 s in artificial saliva. Afterwards the incorporated pore former was dissolved and due to the swelling of MCC the matrix coating layer was disrupted and the API was released.

The results of the in vitro taste assessment had a high standard deviation. The batches Para2.2.VI and Para2.3.I had a spraying time of 21 min resp. 19 min, which is too short to ensure a homogeneous coating distribution. This variability in coating layer thicknesses influences the functionality of the coat and causes also variability of the drug release. For the in vitro taste assessment 28 minitablets were tested, since this number is equivalent to one dose. Due to the high number in a relative small volume, it led to irregular sticking of minitablets. That is also the root cause of the variability in dissolution testing. Colorcon has showen that the use of specially designed sinker could reduce the variability in dissolution [135].

The dissolution curves of the single measurements exhibited different lag times and therefore the resulting mean curve has a stepwise characteristic. This is also an indicator for the inhomogeneity of the coating layers.

Curing of the coated minitablet at 40°C and 60°C for 24h did not affect the dissolution profiles, even though there were cracks present on the surface of the 60 °C cured minitablets (Table 40).

6.4.2.   Cetirizine Dihydrochloride

6.4.2.1.   Preliminary Coating Trials

Preliminary coating experiments with the cetirizine minitablets and the pH independent polymer Surelease[®] were performed to evaluate the suitable levels for the DoE.

For the first coating trial a high polymer to pore former ratio of 90:10 and a high coating weight gain of 6 % and 12.4 % was chosen. The coating process was performed without any problems and had a high coating process efficiency of 97 % (see Table 32). The spray rate was set for the first 10 minutes to 1 g/min to ensure that the coating liquid did not penetrate into the core. The coated minitablets had a glossy appearance and did not exhibit any coating defects. The taste masking of those minitablets was good with no API released in artificial saliva within the first 5 minutes. However, the minitablets did not meet the immediate release requirements. The minitablets with a weight gain of 6 % had a $t_{85\%}$ (time to 85% drug release) of 1 hour and 10 minutes and the minitablets with the higher weight gain of 12.4 % did not have any release within 5 hours. Therefore the polymer to pore former ratio was reduced to 85:15 and the weight gain to 2.25 % and 4.75 % for the next coating trials.

By the previously mentioned changes the minitablets met the immediate release requirements (see Figure 66) and the minitablet with a weight gain of 4.75 % was sufficiently taste masked for 180 s (see Figure 65).

Discussion

The polymer ratio 90:10 in combination with a high coating weight gain caused an extended release of the cetirizine dihydrochloride and therefore was not suitable for a high level for the DoE.

Hou investigated the mechanism of a cationic drug release coated with Surelease. Cationic APIs could form a poorly soluble complex with the ammonia contained in the surelease dispersion during coating. The author discovered that the curing could decompose this complex and the API would be faster released [136].

As the uncured minitablets (CET1.2.II) reached a 100% drug release in the dissolution in SGF ($t_{100\%}$< 15min) (see Figure 66), it can be assumed that either no complex is formed or that the drug load is low enough that only a negligible amount of the API is present at the interface between the minitablet and the coating layer.

Table 32: Results preliminary coating trials cetirizine with Surelease

	CET1.2.I		CET1.2.II	
Batch	CET1.2.I-1	CET1.2.I-2	CET1.2.II-1	CET1.2.II-2
Description	Sur90:Opa10; 6 %WG	Sur90:Opa10; 12.4%WG	Sur85:Opa15; 2.25%WG	Sur85:Opa15; 4.75%WG
Process evaluation				
LOD before [%]	1.84	1.84	1.84	1.84
LOD after [%]	0.69	1.29	1.14	0.75
Initial MT weight [mg]	16.670	16.670	16.670	16.670
Final MT weight [mg] MT50	17.433	18.567	16.9	17.205
Srel weight [%]	0.71	0.81	1.25	1.28
Weight gain [%]	5.80	12.00	2.10	4.36
Polymer applied [mg/cm²]	2.534	5.242	0.893	1.801
Coating Uniformity	0.122	0.293	0.208	0.218
Coating Process Efficiency [%]	97.272	96.432	93.453	91.693
IPC coated MT				
Hardness [N]	34.8	43	32.9	35.5
Height [mm]	2.97	3.01	2.95	2.96
Dissolution SGF immediate release [hh:mm:ss]	01:10:58	no release within 05:17:36	00:02:41	00:06:04
Taste masking [µg/ml]: 60s; 180s; 300s	0; 0; 0	0; 0; 0	0; 2.067; 65.534	0; 0; 14.861
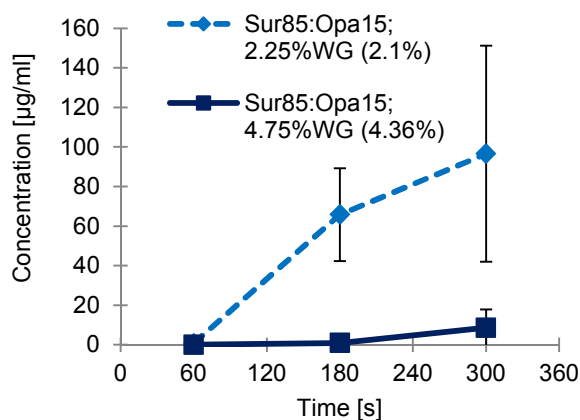
Figure 65: In vitro taste assessment in AS: cetirizine MT coated with Surelease® (CET1.2.II)
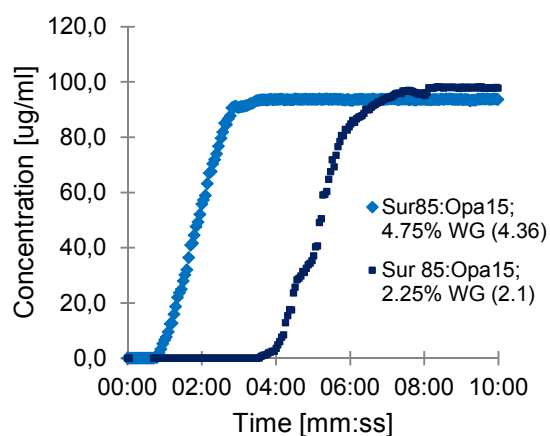
Figure 66: Dissolution in SGF: cetirizine MT coated with Surelease® (CET1.2.II)

6.4.2.2.   Design of Experiments

The pH dependent polymers need a specific amount of coating thickness and then full taste masking (0 % API release within 5 min) is achieved. No negative influence on the release in SGF was observed even at high coating levels. Since the pH independent polymer Surelease® extends the drug release in case of a too high coating level or if too less pore former is incorporated, a DoE was performed with this polymer to find acceptable process and formulation ranges. The compromise between the requirements for a sufficient taste masking and an immediate release profile should be investigated. The DoE was performed with the cetirizine dihydrochloride minitablets.

The main goal of the DoE was to evaluate the individual and joint effects of the polymer to pore former ratio, the spraying rate and the spraying time on relevant critical quality attribute responses (CQAs) related to taste masking, dissolution and other properties of the coated minitablets, and also on the efficiency of the coating process.

Factor Levels and Run Order
Table 33 shows the ranges over which the factors were investigated. In this table, column "Label" shows the factor names as used by the R software to generate all plots included in this thesis. The column "CodedName" includes the names used for fitting regression models. The used R code is shown in Appendix XII.

Table 33: Experimental factors and levels

Name	Label	Unit	CodedName	Low	Target	High
Polymer Ratio	Polymer.Ratio	% w/w	Pol.Ratio	75	80	85
Spraying rate	Spraying.Rate	g/min	Spray.Rate	1	2	3
Spraying Time	Spraying.Time	min	Spray.Time	45	70	95

The experiment was designed as a 2^3 full factorial design with three center points (CP) to investigate also the variability across the experimental space of the DoE. The initial order of the factorial runs was randomized and the CPs were placed at the beginning, middle and end of the DoE. However the run order was changed so that the number of coating solution preparations could be minimized for logistical reasons. The actual run order is given in Table 35. The solution for runs 3, 4 and 5 was prepared at the same time and similarly for runs 7 and 8, and for 9 and 10. The composition of the coating suspensions is shown in Table 34.

Table 34: Coating suspension composition DoE

	Surelease 75:Opadry25	Surelease 80:Opadry20	Surelease 85:Opadry15
	Composition [%]	Composition [%]	Composition [%]
Surelease	44.00	47.75	50.00
Opadry II clear	23.33	19.75	13.33
colorant	0.50	0.50	0.50
Water	32.17	32.00	36.17
Sum	*100.00*	*100.00*	*100.00*

Table 35: Factor Levels and Run Order

Run	Pattern	Polymer.Ratio	Spraying.Rate	Spraying.Time
1	+−−	85	1	45
2	0	80	2	70
3	++−	85	3	45
4	+−+	85	1	95
5	+++	85	3	95
6	0	80	2	70
7	−−+	75	1	95
8	−−−	75	1	45
9	−++	75	3	95
10	−+−	75	3	45
11	0	80	2	70

The process parameters, which were not investigated in the DoE, were kept constant at the following level:

air volume rate	100 m³/h
distance base plate-Wurster column	14 mm
atomization pressure	1.25 bar
nozzle bore diameter	0.5 mm
nozzle cap type	A
Spray rate [g/min]	1 ; after 10 min adjusted to level
inlet air temperature	58-71 °C
	adjusted that the product temperature stayed at 43±0.5 °C

Table 36 includes all responses of interest, their units and the corresponding labels used for statistical analysis. The response taste masking is the drug concentration in artificial saliva after the specific time assessed by the in vitro taste assessment (5.7. In vitro Taste Assessment).

Table 36: Responses related to minitablet properties and coating process efficiency

Name	Label	Unit
Taste Masking at 60 seconds	Taste.masking.60s	µg/mL
Taste Masking at 180 seconds	Taste.masking.180s	µg/mL
Taste Masking at 300 seconds	Taste.masking.300s	µg/mL
Time to 85% Dissolved	Dissolution	sec
Coating Uniformity	Coating.Uniformity	unitless
Coating Process Efficiency	Coating.Process.Efficiency	%
Hardness	Hardness	N
Height	Height	mm

Linear regression models that included all main and two-factor interaction effects were fitted to the experimental data to analyze the individual and joint effects of the factors on all relevant responses, except for Taste.masking.60s and Taste.masking.180s. These responses had only two, respectively three, non-zero values over all experimental runs and statistical analysis did in so has been unable to make a conclusion based on these results (Appendix IX).

All factors investigated in the DoE were considered continuous; that is, theoretically, these factors could be set at any value within their considered range. During the factorial runs, the factors were set either at low or high values. For the CP runs, the factors were set at mid-range level.

When fitting regression models, the low factor levels were coded with -1, high levels with +1 and mid-range values with 0. To achieve that, the actual levels of a factor F were transformed as follows (see Equation (22))

$$x_F = \frac{F - (F_{low} + F_{high})/2}{(F_{high} - F_{low})/2} \tag{22}$$

where x_F is the coded variable corresponding to factor F, and F_{low} and F_{high} are the values corresponding to the low and high levels of factor F, respectively.

As an example for the regression model the joint effect of the three factors on the minitablet hardness could be determined with the following Equation (23). It includes all three main effects and three two-factor interactions (2FI).

$$\text{Hardness} = \hat{\alpha} + \hat{\beta}_{\text{Pol.Ratio}} x_{\text{Pol.Ratio}} + \hat{\beta}_{\text{Spray.Rate}} x_{\text{Spray.Rate}} + \hat{\beta}_{\text{Spray.Time}} x_{\text{Spray.Time}} +$$
$$+ \hat{\beta}_{\text{Pol.Ratio:Spray.Rate}} x_{\text{Pol.Ratio}} x_{\text{Spray.Rate}} + \hat{\beta}_{\text{Pol.Ratio:Spray.Time}} x_{\text{Pol.Ratio}} x_{\text{Spray.Time}} +$$
$$+ \hat{\beta}_{\text{Spray.Rate:Spray.Time}} x_{\text{Spray.Rate}} x_{\text{Spray.Time}}$$

(23)

The β's in Equation (23) are the estimates of the coefficients corresponding to the main effects and 2FIs. Note that the coefficients for the interaction effects have the names of the two corresponding factors as a subscript (e.g., coefficient for the interaction between spraying rate and spraying time is denoted by $\beta_{\text{Spray.Rate:Spray.Time}}$). These estimates are included in Table 38. In this table, the β's from Equation (23) are denoted by the name of their corresponding effects; that is, only the subscripts of the β's are included. For example, the main effect of spraying rate is denoted by Spray.Rate, whereas the interaction between spraying rate and spraying time is denoted by Spray.Rate:Spray.Time. The values corresponding to the intercept α can be found in Table 37 as the grand mean of the corresponding response.

We interpret the estimates of the regression coefficients in Equation (23) as half of the corresponding effect sizes (or simply, the effects). That is, the effects are computed as the estimates of the regression coefficients are multiplied by 2.

In general, the effect corresponding to a certain factor is called a main effect, whereas the joint effect of two factors is called an interaction effect. The main effects are interpreted as the average change in response when the factor is varied from low to high level, where the average is taken over all levels of the other experimental factors.

Having large interaction effects between two factors means that the effect of one of the factors depends on the level of the other For example the response Taste.masking.300s shows a large interaction effect between spraying rate and spraying time. The effect of spraying rate depends on the level of spraying time (see Figure 67). That is, when the spraying time is set at high level (95), the average change in Taste.masking.300s is Spray.Rate+Spray.Rate:Spray.Time=-29.623 µg/ml, when we change spraying rate from low (1) to high (3). However, when the spraying time is set at low level (45), the average change in Taste.masking.300s is Spray.Rate-Spray.Rate:Spray.Time=-130.233 µg/ml, when we change spraying rate from low to high.

Table 37: Summary Statistics of responses

Response	Min	Max	Range	Median	Mean	Std.Dev	CV
Taste.masking.60s	0.00	1.41	1.41	0.00	0.14	0.42	293.83
Taste.masking.180s	0.00	49.03	49.03	0.00	7.35	16.33	222.09
Taste.masking.300s	0.00	143.11	143.11	0.26	29.43	52.34	177.84
Dissolution	161.00	1860.00	1699.00	434.00	589.36	532.80	90.40
Coating Uniformity	0.18	0.24	0.06	0.22	0.22	0.02	8.50
Coating Process Efficiency	84.26	98.15	13.90	93.45	93.40	4.08	4.37
Hardness	30.60	41.70	11.10	36.30	35.71	3.25	9.10
Height	2.94	3.06	0.12	2.95	2.97	0.04	1.42
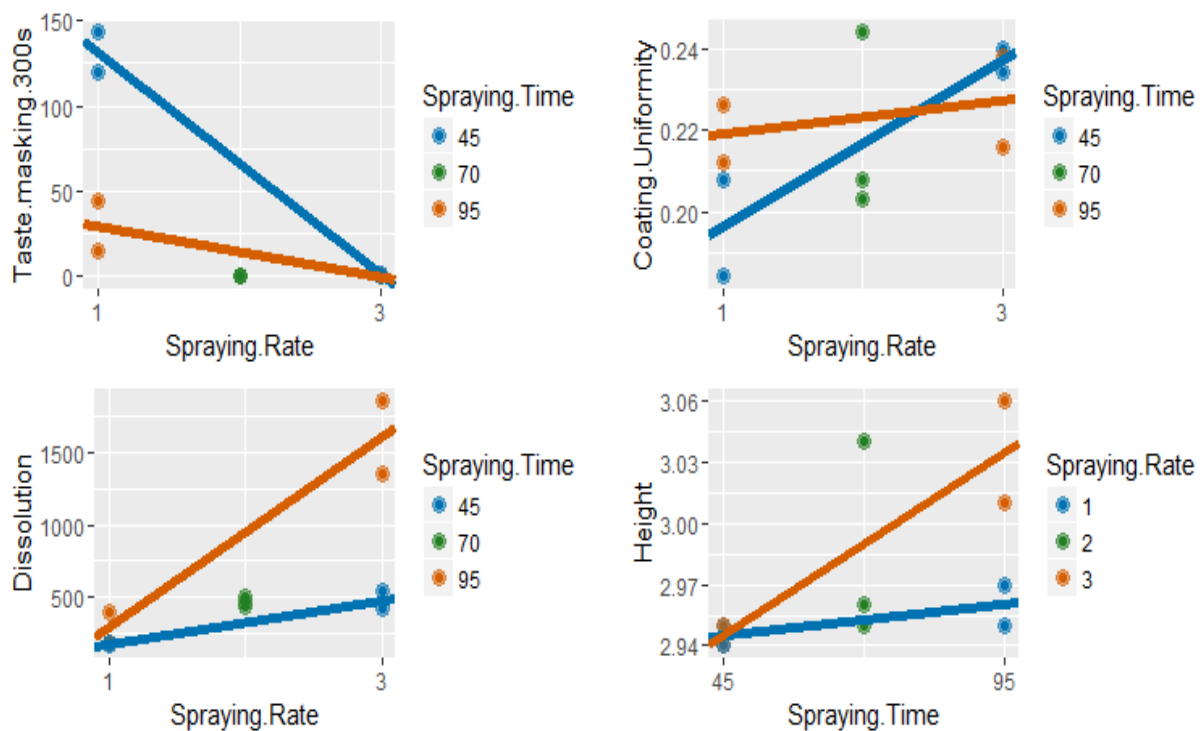
Figure 67: Interaction effects plot

Results

Most of the taste masking values at 60 and 180 seconds were zero. For Taste.masking.60, there were two values larger than zero, 0.174 and 1.41 µg/ml, both values being generated when the spraying rate and spraying time were low. For Taste.masking.180s, there were three values larger than zero with a maximum of 50 µg/ml, all of them being generated at low spraying rate and spraying time.

Table 38: Output linear regression models

Response	Effect	Effect Size	Estimate	Std.error	p.value
Taste.masking.300s	Spray.Rate	-79.93	-39.96	10.57	0.02
Taste.masking.300s	Spray.Time	-51.32	-25.66	10.57	0.07
Taste.masking.300s	Spray.Rate:Spray.Time	50.30	25.15	10.57	0.08
Taste.masking.300s	Pol.Ratio:Spray.Rate	13.69	6.85	10.57	0.55
Taste.masking.300s	Pol.Ratio	-12.94	-6.47	10.57	0.57
Taste.masking.300s	Pol.Ratio:Spray.Time	-1.82	-0.91	10.57	0.94
Dissolution	Spray.Rate	813.00	406.50	46.45	0.00
Dissolution	Spray.Time	624.50	312.25	46.45	0.00
Dissolution	Spray.Rate:Spray.Time	508.50	254.25	46.45	0.00
Dissolution	Pol.Ratio	200.50	100.25	46.45	0.10
Dissolution	Pol.Ratio:Spray.Time	152.00	76.00	46.45	0.18
Dissolution	Pol.Ratio:Spray.Rate	109.50	54.75	46.45	0.30
Coating.Uniformity	Spray.Rate	0.02	0.01	0.01	0.10
Coating.Uniformity	Spray.Rate:Spray.Time	-0.02	-0.01	0.01	0.23
Coating.Uniformity	Pol.Ratio	0.02	0.01	0.01	0.23
Coating.Uniformity	Spray.Time	0.01	0.00	0.01	0.61
Coating.Uniformity	Pol.Ratio:Spray.Rate	0.00	0.00	0.01	0.84
Coating.Uniformity	Pol.Ratio:Spray.Time	0.00	0.00	0.01	0.90
Coating.Process.Efficiency	Pol.Ratio	4.06	2.03	1.93	0.35
Coating.Process.Efficiency	Spray.Rate:Spray.Time	-2.03	-1.01	1.93	0.63
Coating.Process.Efficiency	Pol.Ratio:Spray.Rate	1.20	0.60	1.93	0.77
Coating.Process.Efficiency	Spray.Rate	-1.17	-0.59	1.93	0.78
Coating.Process.Efficiency	Pol.Ratio:Spray.Time	0.23	0.12	1.93	0.96
Coating.Process.Efficiency	Spray.Time	0.17	0.09	1.93	0.97
Hardness	Spray.Rate	6.42	3.21	0.37	0.00
Hardness	Spray.Time	2.33	1.16	0.37	0.03
Hardness	Pol.Ratio:Spray.Time	-1.57	-0.79	0.37	0.10
Hardness	Spray.Rate:Spray.Time	0.92	0.46	0.37	0.28
Hardness	Pol.Ratio:Spray.Rate	-0.78	-0.39	0.37	0.35
Hardness	Pol.Ratio	-0.18	-0.09	0.37	0.82
Height	Spray.Time	0.05	0.03	0.01	0.13
Height	Spray.Rate:Spray.Time	0.04	0.02	0.01	0.25
Height	Spray.Rate	0.04	0.02	0.01	0.25
Height	Pol.Ratio:Spray.Rate	0.01	0.01	0.01	0.68
Height	Pol.Ratio	0.01	0.00	0.01	0.80
Height	Pol.Ratio:Spray.Time	0.01	0.00	0.01	0.80

The largest effect on Taste.masking300s are the individual effects of spray rate and spray time and the joint effect of both. As shown in Figure 67 Taste.masking.300s decreases when the spraying rate is increased, i.e. the taste masking is more efficient. However, when the spraying time is set at low level, the decrease in Taste.masking300s is much steeper than in the case where the spraying time is high. Taste.masking300s should be as close to zero as possible. Setting the spraying rate at 3 g/min generates Taste.masking300s values equal to zero, no matter of the spraying time or polymer to pore former ratio levels. From the generated data the hypothesis can be proposed that when the spraying rate is set at the high level, the coating process is robust to changes in the levels of the other factors with respect to Taste.masking300s, which indicates that a spray rate of 3 g/min is the optimal setting with regards to the Taste.masking.300s. The higher the spray rate the higher is the Weight gain, which ensures efficient taste masking. However, the compromise between taste masking and dissolution has to be found.

Dissolution is defined here as the average time until 85 % of the API is released. Run 5 did not have any drug release within the duration of the analysis (30 min), therefore the value was set to 31 minutes, i.e., 1860 seconds (even was not released). The upper specification limit for Dissolution is 15 minutes (i.e., 900 seconds). The largest effect on Dissolution is the join effect of spraying rate and spraying time. Figure 67 shows that the time to 85% drug release increases with spraying rate; however, this effect is small when the spraying time is low and is much larger when the spraying time is high. The setting where the spraying rate is low generates low dissolution time values regardless of the levels of the other factors. However, both responses Taste.masking300s and Dissolution should be optimized. There are two settings where both responses are low; one corresponds to the center-point runs where the spraying rate is 2 g/min and the spraying time is 70 min. The second setting corresponds to high spraying rate and low spraying time.

Polymer to pore former ratio in the examined range had no significant influence on taste masking, which is shown in Table 38 where the factor Pol.Ratio exhibit only low values in the effect size of the responses Taste.masking.300s and Dissolution.

The largest effect on Coating.Uniformity is the join effect of spraying rate and spraying time (see Figure 67). When the spraying time is set at high level there is almost no effect of spraying rate on Coating.Uniformity. However, when the spraying time is set at low level, Coating.Uniformity increases with the spraying rate. As in the case of Taste.masking.300s and Dissolution, low variability for the Coating.Uniformity. During the DoE, low values were obtained at CP setting and when both the spraying rate and time were low. One of the CP values was unusually large and could be explained by some process issues encountered during that run.

The spraying rate and time are the two process parameters that determine the minitablet weight gain (%) after coating. For the setup of the DoE, the weight gain is given by the following formula (24):

$$\text{Weight. Gain} = 0.15 \times \frac{\text{Spraying. Rate} \times \text{Spraying. Time} - 10 \times (\text{Spraying. Rate} - 1)}{3} \qquad \textbf{(24)}$$

Figure 68 includes a contour plot of Weight Gain over the experimental space of the different spraying rate and spraying time settings of this DoE. The five black dots in the plot represent the Weight Gain values corresponding to the DoE factorial runs and CPs. The Weight Gain values mostly increase with the spraying rate as long as the spraying rate is low. However, as the spraying rate increases Weight Gain is also influenced by the spraying time. For example, when the spraying rate is around 3 g/min, Weight Gain increases from around 5 to 14% when the spraying time is increased from 45 to 95 min. As shown in Equation (24) and in the contour plot, we note that the largest effects on Weight Gain is the individual and join effects of spraying rate and spraying time. As for both Taste.masking.300s and Dissolution the largest effect was the effect of spraying rate, - time and their interaction and knowing that these two parameters determine the weight gain after coating in an interactive manner, it is plausible that it is Weight Gain that mainly drives Dissolution and Taste.masking.300s.
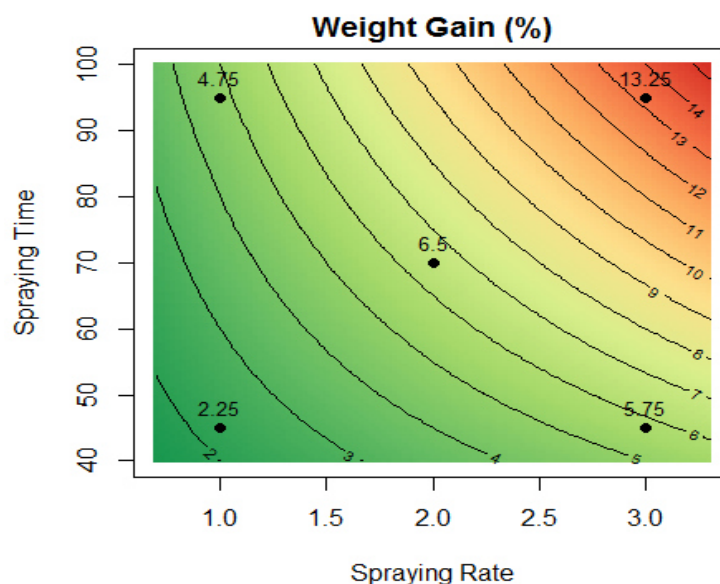
Figure 68: Contour plot of weight gain [%]

Figure 69 shows a scatter plot of Dissolution vs. Taste.masking.300s where the data points are color-coded based on the Weight Gain levels. Efficient taste masking is achieved when the Dissolution values are below 15 min and Taste.masking.300s values are close to zero.

That is obtained when Weight.Gain is between 5.75 and 6.5%. This range covers the CP setting and run 3 and 10 where the spraying rate is 3 g/min and spraying time is 45 min.
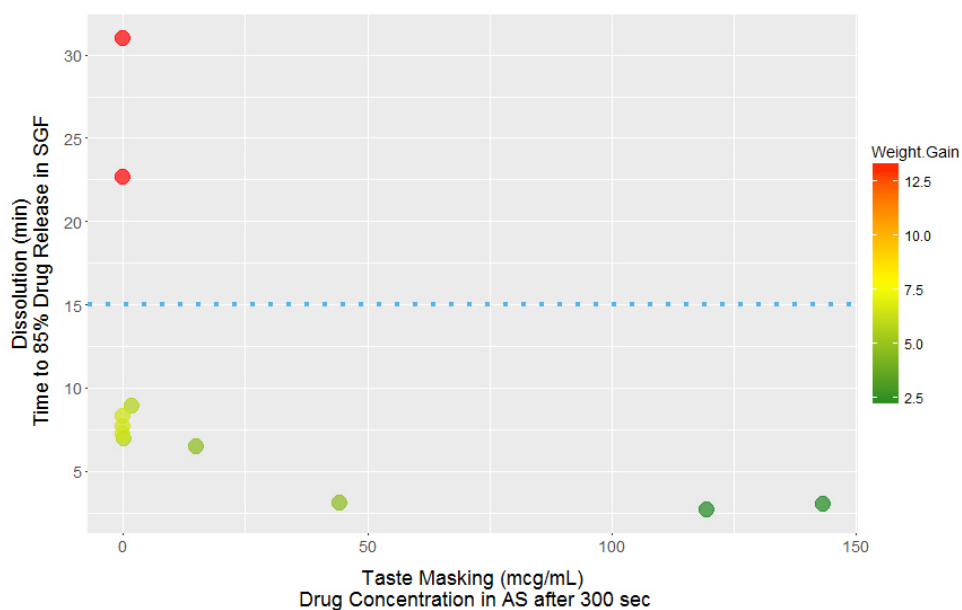
Figure 69: Scatter plot of Dissolution (Time to 85% drug release [min]) vs Taste masking (Drug concentration is AS after 300s [µg/ml]) by weight gain [%]

Discussion

The validity of the hypothesis that other process settings of spray rate and spray time, which were not investigated during the DoE, that would yield a Weight.Gain between 5.75 and 6.5 % could also generate minitablets with Taste.Masking.300s close to zero and low Dissolution values and could be further investigated in a follow-up study.

As already mentioned the DoE was initially designed as a completely randomized full-factorial experiment. But the DoE was performed in a sequence with 3 runs having the high polymer ratio and later on 4 runs with low polymer ratio so that the number of coating solution preparations could be minimized. Therefore, the effect of polymer ratio could be confounded with the effect of any other unknown process parameters that varies in a same manner as the polymer ratio. That could also be the case for the response Coating Process Efficiency. The largest effect on this response has the polymer ratio. Process efficiency increases with the polymer ratio. There is no scientific explanation for such an effect. The process efficiency decreases over time most likely due to some other reasons such as the clogging of the filters in the fluid bed coater or the filter for the exhaust air of the RABS. This might be a possible the explanation for the spurious effect of polymer ratio on the process efficiency. As the polymer to pore former ratio had no effect on the taste masking and dissolution, the levels of the factor may have been set in a too narrow range to observe any significant effect.

6.5.   *X-ray µCT and SEM*

6.5.1.   Acetaminophen Minitablets
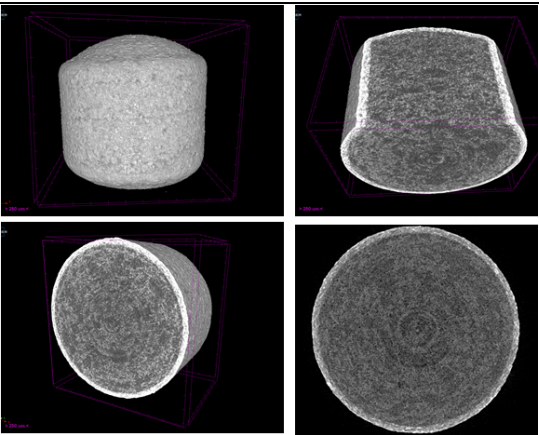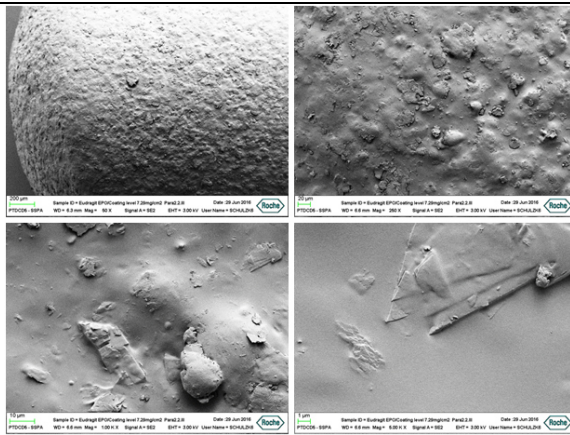
In Table 39, the X-Ray µCT and SEM images of the acetaminophen minitablets coated with the pH dependent polymers Eudragit E PO® and Kollicoat® Smartseal 30D are shown. The X-ray µCT images display different cross-sections of the 3D image. The SEM picture shows the coating morphology with different magnifications factors of 50x; 250x; 1000x and 5000x.

The core of the minitablet looks very homogeneous and does not exhibit any signs of solid phase separations. The surface of the EPO coated tablet seems to be very rough, possibly due to blockage of the filter, the solid particles of spray dried coating suspension were deposited on the surface.

SEM images of the Kollicoat Smartseal coated minitablets (magnification factor of 1000x and 5000x of Para2.2.V and Para2.3.V-2) depict cracks on the surface; however were fully taste masked wihout any API release in artificial saliva. Crack formation could result from the sample preparation when the minitablets are in vacuum during SEM analysis, where they will automatically dry and shrink due to the loss of water. The reason why the EPO coated minitablets do not exhibit cracks could be due to the higher elasticity of the coating polymer.

As discussed in chapter 6.4.1.1 a coating level of 4 mg/cm² of Kollicoat® Smartseal 30D was necessary for taste masking for the acetaminophen minitablets. This coating level results in a thickness of 37 µm.

Table 39: X-Ray µCT and SEM images of EPO and SMA coated MTs

Para2.3.IV-1(SMA)	Para2.3.V-1 (SMA)	Para2.3.V-2 (SMA)	Para2.2.V (SMA)
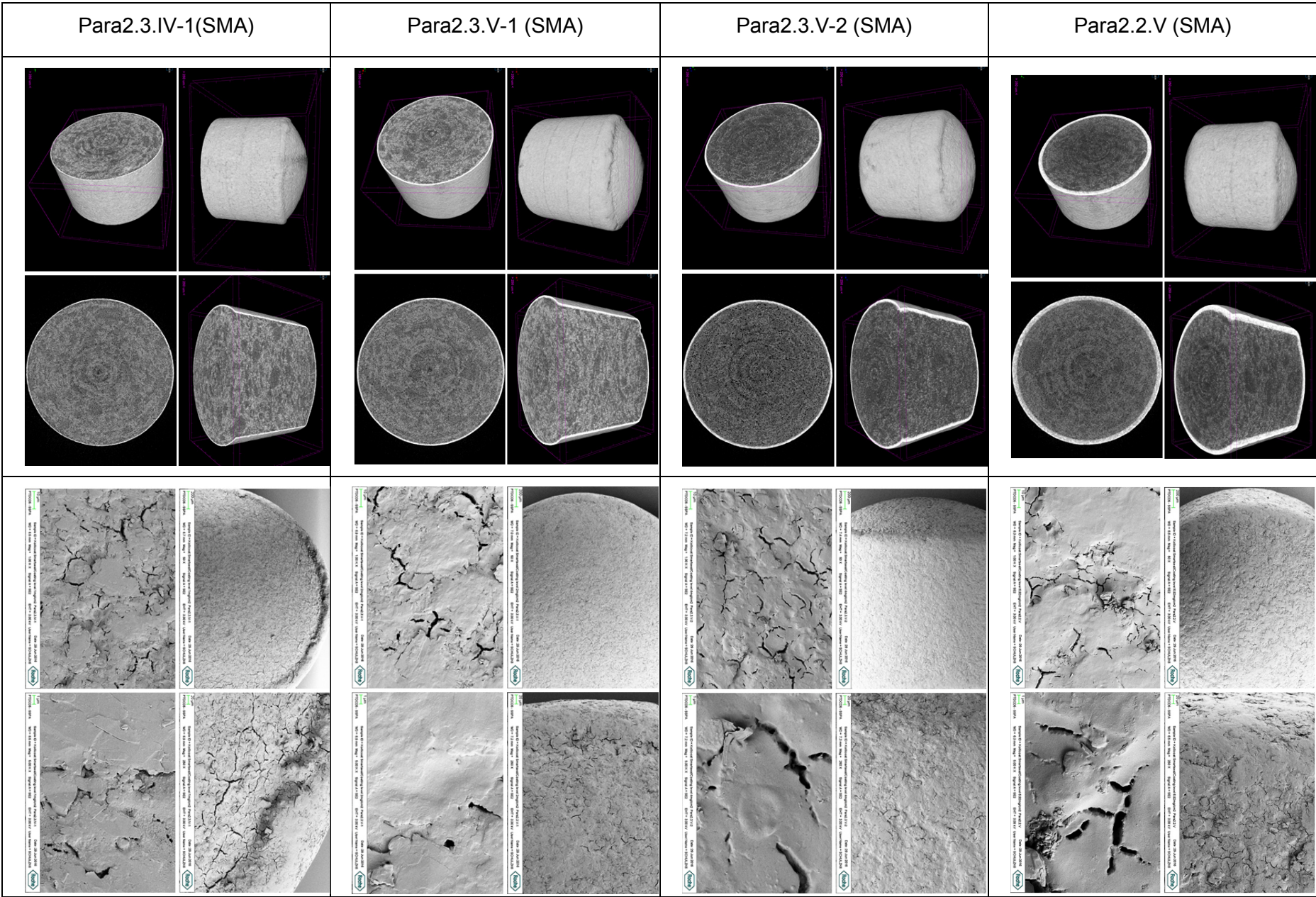
The coating thicknesses were measured with SEM and X-ray µCT (Appendix XIV & 0). For the SEM imaging the minitablet was cut in two pieces and the thickness was measured on the cross section, which is shown in Figure 70 and Figure 71. SEM has a greater resolution, but is just measured at two locations. In comparison the X-ray µCT has a lower resolution of 1µm, but it is statistically more accurate due to the high number of measuring point (between 600 -700). Furthermore the SEM measurement is needed to make sure that no artifact is measured with the X-ray µCT. In summary there is a good correlation between the X-ray µCT and SEM measured coating thicknesses, which is shown in Figure 72.
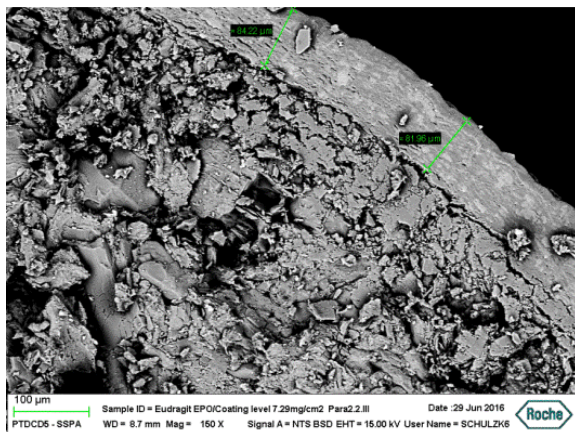
Figure 70: Coating thickness of Para2.2.III (EPO 6.31mg/cm²) determined by SEM
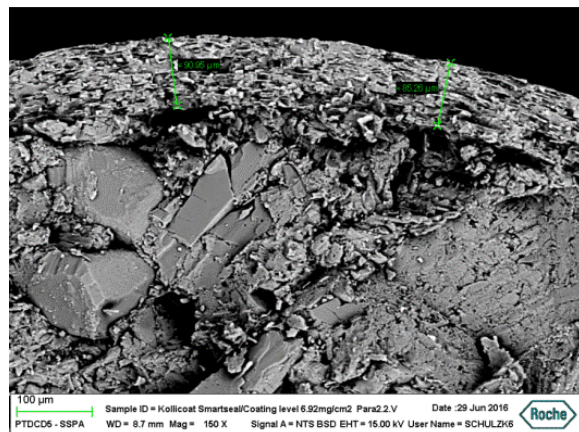
Figure 71: Coating thickness of Para2.2.V (SMA 6.92mg/cm²) determined by SEM
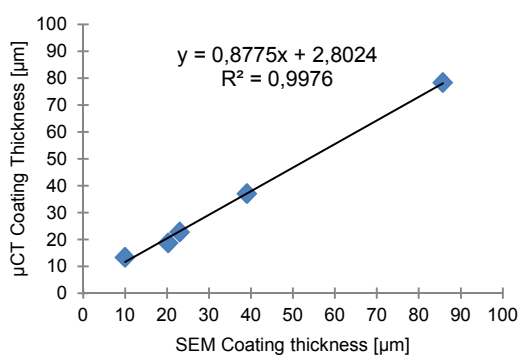
Figure 72: Correlation X-ray µCT and SEM coating thicknesses
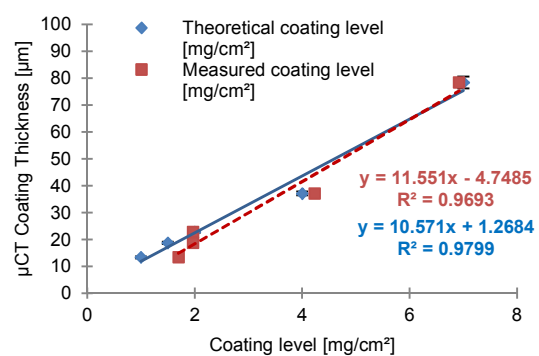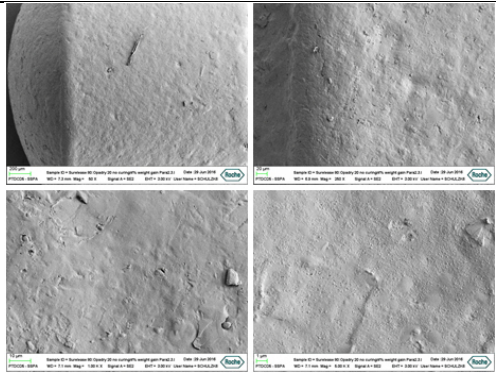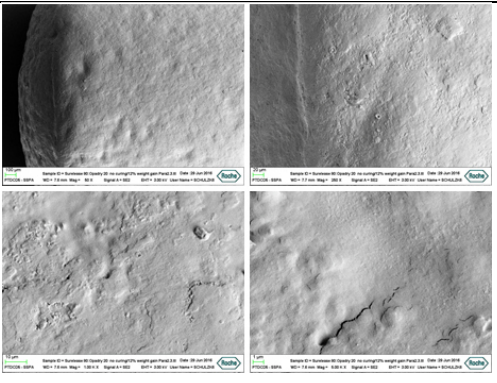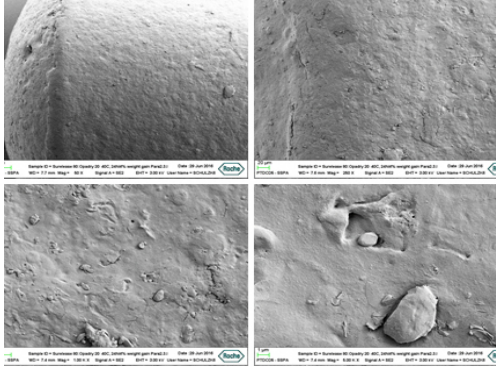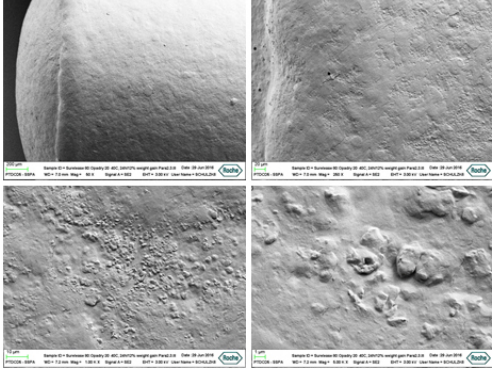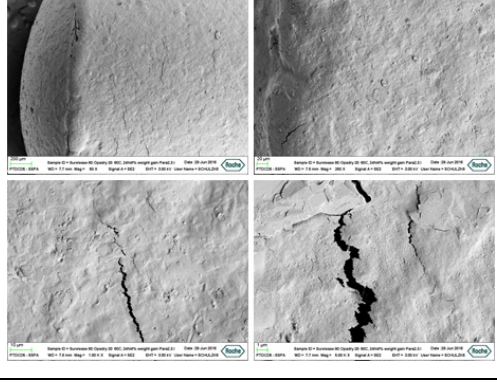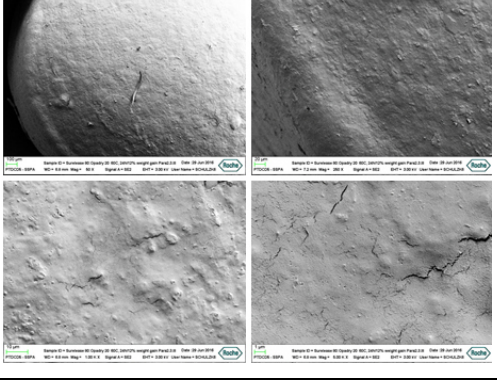
Figure 73: Correlation of coating thickness with theoretical and measured coating level

In Figure 73 the linear relationship between the coating layer thickness and the theoretical and measured coating level is shown. The difference between the theoretical and the measured coating level is not only because of the coating losses, also because determining coating level just by weighing can be inaccurate due the weight variations of the cores itself. Anyhow it is a good correlation taking into account experimental error

Table 40 shows the surface morphology of Surelease® coated minitablets undergoing different curing conditions. The minitablets which were cured at 60 °C for 24 h exhibited cracks. Minitablets with the lower weight gain exhibiting larger cracks and with the higher weight gain just smaller ones. The surface was smooth except some deposited spray dried droplets.

Table 40: SEM images acetaminophen MT coated with Surelease®

	Sur80:Opa20, 4%WG (Para2.3.I)	Sur80:Opa20, 12%WG (Para2.3.III)
No curing		
40°C, 24 h		
60°C, 24 h		

6.5.2.   Cetirizine Minitablets

Figure 74 shows the X-ray µCT image of the minitablets coated with the center point parameter setting in the DoE. The core of the cetirizine minitablet exhibit light spots in the X-ray µCT image. These light spots are in general materials having a higher X-ray extinction coefficient as a result of a higher density (resp. electron density or nucleus weight) or a different chemical composition. Therefore it can be assumed that these light spots represent the
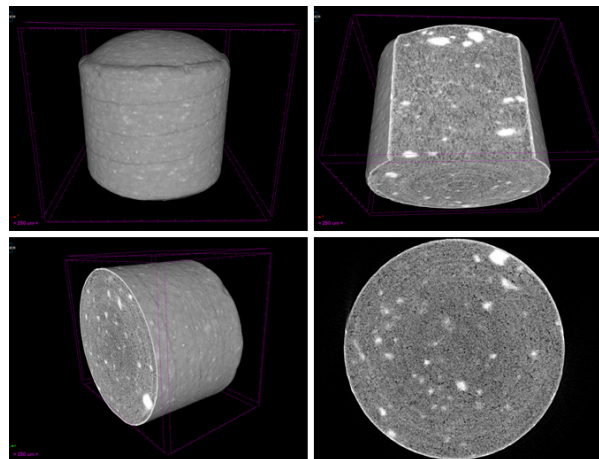
Figure 74: X-Ray µCT: center point (Sur80:Opa20; 2g/min, 70min)

cetirizine possessing chloride atoms. These spots in the minitablet seem from visual stand point not to be homogeneously distributed. However during the dissolution of the minitablets 100±5% drug was released over all batches; therefore it can be assumed that the overall distribution was good enough. Nevertheless further particle size reduction of the rather broad distribution (Table 19) would make sense to improve the homogeneity (e.g. via hammer milling, pin milling).

The minitablets had a glossy appearance, however the surface was still relatively rough (see Figure 75), which is an indication for a too dry process.
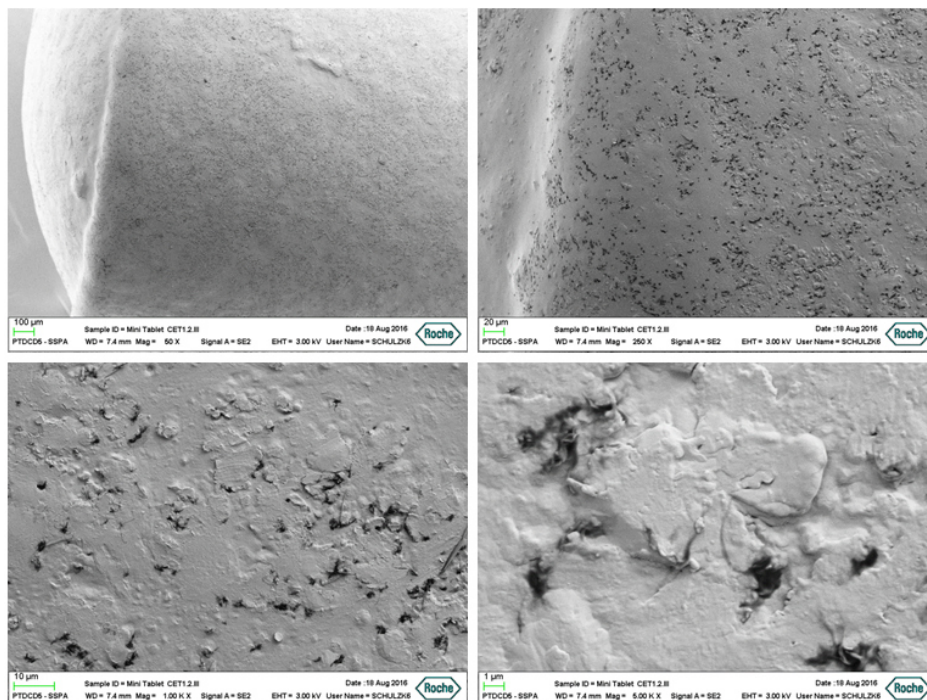
Figure 75: SEM image: center point (Sur80:Opa20, 2g/min, 70min)

6.6.   Determination of the Bitterness Threshold of Cetirizine Dihydrochloride

6.6.1.   E tongue measurement

The goal of these measurements was, to determine the bitterness threshold of cetirizine dihydrchloride. The bitterness threshold is needed as an acceptance criterion for the in vitro taste assessment. Concentrations of cetirizine and bitterness standard (similar compound with known bitterness threshold) should be measured with the e tongue and the sensor responses compared. The compound quinine hydrochloride was chosen as a bitterness standard because in vivo data and the bitterness threshold are available for this drug. Additionally the substance also exists as a hydrochloride form.

Figure 76: Stock solution cetirizine in artificial saliva

The e-tongue measurements should be conducted in the described artificial saliva, since this media was used for the all in vitro taste assessment in this thesis. It was observed while the preparation of the stock solution of cetirizine in artificial saliva that a slime was built when the artificial saliva was added to the cetirizine. The dissolved cetirizine decreased the pH of the artificial saliva, and the contained enzymes precipitated at the lower pH. As mitigation the stock solution was then prepared with phosphate puffer pH 6.8 according USP/Ph.Eur. to ensure that precipitation of the enzymes had caused the slime formation (Figure 77). No precipitation or slime formation occurred,

Figure 77: Stock solution cetirizine in phosphate puffer pH 6.8

therefore the API should be first dissolved in 5 ml water and then the remaining artificial saliva added.

The following series of concentrations were measured (see Table 41).

Table 41: Series of concentration for e-tongue measurement

Measurement	Cetirizine dihydrochloride		Quinine hydrochloride	
	Conc. [mg/l]	Conc. [mM]	Conc. [mg/l]	Conc. [mM]
1	$2*10^{-1}$	$4.331*10^{-1}$	$1.7*10^{-1}$	$4.331*10^{-1}$
2	$2*10^{-2}$	$4.331*10^{-2}$	$1.7*10^{-2}$	$4.331*10^{-2}$
3	$2*10^{-3}$	$4.331*10^{-3}$	$1.7*10^{-3}$	$4.331*10^{-3}$
4	$2*10^{-4}$	$4.331*10^{-4}$	$1.7*10^{-4}$	$4.331*10^{-4}$

First the concentration series of both compounds were measured in artificial saliva (composition as described in chapter 5.7). The sensor responses are shown in Figure 78.
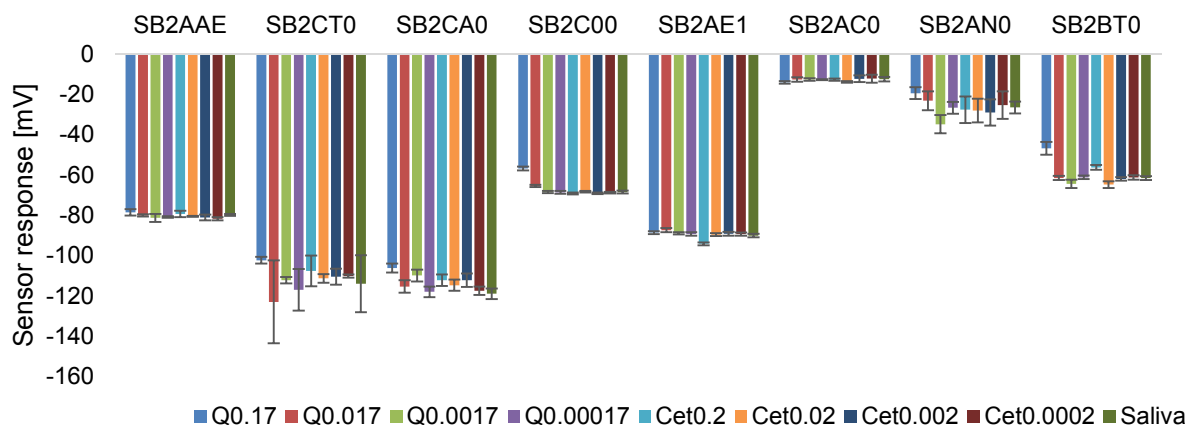
Figure 78: Sensor responses in artificial saliva

There was no concentration dependent sensor response present. Sensor SB2AC0 showed even for all concentrations the same response. However sensor SB2AN0 showed a change in the response depending on the concentration, but the standard deviation was then too high. As hypothesis it could be interpreted, that the salts of the artificial saliva may overlay the sensor responses at the fairly low concentrations of the two measured drug compounds.

Therefore a dilution series from the stock solution in artificial saliva was performed with deionized water. The blank resp. pure artificial saliva was also diluted 1/10. The responses of the diluted solutions are shown in Figure 79.
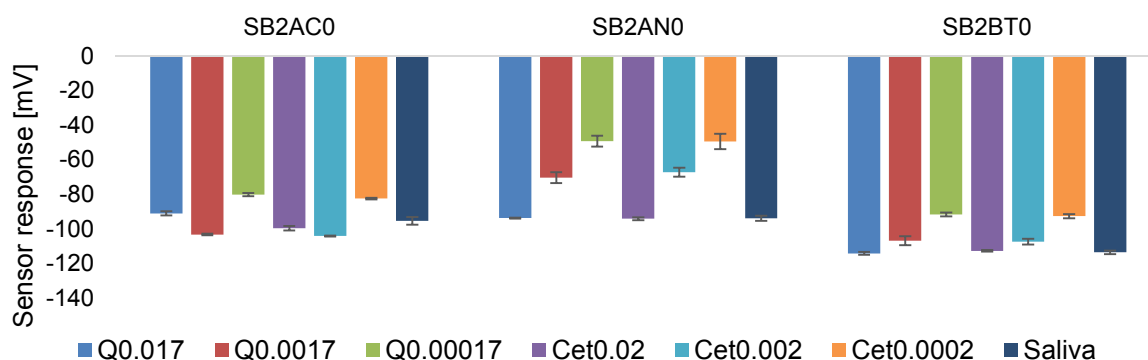
Figure 79: Sensor responses diluted artificial saliva

The sensors SB2AN0 and SB2BT0 showed now a concentration dependent sensor response. But it cannot be distinguished if the concentration dependency is due to the diluted saliva medium at different ionic strength or could be linked to the API. Therefore a third measurement of the compounds in water was performed. The sensor responses are shown in Figure 80. The bitterness sensors SB2AC0, SB2AN0 und SB2BT0 showed a

concentration dependent sensor response. The other sensors are taste sensors. They show as well a concentration dependency, but the standard deviations are too large.
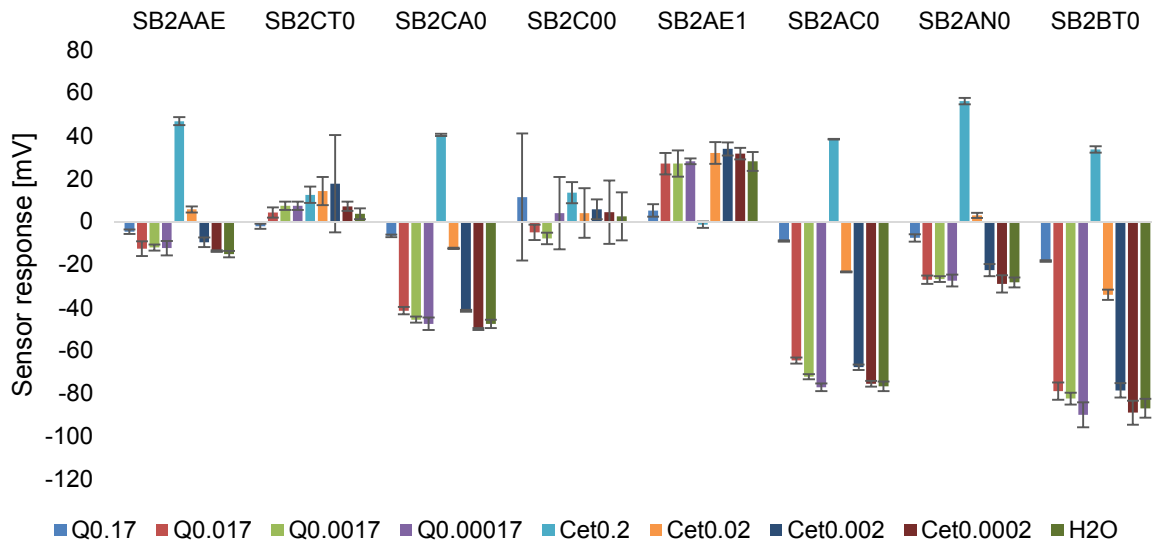
Figure 80: Sensor responses in water (Univariate analysis)

Figure 81 illustrates the sensor responses of quinine and cetirizine depending on their concentration displayed on logarithmic scale. The compounds exhibit a linear relationship in a specific concentration range. It is visualized that cetirizine causes a higher sensor response than quinine. This could be an indication that cetirizine has higher bitterness than quinine. From the known bitterness threshold of quinine at 9 mg/l the sensor response according to the linear equation was calculated. Similarly the bitterness threshold of cetirizine was determined for the different sensors (see Table 42).
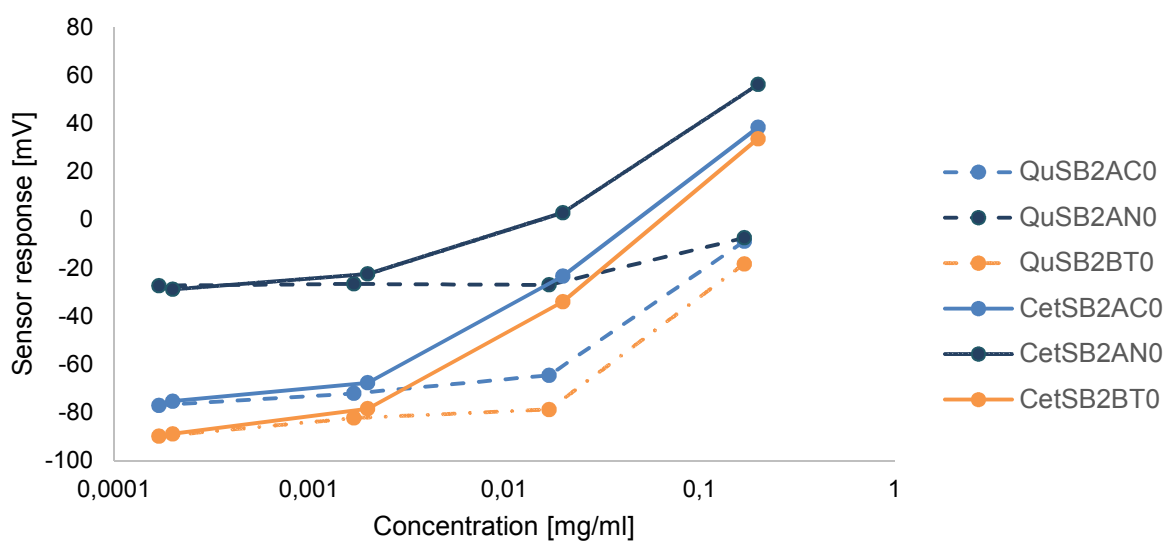
Figure 81: Concentration dependent sensor response (logarithmic scale)

Table 42: Bitterness threshold cetirizine depending of use sensor

Sensor	Bitterness Threshold Cetirizine [µg/ml]
SB2AC0	1.6782
SB2AN0	0.7814
SB2BT0	1.6246

Discussion

As shown in Figure 80 the sensor SBAN0 exhibit large difference in the sensor responses at different concentrations. This indicates a high sensitivity and the error bars are narrow. Also sensor SB2BT0 has a high sensitivity and this sensor is particularly recommended for bitter hydrochloride salts. Therefore the bitterness threshold of 1.6246 µg/ml of sensor SB2BT0 was used as an acceptance criteria for the in vitro taste assessment.

The compound quinine is a hydrochloride whereas cetirizine a dihydrochloride. The different resulting pH resp. ion strengths of the solutions might have an influence on the sensor responses. Due to the different pH the protonation grade could be different between cetirizine and quinine.

6.6.2.   Human taste panel

The human taste panel was conducted with 12 healthy volunteers (50% men, 50% female). The volunteers were between 23 and 37 years old (average 28.9±4.7 y) and one of the panelists was a smoker.

The raw data of the human taste panel are shown in Appendix XIV. The modeled bitterness score depending on the concentration of the cetirizine solution of all panelists is shown in Figure 82. An ordered nominal logistic regression was performed using the software JMP (Version 12, SAS Institute, Cary, NC, USA) [137]. Figure 83 shows the on y-axis the probability on the bitterness sc

ores depending on the concentration of the test solution. The three curves represent the change of the probabilities of the different bitterness scores. The bitterness score of 2 represent the first perception of a bitter taste by the panelist, consequently all scores above 1 exhibit a bitter taste. The bitterness threshold of 25 µg/ml was determined, where the probability is 75 % that the panelist would perceive a bitter taste, which is shown in Figure 83 (probability of bitterness score 1 is 0.25). There is also the highest probability (38.1 %) that the panelist would evaluate the taste with a bitterness score of 2.

This value is significant higher than the bitterness threshold of the e tongue. According to the bitterness threshold of the human taste panel all formulations of the DoE except of the runs having a weight gain of 2.25 % and 4.75 % (Run 7) were taste masked for 300 s (Appendix IX and X).

In the second part of the human taste panel the in vivo relevance of the in vitro taste assessment was evaluated. Therefore the duration until the first bitterness sensation of two samples was measured. Sample A were minitablets of the center point (run 2) in the DoE and represents the optimum of the factors. Sample B were minitablets from run 8 and had the lowest taste masking efficiency. The results are shown in Figure 84.

An outliner test according Grubbs was performed using g_{crit} (n=12, α=0.05) = 2.285. Based on Equation (25) the outliner could be evaluated, where $x_{min/max}$ are the limiting values, $\bar{x}$ is the mean and s the standard deviation. The result of one panelist was therefore neglected.

$$g_{crit} = \frac{\left|x_{min/max} - \bar{x}\right|}{s} \tag{25}$$
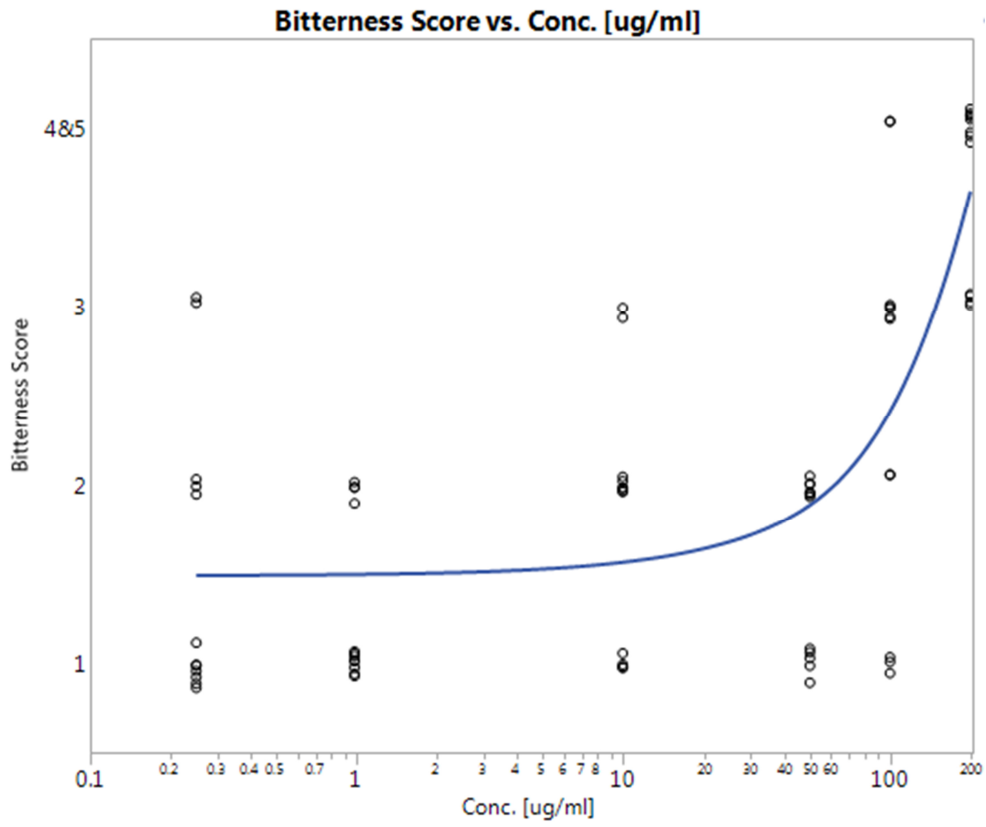
Figure 82: Bitterness scores of cetirizine dihydrochloride solutions
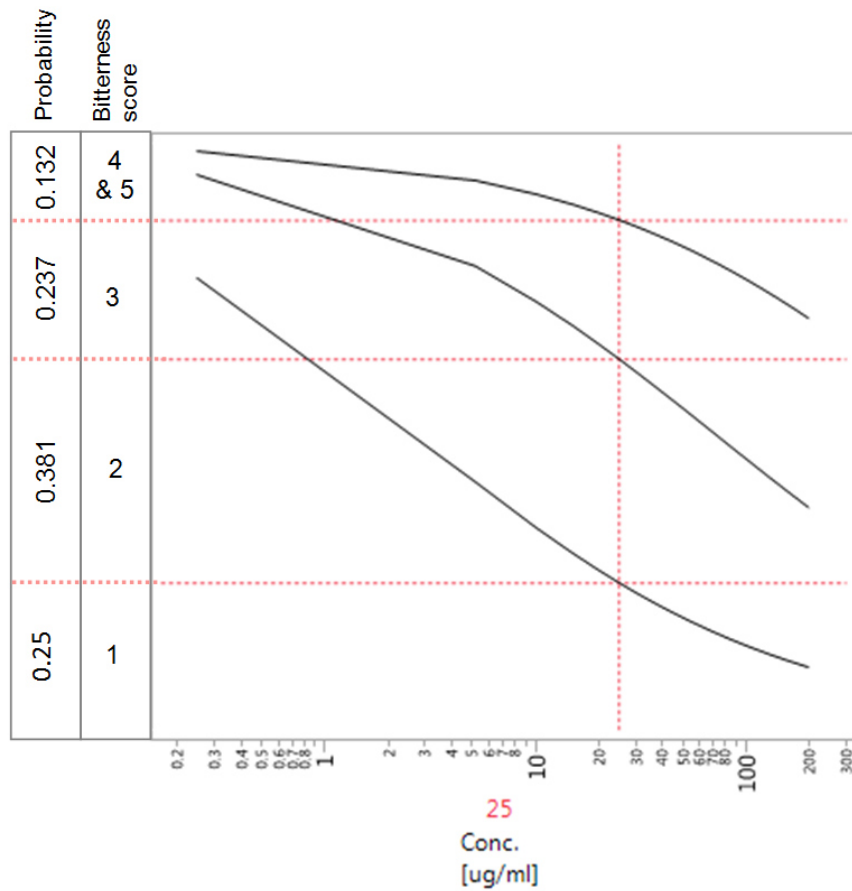
Figure 83: Ordinal logistic regression, 75% probability to receive a bitter taste

The panelists reported that when the coating layer cracked, they had immediately a strong bitter sensation. That happened with Sample B after an average time of 65.4 s and with Sample A after 260.7 s. As the test was stopped after 300 s the average of Sample A is underrepresented, hence 50 % did not detect any bitterness after 300 s and could be even longer.
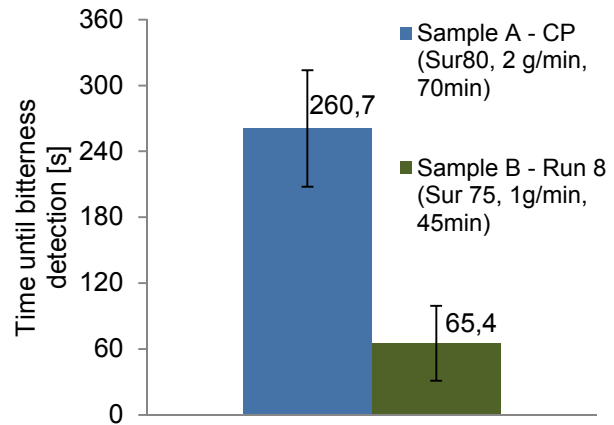
Figure 84: Biorelevance test - time until bitterness detection [s]

Figure 85 shows the correlation between the result of the human taste panel and the in vitro taste assessment. The lower part of the diagram visualizes the drug releases of the coated cetirizine minitablets in artificial saliva. Sample A did not have any drug release in artificial saliva and Sample B had at the sampling point of 60 s a released drug concentration of 1.41 µg/ml. That indicates that the coating layer was already "open". The upper part shows the time until the first bitter sensation was detected by the panelists.
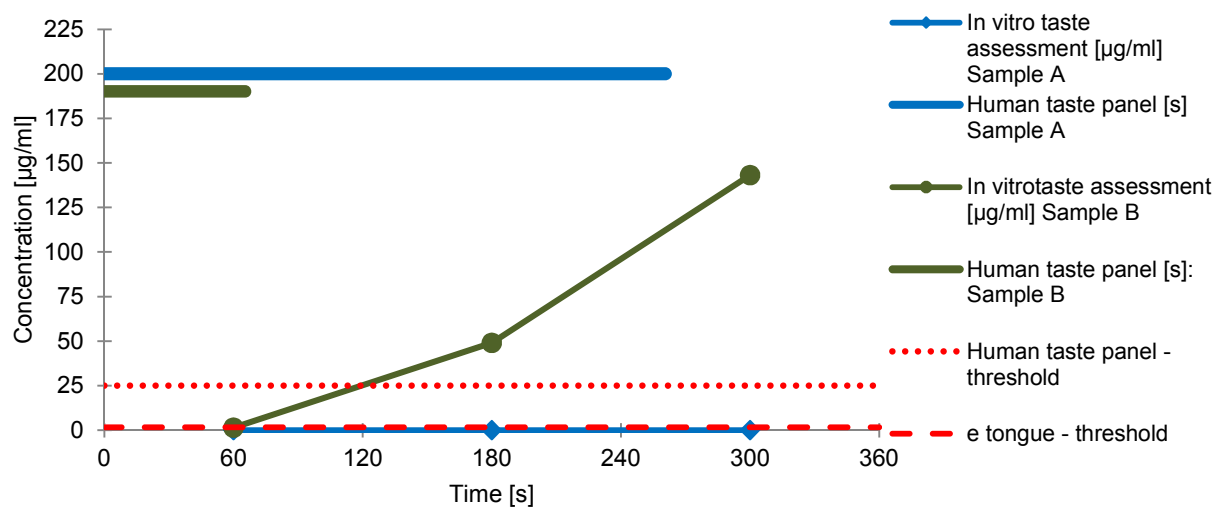
Figure 85: Correlation to in vitro taste assessment

Discussion

The results of the administration of the two DoE samples in the human taste panel showed a good correlation to the in vitro taste assessment, hence the time until bitterness was detected by the panelist equals the time until the first drug is released. That is an indication, that the hydrodynamic resp. rotational speed of the analytical method and the composition of the artificial saliva simulate the condition in the human oral cavity. Contrary according the evaluated bitterness threshold from the human taste panel sample B is taste masked for approximately 120 s. That could not be proven by the in vivo relevance test. As the samples were directly placed on the tongue the local concentration is probably much higher when the coating layer ruptures. That is not comparable with a clear aqueous API solution which was tested in the first part of the human taste panel.

Nevertheless the results from adult human taste panel cannot be transferred to pediatric population. Children are typically more sensitive to bitterness than adults [40]. Furthermore the taste impression of children varies very much over age [138]. The variation of the taste depending on age was also present in this human taste panel, the bitterness sensitivity decreased with age, this was even more dominant in female panelists. According the model the bitterness score evaluated by adult woman increases by 0.1 per years and that would result in a higher bitterness threshold. From the resulting data it is also visual that the female population is more sensitive to bitterness (Figure 86).
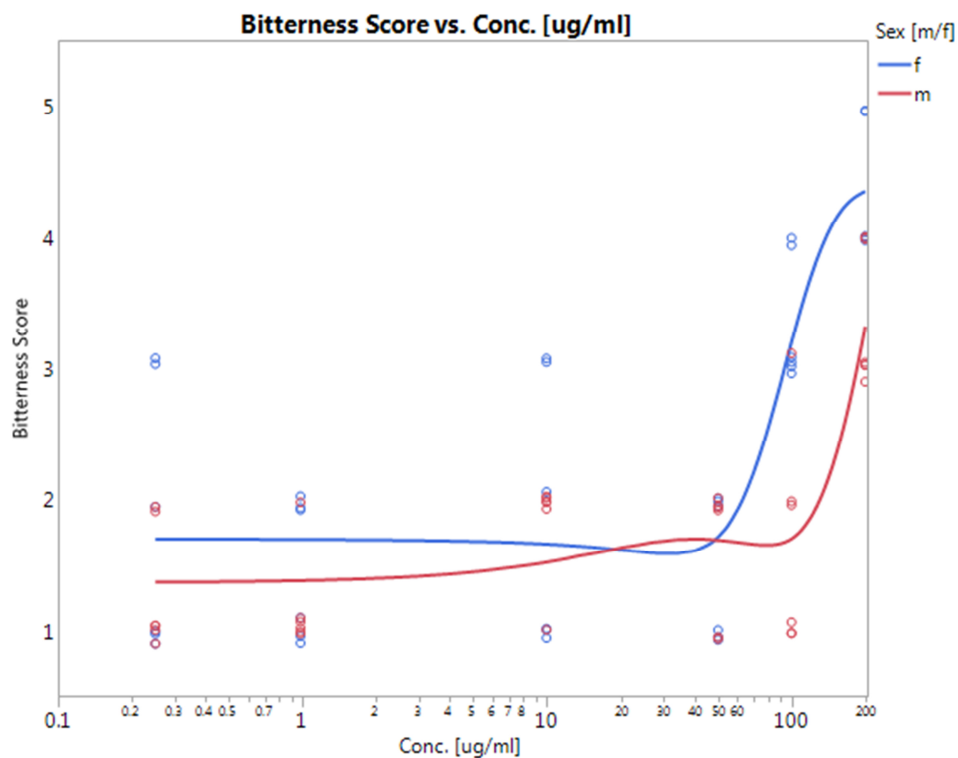
Figure 86: Bitterness scores vs. concentration of cetirizine difference of sex

6.7.   Technology Comparison

The GMPC-1 (Glatt GmbH Process Technology, Germany) is equipped with a perforated drum. The perforation is larger than the diameter of the minitablets, therefore the minitablets would fall through the perforation during the drum coating process. A tailor-made inlet bag was designed and manufactured by the company Lanz Anliker AG (Figure 87) for the 1.6 l drum. The inlet bag was manufactured from antistatic polyester and a 700 µm polyamide mesh. The inlet bag was fixed at the back with the screw which mounts the drum. For the incoperation of the inlet bag into the drum, the baffles were removed and mounted above the inlet bag (Figure 88 and Figure 89). In the front the inlet bag was pulled over the drum opening and fixed with the elastic strap.
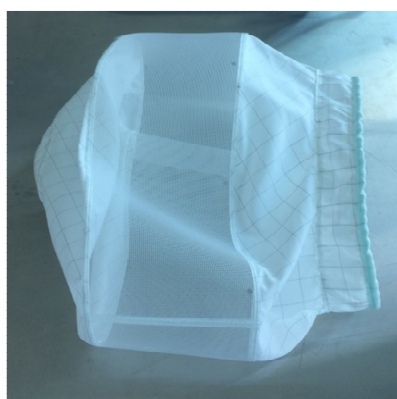
Figure 87: tailor-made inlet bag
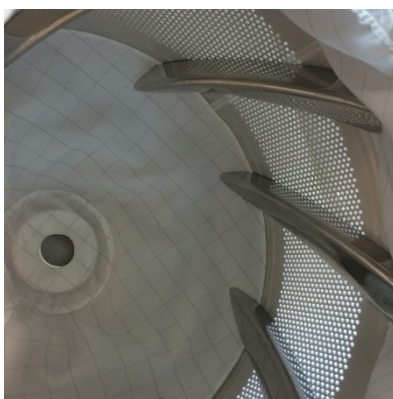
Figure 88: Mounted inlet bag

Figure 89: Mounted inlet bag (close up)

6.7.1.   Feasibility Trial Acetaminophen Minitablets

The goal of the trial was to test the feasibility of coating minitablets with the tailor made inlet bag in the drum. Therefore the process parameters were chosen carefully, as described in chapter 5.1.5.1.

Due to the large amount of required coating suspension indigo carmine was used as a colorant instead of iron oxide yellow to facilitate the assessment regarding progress of the coating process in the drum. Samples have been taken after 2, 4, 6 and 8 mg/cm². At a coating level of 2 mg/cm^2 the color distribution was still inhomogeneous (Spraying time = 183 min). The coating process was feasible without twinning or sticking together of minitablets. It has also shown high coating process efficiency between 87 and 94.5 % (Table 43). But the minitablets had a rough surface, which became visible in the X-ray µCT and SEM pictures (Figure 90 and Figure 91).
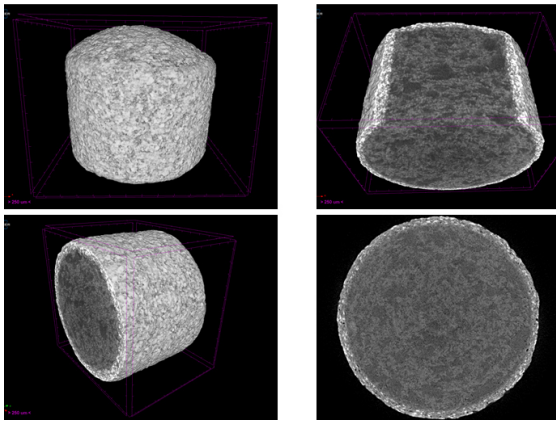
Figure 90: X-ray μCT Feasibility trial acetaminophen minitablets, 8mg/cm²
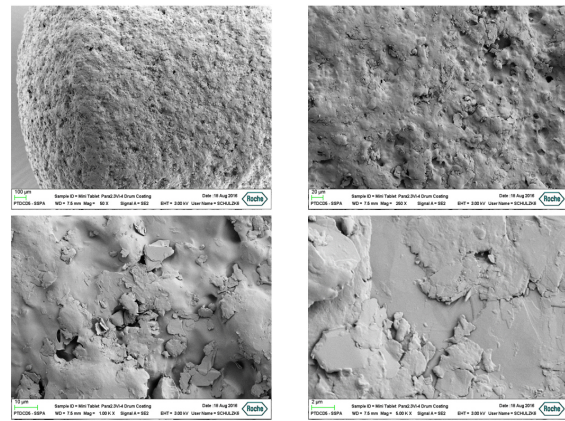
Figure 91: SEM Feasibility trial acetaminophen minitablets, 8 mg/cm²
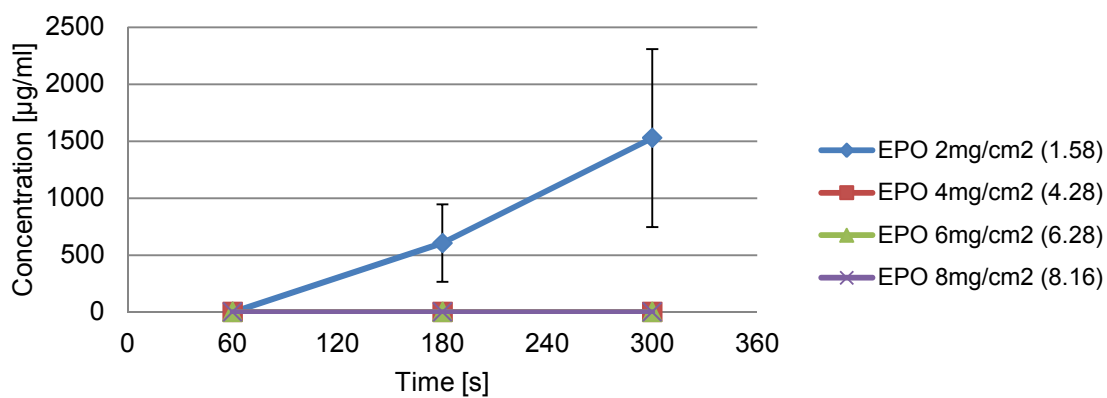
Figure 92: In vitro taste assessment in AS: drum coated acetaminophen MT coated with EPO

Discussion

Compared to the fluid-bed based Wurster process less dissolved surfaces and flaked coating were observed with the drum coating process. This could be due to the very low spray rate. Contrary a rough coated surface could be caused because of the low spray rate and resulting spray drying effects. Another reason could be that the indigo carmine was not dissolved in the 60°C hot water prior adding to the coating suspension – undissolved indigo carmin would then end-up as solid particles on the coated tablet surface.

After a spraying time of 183 min the minitablets did not show a homogeneous coating distribution. The batch size of 1000 g is the largest for the 1.6 l drum. By reducing the batch size the mixing quality may improve.

Despite the rough surface the coating layer exhibited good functionality. Efficient taste masking in the in vitro taste assessment could be reached at a coating level of 4mg/cm² (Figure 92).

Table 43: Results feasibility trial drum coater

Batch	Para2.3.VI			
Polymer	EPO; 2mg/cm^2	EPO; 4mg/cm^2	EPO; 6mg/cm^2	EPO; 8mg/cm^2
Process evaluation				
LOD before [%]	2.02	2.02	2.02	2.02
LOD after [%]	2.07	1.98	1.86	1.92
Initial MT weight [mg]	14.22	14.22	14.22	14.22
Final MT weight [mg]	15.192	15.912	16.899	17.869
Srel weight [%]	6.05	6.58	7.46	7.04
Weight gain [%]	6.78	11.94	19.03	25.79
Polymer applied [mg/cm²]	2.22	3.90	6.22	8.42
Coating Uniformity [ ]	0.9	1.027	1.237	0.984
Coating Process Efficiency [%]	100.8	87.5	93.6	95.3
IPC coated MT				
Appearance	Inhomogeneous in color	rough surface	rough surface	rough surface
Hardness [N]	44.8	39.4	50.2	52
Height [mm]	2.77	2.8	2.88	2.92

6.7.2.   Process Transfer

The center point of the DoE performed for the fluid-bed process represented the experimental point with optimal parameter setting to reach efficient taste masking and immediate release during dissolution in SGF. Key parameter settings should therefore be transferred to the drum coating process to evaluate which technology would be more suitable for the minitablet coating and to be more efficient.

The Wurster coating trials were performed with a batch size of 300 g, but for the drum coating process a higher batch size (700 – 1000 g) was required. Therefore comparison is difficult compare. The following two approaches were used:

1. Approach:

The first approach was to keep the drying condition equal. Hence the drying condition of the center points in the Wurster process needed to be calculated. The recorded values of the Wurster process (air volume rate, inlet air temperature, spray rate, room temperature and room relative humidity) were used to calculate the exhaust humidity according am Ende's thermodynamical model [16]. The average exhaust humidity of the three center points were 15.7 %rH (Run1 16.14 %, Run6: 15.8 %, Run11: 15.3 %).

Due to the fact that the product temperature and the relative humidity in the drum coating tablet bed cannot be directly measured, the exhaust temperature and the exhaust humidity

are used. The heat loss factor of the GMPC-1 was already evaluated by previous trials and is 0.011 KJ/s*K. By using the thermodynamic model, the spray rate and the inlet air temperature were modeled to reach the same coating/drying condition (resp. same exhaust temperature and relative humidity). Due to prior knowledge the air volume rate was set to 80 m³/h. The parameters were modeled as follows: spray rate 3 g/min, inlet air temperature 57.8 °C to reach the exhausted relative humidity of 15 % rH.

2. Approach:

The second approach was to scale the spray rate with the batch size so that the spraying time became the same. The normalized spray rate of the center point was 6.7 g/min*kg. That would result in a spray rate of 5.3 g/min for a batch size of 700 g in the drum. The inlet air temperature was modeled to reach the exhaust temperature of 43 °C. That would lead theoretically to a more humid process having an exhaust relative humidity of 18.7 % rH according the Ende's thermodynamical model.

3. Approach:

The third approach was to optimize the drum coating process to reach the same product quality as obtained in the Wurster coating process.

Results

The first approach led to an inhomogeneous coating distribution (Figure 93). The minitablets varied regarding their color intensity, which is an indication for an inhomogeneous coating distribution. Furthermore few minitablets stuck together and built twins.

Figure 93: CET1.2.XIII inhomogeneous distribution

Figure 94: CET1.2.XIV inhomogeneous distribution

Figure 95: CET1.2.XIV twinning

The second approach led to even more inhomogeneous color distribution and extensive twinning effect with 2 to 5 minitablets sticking together (Figure 94 and Figure 95). 5.3 % of the minitablets stuck together. Furthermore the agglomerates had a stronger coloring which means a higher coating weight gain. The reason could be that the agglomerates have in total a higher minitablet weight, therefore the centripetal force would increase and push these

agglomerates to the wall of the drum. Then at the turn over point the twins are present at the surface and the probability was much higher compared to single minitablets that they will pass the spraying zone.

With the 3rd trial the same product quality could be reached without any twinning. Therefore the spray rate was reduced to increase the spraying time and ensure homogeneous distribution. Furthermore the pattern air pressure was increased to 0.9 bar that the spray cone is more elliptical shaped and covers a larger area of the tablet bed. Due to the reduced spray rate the spraying time was more than twofold longer compared to the Wurster coating process. Also the values for the Coating uniformity and the Coating Process efficiency were worse (CU$_{drum}$=0.23, CU$_{wurster}$=0.22; CPE$_{drum}$= 89.0 %, CPE$_{wurster}$= 92.4 %) (Table 44) and the minitablets coated in the drum were less glossy compared to the Wurster coating. Despite this, the minitablets were taste masked and had immediate drug release (Figure 96 and Figure 97).

Table 44: Results Process transfer drum coater

Trial	1	2	3
Batch	CET1.2.XIII	CET1.2.XIV	CET1.2.XV
Description	Sur80:Opa20, 6.5%WG	Sur80:Opa20, 6.5%WG	Sur80:Opa20, 6.5%WG
Process evaluation			
LOD before [%]	1.84	1.84	1.84
LOD after [%]	1.21	1.28	1.26
Initial MT weight [mg]	16.67	16.67	16.67
Final MT weight [mg]	17.51	17.53	17.53
Srel weight [%]	1.42	1.74	1.35
Weight gain [%]	5.73	5.78	5.79
Polymer applied [mg/cm²]	2.37	2.39	2.39
Coating Uniformity [%]	0.25	0.302	0.23
Coating Process Efficiency	88.1	89.0	89.0
Spraying time [min]	109	70	148
IPC coated MT			
Appearance	less glossy, not homogeneous coloring	less glossy, not homogeneous coloring, twinning	less glossy
Hardness [N]	40.1	38.1	38.6
Height [mm]	2.95	2.96	2.95
Dissolution SGF immediate release [hh:mm:ss]	00:03:58	00:04:16	00:05:17
Taste masking [µg/ml]: 60s; 180s; 300s	0; 0; 0.48	-	0; 0; 0.30
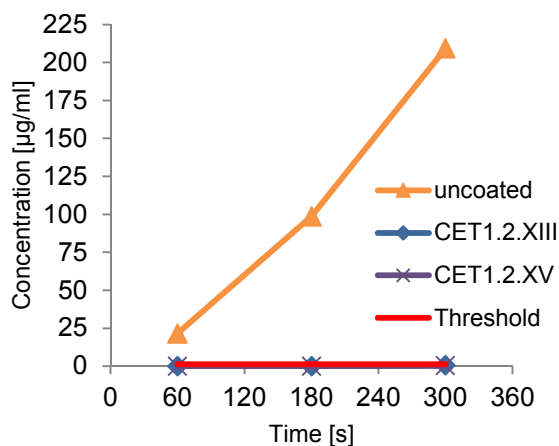
Figure 96: In vitro taste assessment, process transfer
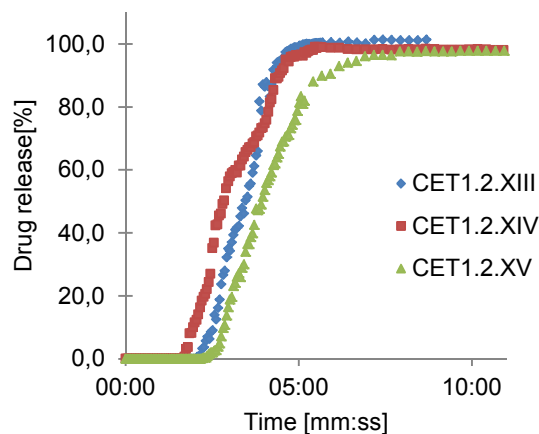
Figure 97: Dissolution, process transfer

Discussion

Uniform coating distribution depends mainly on two factors:

- Uniformity of application of the coating liquid (number of spray guns, atomization fineness, type of spray pattern, etc.)
- Uniformity of mixing (pan speed, baffle design, tablet size and shape)

The fine droplets could positively influence the coating uniformity. The fineness of the atomization can be adjusted by the diameter of the nozzle bore. During the coating process a 0.8 mm nozzle bore was used. Smaller nozzle bores exist but were not available in house. The droplet size can be also be adjusted by the atomization pressure. If the atomization pressure is higher the droplets will be smaller as well. The atomization pressure could not be increased; due to the small weight of the minitablets the atomization pressure formed a dent onto the tablet bed surface (Figure 98). Further increase of the atomization pressure would consequently lead to higher coating losses; hence the drum will be coated.

The spray area does cover only 1/3 of the width of the minitablet bed, which limits the possibility to achieve an optimal coating uniformity. Installing a second spray nozzle, increasing the distance between the spray nozzle and minitablet bed or flattening of the spray cone could improve this situation. The spray cone could be flattened by increasing the spray pattern air pressure from 0.7 to 0.9 bar. The distance between the minitablet bed and the spray nozzle could not be further increased due to minimal loading.

Another observation during the experiment was that the textile rubbed at the window of the coater and produced textile bunching (Figure 99), where the minitablets were kept for several rotations on the sloped surface of the window. This decreased mixing quality and also negatively influenced the homogeneous distribution of the coating suspension

Figure 98: Dent on minitablet bed surface   **Figure 99: textile bunching**

Twinning

Twinning typically occurs during coating when not enough drying capacity is available, either due to a high spray rate, a too low inlet air temperature or a too low inlet air volume rate. The size of the droplets has also an influence, but as described previously the droplet size cannot be reduced. Furthermore there are less shear forces in the drum available compared to the Wurster coating process, which increases the risk of sticking.

By reducing the spray rate and changing the spray pattern the twinning was prevented and distribution of the coating suspension could be significantly improved. On the downside this led then to a 2.1 fold higher spraying time: achieving a spraying time of 148 min for a batch size of 700 g is very long and could become critical in case of scaling up at commercial scale.

Conclusion

It is feasible to coat minitablets in a drum, but the number of trials was not sufficient enough to judge which of the technologies represents the most suitable process for a successful and reproducible minitablet coating. The described drum coating process would require further optimization as mentioned above. Further comparative studies should be performed at equal batch size to evaluate the most suitable and efficient technologies.

6.8.   Excipient Incompatibility Study

The manufacturer of the pH dependent polymer Eudragit E PO® states that the polymer can interact with APIs having anionic activities [130]. Due to the chemical similarity of Eudragit E PO® (EPO) and Kollicoat® Smartseal 30D (SMA), the compatibility study was performed with both polymers. Douroumis also reported about a degradation of cetirizine with the polymer Eudragit E PO® [131], though no stability data as published in. The compatibility of Cetirizine and both pH dependent polymers was tested according Chapter 5.8.

The cetirizine content after the storage of 4 weeks (50 °C, 75 %rH) is shown in Table 45. There is a significantly larger decrease of the API content of the physical mixtures to the pure API. The content of the pure API was taken as a reference to calculate the relative loss of API content (Figure 100).

Table 45: Results compatibility study

	Average Content [%]	Standard deviation	Loss of API content [%]
Pure API	94.66	4.87	5.34
CET : EPO	84.03	3.84	15.97
CET : SMA	73.12	11.89	26.88
MT Formulation : EPO Formulation	81.18	14.80	18.82
MT Formulation : SMA Formulation	72.88	7.40	27.12
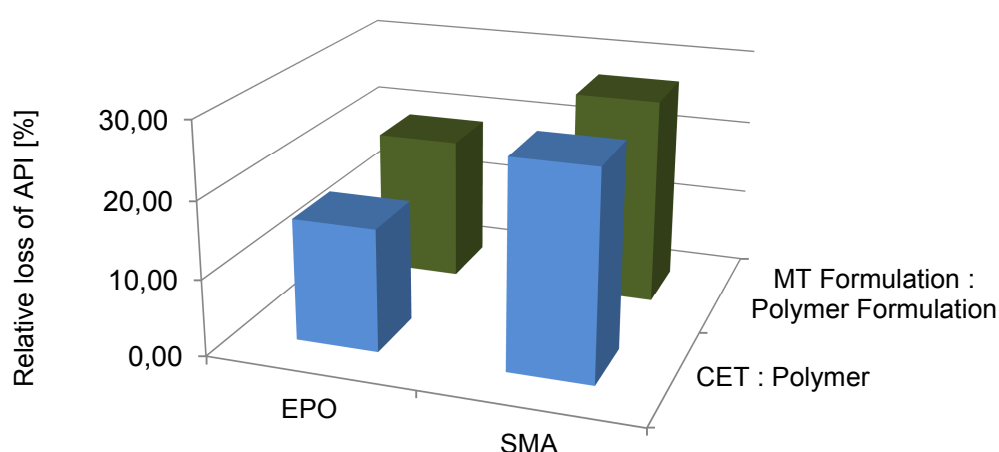
Figure 100: Relative loss of API

The HPLC method was not suitable to quantify degradation products; therefore just the API content was measured. It cannot be acertained which reaction took place or if degradation occured. However an incompatibility can be proven by lowered API content of the samples after storage.

The pKa_1 of 2.7 belongs probably to the acidic group of the cetirizine and is deprotonated at a neutral pH. The deprotonated acidic group could form a complex with the protonated tertiary amine of the pH dependent polymers. This complex would probably have a longer retention time due to the increased hydrophobic moiety and was therefore not detected. The complex could be separated in an highly acidic environment having an pH much lower than 2.7. Due to the fact that the pH in the fed state is between 3 to 6, a proportion of cetirizine will complexated.

The polymer Kollicoat® Smartseal 30D led to a higher decrease of the API compared to Eudragit E PO®. A reason could be the different pKa values for the polymers, which are not specified by the manufacturer.

This interaction of the API with the Polymer can just take place at the interface between the minitablet and the coat. The conditions during the storage were set to be extreme to accelerate the stability study. The storage at these conditions mimic a storage of approx. 1.15 years according Arrhenius equation [139].

Therefore, it could not be recommended to taste mask cetirizine with those polymers.

7. Conclusion

In this work two minitablet formulations were developed using acetaminophen as a high drug load and cetirizine dihydrochloride as a low drug load model compound. The taste masking with three polymers and two technologies (Wurster and drum coater) was investigated.

The choice of the excipients depends mainly on the mechanical and physical properties of the API and with regards to pediatric medication on the safety. Pediatric medication can be developed using a limited number of excipients, e.g. benzylalcohol or propylene glycol is not safe for very young children. Furthermore the required drug load has a great influence. Both APIs have similar mechanical properties, but for acetaminophen the formulation with the high drug load of 50 % caused problems due to the poor mechanical properties of the API (Chapter 6.1.2, page 62). The Amidon prediction model using Hiestand tableting indices can help to reduce the number of formulation screening experiments by predicting the mechanical properties of the powder mixtures. Due to the low final weight of minitablets a poor flowability typically leads to weight and hardness variations. For example the acetaminophen powder mixture, which had an ffc value of 6.7 can be categorized according Jenike as "easy flowing" and represents for normal sized tablets a good value. However for a minitablet powder mixture such a value could already be judged as critical (Chapter 6.2.1, page 65).

Different grades of an excipient can influence the tableting behavior. For example, Avicel PH 102 was worse for the acetaminophen formulation in regards to capping, whereas Avicel PH 101 did not show any tableting defects (Chapter 6.2.1, page 65). For a directly compressible powder mixture, a Hausner factor of lower than 1.3 and Carr's index lower than 30 % seems to be appropriate for minitableting (Chapter 6.2.2, page 72). A tensile strength of 1.6 MPa, resp. a hardness of 30 N was sufficient for coating in fluidized bed and drum coating (Chapter 6.2.2, page 72). The addition of a superdisintegrant for a minitablet formulation is rather not required due to the high surface area with respect to the volume and when using swellable exipients (Chapter 6.2.2, page 72). The use of monoblock multitip punches can be recommended when key ways for the upper and lower punches are available. The tip arrangement should be centered having a narrow outer diameter or rectangular arrangement which should be aligned to the feed frame exit opening to decrease weight variation (Chapter 6.2.1, page 65).

According to the selected acetaminophen formulation one dose would be equal to 28 minitablet units and the cetirizine formulation equal to three minitablets. Concerning the

rather high number of 28 minitablets of the acetaminophen formulation, Klingmann investigated recently the suitability of even a much higher number of minitablets (100-400 minitablets) in children of an age from 2 to 6 years [5]. In this study the swallowability (swallowed intact without chewing) of 100 MT was only 31.2 % but comparable to an oral liquid formulation (syrup). However, it can be assumed that the swallowability of only 28 minitablets should not be inferior but rather better compared to these study results.

Once the minitablet formulations were selected the coating process was investigated. The majority of coating experiments was performed in a **Wurster coater** using pH dependent and independent polymers.

The **pH dependent polymers** Eudragit E PO® and Kollicoat® Smartseal 30D offer an easy and simple approach to taste mask minitablets. The minimum necessary coating level was investigated, however it could be confirmed that no sustained release effects were observed at high coating levels. In this work the taste masking of acetaminophen minitablet with pH dependent polymers (Eudragit E PO®, Kollicoat® Smartseal 30D) was achieved with a coating level of 4 ± 0.5 mg/cm^2 having a coating layer thickness of 37 µm (Chapter 6.4.1.1 and 6.5.1, page 82 and 101). The amount of swellable excipients in the core formulation was evaluated as a critical material attribute. The pH dependent polymers are insoluble at the pH of saliva, but still permeable for water. The permeation of water causes swelling of the core and results in an increase of the internal core pressure. Due to the stress concentration effect, the pressure maximises in the region of the edges due to the specific geometry of the minitablet, causing the coating layer to rupture initially at the edges of the minitablet, when the internal pressure exceeds the elasticity of the coating layer. As a result the taste masking with the polymer Eudragit E PO® was more efficient due to the higher elasticity of the coating layer [134] (Chapter 6.4.1.1, page 82). A drawback of pH dependent polymers is the potential chemical incompatibility of the polymer with APIs acting as proton donator. This could be confirmed experimentally for Cetirizine dihydrochloride showing an incompatibility with the pH dependent polymers (Chapter 6.8, page 121). Another drawback of pH dependent polymers could be their food incompatibility with acidic fruit mush, e.g. applesauce.

The **pH independent polymer** Surelease® can also efficiently taste mask minitablets, though additional factors like curing or the ratio of polymer to pore former needs to be investigated. The effect of swellable excipients in the minitablet formulation is even more critical when using Surelease® and a hydrophilic pore former as a taste masking system as dissolution of the pore former enables faster water penetration into the core. In this work the acetaminophen minitablets could be taste masked for only 60 s at a coating level of 4 mg/cm² (Chapter 6.4.1.2, page 87). Due to the previously mentioned chemical

incompatibilities of cetirizine with the pH dependent polymers, cetirizine minitablets were only coated with the pH independent polymer Surelease®. As Surelease® can extend the drug release the compromise between efficient taste masking and immediate release requirement needs to be found. A two level full factorial DoE was performed to investigate the influence of the spray rate, spray time and the polymer to pore former ration on the responses "taste masking" and "dissolution". The biggest influence had the spray rate, spray time and their joint effect. As these two factors determine the coating weight gain, this factor can be assumed as a critical process parameter. The optimum could be found having a polymer to pore former ratio of 80:20, a spray rate of 2 g/min and a spraying time of 70 min (Chapter 6.4.2.2, page 92). The polymer to pore former ratio had in the examined range no significant influence. The reason could be a too narrow level setting. Due to the pH independence the administration with soft food having a low pH would not limited.

For the coating of minitablets in a conventional **drum coater** typically used for coating of larger tablets (>5 mm) a new tailor-made polyamide insert was designed which was fixed in a conventional 1.6 l perforated drum. The coating of minitablets in a perforated drum is feasible, but required a twofold longer spray time to obtain the same product quality compared to the Wurster coating process (Chapter 6.7.2, page 116). The spray time required additional spraying at a lower rate due to the inhomogeneous coating distribution and twinning. Critical process parameters with regards to minitablet coating are the atomization pressure and the spraying time. The increase of the atomization pressure is limited due to the formed dent on the minitablet bed, therefore larger droplets are formed and the risk of twinning is increased. In addition the drum coating process provides less shear forces due to the low weight of the minitablets compared to the Wurster process, which also increases the risk of twinning.

The taste masking was tested by an **in vitro taste assessment**, where the initial drug release in 5 ml artificial saliva was measured. The artificial saliva contained organic salts, a viscosity enhancer and enzymes and was adjusted to a pH of 7.1. The taste masking was achieved when the drug release was zero or below the bitterness threshold. The bitterness threshold of acetaminophen was published in the literature [117], whereas the bitterness threshold of cetirizine had to be investigated. Therefore e tongue measurements were performed using the bitterness standard quinine hydrochloride. As a result the cetirizine bitterness threshold of 1.624 µg/ml was determined by e tongue (Chapter 6.6.1, page 106). Contrary the human taste panel delivered a surprisingly a higher bitterness threshold of 25 µg/ml (Chapter 6.6.2, page 110). Reasons for this discrepancy might be due to the fact that

the bitterness standard was not a dihydrochloride, secondly the acidity of the cetirizine might have an impact on human taste sensation of bitterness. Furthermore it needs to be kept in mind that the taste of adults cannot be transferred to children as adults are much more used to accept bitter food resp. beverages (e.g. coffee, beer) [40]. Nevertheless a good correlation of the time until the unset of the bitter taste masking between in vitro taste assessment and the human taste panel was found (Chapter 6.6.2, page 110), which is an indication that the performed in vitro taste assessment have some in vivo relevance. The in vitro drug release study is a simple and less time consuming tool for formulation screening, but the bitterness threshold should be determined in addition by a human taste panel preferably in children.

A successful taste masking with an organic polymer for a pediatric population would of course also require an assessment regarding the safety of the excipients and more specifically their amounts. The taste masked acetaminophen minitablets coated with the pH dependent polymers (coating level 4 mg/cm²) would result in a exposure of 1.017mg/kg bw of EPO and 1.373 mg/kg bw of SMA per dose. That is far below the ADI of those polymers (Chapter 4.3.1, page 34), even for the maximum daily dose.

Within the scope of this thesis to sufficiently taste mask minitablet formulations, this could be successfully developed for the model drugs acetaminophen and cetirizine dihydrochloride. A suitable manufacturing process could also be identified. Critical process parameters and material attributes were evaluated. This work has been shown that:

- formulations having drug loads between 5 % and 50 % were successfully developed
- the chemical structure of the API can influence the choice of the polymer selection
- the amount of swellable excipients influence the taste masking efficiency
- the chosen polymers are suitable for taste masking of minitablets
- it is feasible to coat minitablets in a fluidized bed and in a modified drum
- the in vitro taste assessment method has in vivo relevance and can be used for formulation screening

8. References

[1]   European Medicines Agency (EMA), "Report on the survey of all paediatric uses of medicinal products in Europe," London, 2010.

[2]   G. L. Kearns, S. M. Abdel-Rahman, S. W. Alander, D. L. Blowey, J. S. Leeder and R. E. Kauffman, "Developmental Pharmacology - Drug Disposition, Action, and Therapy in Infants and Children," New England Jornal of Medicine, no. 349, pp. 1157-1167, 2003.

[3]   European Medicines Agency, "Guideline on pharmaceutical development of medicines for paediatric use," pp. 1-24, 2013.

[4]   V. W. Yeung and I. C. K. Wong, "When do children convert from liquid antiretroviral to solid formulations," Pharm World Sci, no. 27, pp. 399-402, 2005.

[5]   V. Klingmann, "Suitablility of Multiple Uncoated Mini-Tables in Toddlers and Infants - A Randomized controlled Trial," in 8th EuPHI Conference (Oral presentation), Lisbon, Portugal, 2016.

[6]   N. Spomer , V. Klingmann, I. Stoltenberg, C. Lerch, T. Meissner and J. Breitkreutz, "Acceptance of uncoated mini-tablets in young children : results from a prospective exploratory cross-over study," Archives of Diseases in Childhood, vol. 97, pp. 283-286, 2012.

[7]   H. K. Batchelor , N. Fotaki and S. Klien , "Pediatric oral biopharmaceutics: Key considerations and current challenges," Advanced Drug Delivery Reviews, vol. 73, pp. 103-112, 2013.

[8]   D. Matsui, "Current Issues in Pediatric Medication Adherence," Pediatr Drugs, vol. 9, no. 5, pp. 283 - 288, 2007.

[9]   C. P. Milne and J. B. Bruss, "The econimics of pediatric formulation development for off-patent drugs," Clinical Therapics, vol. 30, pp. 2133-2145, 2008.

[10]   Z. Ayenew, V. Puri, L. Kumar and A. K. Bansal, "Trends in Pharmaceutical Taste Masking Technologies: A Patent Review," Recent Patents on Drug Delivery & Formulation, vol. 3, pp. 26-39, 2009.

[11]   J. Breitkreutz, T. Wessel and J. Boos, "Dosage forms for peroral drug administration

to children," Paediatric and Perinatal Drug Therapy, pp. 25-33, 1999.

[12]   World Health Organization, "Report of the informal expert meeting on dosage forms of medicines for children," Geneva, Switzerland, 2009.

[13]   P. Lennartz and J. Mielck, "Minitabletting: improving the compactability of paracetamol powder mixtures," International Journal of Pharmaceutics, vol. 173, no. 1, pp. 75 - 85, 1998.

[14]   N. C. E. Rouge, E. Doelker and P. Buri, "Screening of potentially floating excipients for minitablets," S.T.P. Pharm. Sci., vol. 7, pp. 386 - 392, 1997.

[15]   A. Kramar, S. Turk and F. Vrecer, "Statistical optimization of diclofenac sodium sustained release pellets coated with polymethacrylic films," International Jornal of Pharmaceutics, vol. 256, pp. 43-52, 2003.

[16]   C. Tuleu, C. Andrieux, P. Boy and J. C. Chaumeil , "Gastrointestinal transit of pellets in rats: effect of size and density," International Journal of Pharmaceutics, vol. 180, no. 1, pp. 123-131, 1999.

[17]   V. Klingmann, N. Spomer, C. Lerch, I. Stoltenberg, C. Frömke, H. M. Bosse, J. Breitkreutz and T. Meissner, "Favorable Acceptance of Mini-Tablets Compared with Syrup: A Randomized Controlled Trail in Infants and Preschool Children," The Jornal of Pediatrics, vol. 163, no. 6, pp. 1728-1732, 2013.

[18]   V. Klingmann, A. Seitz, T. Meissner , J. Breitkreutz, A. Moeltner and M. H. Bosse , "Acceptability of Uncoated Mini-Tablets in Neonates- A Randomized Controlled Trail," The Jornal of Pediatrics, vol. 167, no. 4, pp. 893-896, 2015.

[19]   C.-M. Su, Y.-H. Yang and T.-Y. Hsieh, "Relationship between oral status and maximum bite force in preschool children," Journal of Dental Sicence, vol. 4, no. 1, pp. 32 - 39, 2009.

[20]   S. Braun , J. W. Freudenthaler and K. Hönigle, "A study of maximum bite force during growth and development," The Angle Orthodontist, vol. 66, no. 4, pp. 261 - 264, 1996.

[21]   D. A. Van Riet-Nales, P. Kozarewicz, B. Aylward, R. d. Vries, T. C. G. Egberts, C. M. A. Rademaker and A. F. A. M. Schobben, "Paediatric Drug Development and Formulation Design - a European Perspective," AAPS PharmSciTech, 2016.

[22]   A. Kluk, M. Sznitowska, A. Brant, K. Sznurkowska, K. Plata-Nazar, M. Mysliwiec

and H. Kaminska, "Can preschool-aged children swallow several minitablets at a time? Results from a clinical pilot study," International Journal of Pharmaceutics, vol. 485, pp. 1-6, 28 02 2015.

[23]   V. Klingmann, "Suitablility of Multiple Uncoated Mini-Tables in Toddlers and Infants - A Randomized controlled Trial," in Oral presentation, 8th EuPHI Conference, Lisbon, Portugal, 2016.

[24]   S. M. Iveson, J. D. Litster, K. Hapgood and B. J. Ennis, "Nucleation, growth and breakage phenomena in agitated wet granulation prossess: a review," Powder Technology, vol. 117, pp. 3 - 39, 2001.

[25]   Bossche, "Making compressable mass," in Sticking, Capping, Lamination, Berlin, 2015.

[26]   J. B. Mielck and J. Flemming, "Requirements for the Production of Microtablets: Suitability of Direct-Compression Excipients Estimated from Powder Characteristics and Flow Rates," Drug Development and Industrial Pharmacy, vol. 21, no. 19, pp. 2239 - 2251, 1995.

[27]   A. Aleksovski, R. Dreu, M. Gasperlin and O. Planinsek, "Mini-tablets: a contemporary system for oral drug delivery in targeted patient groups," Expert Opinion on Drug Delivery, vol. 12, no. 1, pp. 65 - 84, 2015.

[28]   E. Hershberg, "Apparatus for punching miniature tablets". United States of America Patent US53175521A, 30 03 1965.

[29]   I Holland Ltd., "Tablettingscience," [Online]. Available: http://tablettingscience.com/PDFs/Downloads/multi-tip-tablet-tooling.pdf. [Accessed 06 09 2016].

[30]   K. Becker, S. Salar-Behzadi and A. Zimmer, "Solvent-Free Melting Techniques for the Preparation of Lipid - Based Solid Oral Formulations," Pharm Res, vol. 32, pp. 1519-1545, 2015.

[31]   C. Bindschaedler, R. Gurny and E. Doelker, "Theoretical concepts regarding the formation of films from aqueous microdispersions and application to coating," Labo-pharma, Problemes et Techniques, vol. 31, pp. 389 - 394, 1983.

[32]   J. Khinast, "Pharmaceutical Engineering II Lecture - 6b Coating," Graz, 2014.

[33]   A. Grave, "Von Der Entwicklung Zur Produktion - Scale Up Für Wirbelschicht -

Prozesse," Binzen, 2013.

[34]   G. S. Sonar and S. S. Rawat, "Wurster Technology: Process variables involvied and Scale up science," Innovations in Pharmacy and Pharmaceutical Technology, vol. 1, no. 1, pp. 100-109, 2015.

[35]   S. Gittings, N. Turnbull, C. J. Roberts and P. Gershkovich, "Dissolution metholgy for taste masekd oral dosage forms," Journal of Controlled Release, vol. 173, pp. 33-40, 2013.

[36]   P. A. Breslin, "An Evolutionary Perspective on Food and Human Taste," Current Biology, vol. 23, pp. 409-419, 2013.

[37]   T. H. Hoang Thi, S. Morel, F. Ayouni and M.-P. Flament, "Development and Evaluation of taste-masked drugs for paediatric medicines - Application to acetaminophen," International Journal of Pharmaceutics, vol. 434, pp. 235-242, 2012.

[38]   J. Walsh, A. Cram , K. Woertz, J. Breitkreutz, G. Winzenburg, R. Turner and C. Tuleu, "Playing hide and seek with poorly tasting paediatric medicines: Do not forget the excipients," Advanced Drug Delivery Reviews, vol. 73, pp. 14 - 33, 2014.

[39]   S. Joshi and H.-U. Petereit, "Film coatings for taste masking and moisture protection," International Journal of Pharmaceutics, vol. 457, pp. 395-406, 2013.

[40]   J. A. Mennella, A. C. Spector and D. R. Reed, "The Bad Taste of Medicines: Overview of Basic Research on Bitter Taste," Clinical Therapeutics, vol. 35, no. 8, pp. 1225 - 1246, 2013.

[41]   S. V. Lipchock, D. R. Reed and J. A. Mennella, "Relationship Between Bitter-Taste Receptor Genotype and Solid Medication Formulation Usage Among Young Children: A retrospective Analysis," Clincal Therapeutics, vol. 34, no. 3, pp. 728-733, 2012.

[42]   European Medicines Agency, "Reflection paper: Formulations of choice for the pediatric population," 2006.

[43]   M. Singh, K. Hemant, M. Ram and H. Shivakumar, "Microencapsulation: A pormising technique for controlled drug delivery," Research in Pharmaeutical Science, vol. 5, no. 2, pp. 65 - 77, 2010.

[44]   R. J. Mrsny, "Oral Drug delivery research in Europe," Jornal of Controlled Release,

no. 161, pp. 247-253, 2012.

[45] D. M. Gaber, N. Nafee and O. Y. Abdallah, "Mini-tablets versus pellets as promising multiparticulate modified release delivery systems for highly soluble drugs," International Jornal of Pharmaceutics, vol. 488, pp. 86-94, 2015.

[46] N. Passerini, B. Albertini, B. Perissutti and L. Rodriguez, "Evaluation of melt granulation and ultrasonic spray congealing," International Journal of Pharmaceutics, vol. 318, pp. 92 - 102, 2006.

[47] S. G. Sudke and D. M. Sakarakar, "Lipids - An Instrumental Excipient in Pharmaceutical Hot-Melt Coating," International Journal of PharmTech Research, vol. 5, no. 2, pp. 607 - 621, 2013.

[48] D. G. Lopes, K. Becker , M. Stehr, D. Lochmann, D. Haak, A. Zimmer and S. Salar-Behzadi, "Role of Lipid Blooming and Crystallite Size in the Perfomence of Highly Soluble Drug-Loaded Microcapsules," Journal of Pharmaceutical Science, vol. 104, pp. 4257 - 4265, 2015.

[49] M. Maniruzzaman, J. S. Boateng, M. Bonnefille, A. Aranyos and J. C. Mitchell, "Taste masikng of paracetamol by hot-melt extrusion: An in vitro and in vivo evaluation," European Journal of Pharmaceutics and Biopharmaceutics, vol. 80, pp. 433 - 442, 2012.

[50] B. A. Becker and J. G. Swift, "Effective Reduction of the Acute Toxcicity of pertain Pharmacologic Agents by Use of synthetic Ion Exchange Resins," Toxicology, vol. 1, pp. 42 - 54, 1959.

[51] R. McGregor, A. Taylor and J. Hort, "Bitter blockers in foods and pharmaceuticals," Modifying Flavour in Food, pp. 221 - 231, 2007.

[52] B. Eileen and A. S. Mankoo.Montenegro Patent WO9704666, 1997.

[53] D. D. Douroumis, A. Gryczke and S. Schminke, "Development and Evaluation of Cetirizin HCL Taste-Masked Oral Disintegrating Tablets," AAPS PharmSCiTech, vol. 12, no. 1, pp. 141-151, 2010.

[54] A. H. Mohamed-Ahmed , J. Soto, T. Ernest and C. Tuleu, "Non-human tools for the evaluation of bitter taste in the design and development of medicines: a systematic review," Drug Discovery Today, vol. 00, no. 00, pp. 1 - 11, 2016.

[55] M. Pein, M. Preis , C. Eckert and F. E. Kiene, "Taste-masking assessment of solid

oral dosage forms- A critical review," International Journal of Pharmaceutics, vol. 465, pp. 239-254, 2014.

[56]   J. Breitkreutz and J. Boos, "Paediatric and geriatric drug delivery," Expert Opinion on Drug Delivery, vol. 4, no. 1, pp. 37 - 45, 2007.

[57]   SIMS Sensory Quality Panel Software System, "SIMS Sensory Software," Sensory and cosumer smiley face testing Questionaire, [Online]. Available: http://www.sims2000.com/sample4children.asp. [Accessed 26 09 2016].

[58]   A. Nakamura and S. Imaizumi, "Auditory Verbal Cues Alter the Perceived Flavor of Beverages and Ease of Swallowing: A Psychometric and Electrophysiological Analysis," BioMed Research International, vol. 2013, 2013.

[59]   Davies, Elin Haf; Tuleu, Catherine, "Medicines for Children: A Matter of Taste," Journal of Pediatrics, vol. 153, pp. 599 - 604, 2008.

[60]   M. Cocorocchio, "Amoeba Tastes Bitter: A novel non-animal model for bitterness research," in 8th EuPHI Conference (Oral presentation), Lisbon, Portugal, 2016.

[61]   V. Anand, M. Kataria, V. Kukkar, V. Saharan and P. K. Choudhury, "The latest trends in the taste assessment of pharmaceuticals," Drug Discovery Today, vol. 12, no. 5/6, pp. 257 - 265, 2007.

[62]   T. Yajima, Y. Fukushima, S. Itai and Y. Kawashima, "Method of Evaluation of the Bitterness of Clarithomycin Dry Syrup," Chem. Pharm. Bull. , vol. 50, no. 2, pp. 147 - 152, 2002.

[63]   M. J. Siewert, C. K. Brown and V. P. Shah, "FIP/AAPS Guidelines to Dissolution / in vitro Release Testing of novel/special Dosage forms," PharmSiTech, vol. 4, 2003.

[64]   N. Guffon, Y. Kibleur, W. Copalu, C. Tissen and J. Breitkreutz, "Developing a new formulation of sodium phenylbutyrate," Arch Dis Child, vol. 97, pp. 1081 - 1085, 2012.

[65]   K. Becker, E.-M. Saurugger, D. Kienberger, D. Lopes, D. Haack, M. Köberle, M. Stehr, D. Lochmann, A. Zimmer and S. Salar-Behzadi, "Advanced stable lipid-based formulations for patient-centric product design," International Journal of Pharmaceutics, vol. 497, pp. 136 - 149, 2015.

[66]   National Center for Biotechnology Information, "National Center for Biotechnology Information," [Online]. Available: https://pubchem.ncbi.nlm.nih.gov/compound/1983.

[Accessed 19 02 2016].

[67]   FDA, "FDA - U.S. Food and Drug Administration," 15 08 2013. [Online]. Available:
         http://www.fda.gov/Drugs/DrugSafety/DrugSafetyPodcasts/ucm284611.htm.
         [Accessed 20 06 2016].

[68]   D. Klauwer, C. Neuhäuser, J. Thul and R. Zimmermann, Pädiatrische
         Intensivmedizin - Kinderkardiologische Praxis, Köln: Deutscher Ärzte Verlag GmbH
         , 2003.

[69]   Pharmacin B.V., "RMS Day 70 Preliminary Assessment Report," 12 2011. [Online].
         Available:
         http://mri.medagencies.org/download/NL_H_2791_001_FinalSPC_4of4.pdf.
         [Accessed 20 06 2016].

[70]   FDA, "Over-the-Counter Pediatric Oral Liquid Drug Products Containing
         Acetaminophen - Guidance for Industry," 08 2015. [Online]. Available:
         http://www.fda.gov/downloads/Drugs/GuidanceComplianceRegulatoryInformation/G
         uidances/UCM417568.pdf. [Accessed 20 06 2016].

[71]   R. Shawahna, "Pediatric Biopharmaceutical Classification System: Using Age-
         Appropriate Initial Gastric Volume," The AAPS Jornal, vol. 18, no. 3, pp. 728-736,
         05 2016.

[72]   O. Boutaud, D. Aronoff and J. Richardson, "Determinants of the cellular specificity
         of acetaminophen as an inhibitor of prostaglandin H2 synthases," Proceedings of
         the National Academy of Sciences, vol. 99, no. 10, pp. 7130-7135, 2002.

[73]   Mc Neil, "FDA - U.S. Food and Drug Administration," 19 09 2002. [Online].
         Available: http://www.fda.gov/ohrms/dockets/ac/02/briefing/3882B1_13_McNeil-
         Acetaminophen.htm#_Toc18717569. [Accessed 20 06 2016].

[74]   P. Piletta , H. Porchet and P. Dayer, "Pharmacodynamics and drug action: Central
         analgesic effect of acetaminophen but not of aspirin," Clinical Pharmacology &
         Therapeutics, vol. 49, no. 4, pp. 350-354, 1991.

[75]   A. Milton , "Modern views on the pathogenesis of fever and the mode of action on
         antipyretic drugs," Journal of Pharmacy and Pharmacology, vol. 28, pp. 393-399,
         1976.

[76]   D. L. Simmons, R. M. Botting, P. M. Robertson, M. L. Madsen and J. R. Vane,
         "Induction of an acetaminophen-sensitive cyclooxygenase with reduced sensitivity

to nonsteroid antiinflammatory drugs," Proceedings of the National Acedemy of Sciences of the United States of America, vol. 96, no. 6, pp. 3275 - 3280, 1999.

[77]   D. L. Simmons, D. Wagner and K. Westover, "Nonsterioidal Anti-Inflammatory Drugs, Acetaminophen, Cyclooxygenase 2 and Fever," Clinical Infectious Diseases, vol. 31, no. 5, pp. 211 - 218, 2000.

[78]   A. Wiener, M. Shudler, A. Levit and M. Y. Niv, "BitterDB: a database of bitter compounds," The Hebrew University of Jerusalem, Institut of Biochemistry, Food Science and Nutrition, Faculty of Agriculture, 2012. [Online]. Available: http://bitterdb.agri.huji.ac.il/compound.php?id=121. [Accessed 10 10 2016].

[79]   PubChem Compound Database, "National Center for Biotechnology Information," [Online]. Available: https://pubchem.ncbi.nlm.nih.gov/compound/55182. [Accessed 19 02 2016].

[80]   K. Ng, D. Chong, C. Wong, H. Ong, C. Lee, B. Lee and L. Shek , "Central nervous system side effects of first- and second generation antihistamines in school children with perennial allergic rhinitis: a randomized, double-blind, placebo-controlled compatative study," Pediatrics, no. 113, pp. 16-121, 2004.

[81]   UCB Pharma Inc., "FDA," 2002. [Online]. Available: http://www.fda.gov/ohrms/dockets/AC/03/briefing/3999B1_23_Zyrtec.pdf. [Accessed 20 06 2016].

[82]   M. Melissa Conrad Stöppler, "RxList Inc.," 02 04 2015. [Online]. Available: http://www.rxlist.com/zyrtec-side-effects-drug-center.htm. [Accessed 20 06 2016].

[83]   Drugs.com, "Drugs," [Online]. Available: https://www.drugs.com/ppa/cetirizine.html. [Accessed 23 06 2016].

[84]   EMC, "EMC," 2015 12 26. [Online]. Available: https://www.medicines.org.uk/emc/medicine/29498. [Accessed 23 05 2016].

[85]   Evonik Industries, "Evonik Industries - Eudragit EPO," [Online]. Available: http://eudragit.evonik.com/product/eudragit/en/products-services/eudragit-products/protective-formulations/e-po/pages/default.aspx. [Accessed 28 03 2016].

[86]   Y. Hou, H. Wang, X. Zhang, M. Zou and G. Cheng, "Study of the mechanism of cationic drug release increas coated with Surelease after curing," Asian Journal of Pharmaceutical Science, vol. 8, pp. 295-302, 2013.

[87]   V. M. Velasco, J. L. Ford and A. R. Rajabi-Siahboomi, "Use of Dynamic Differential Scanning Calorimetry in Identifying Glass Transition Temperatures of Ethylcellulose and Surelease Film," Pharmacy and Pharmacology Communications, vol. 5, no. 4, pp. 259-263, 1999.

[88]   S. A. Kucera, "Eudragit E PO: The Pow(d)er for Superior Formulaiton Options," Presentation , p. 10, 28 10 2010.

[89]   D. A. Quinteros, V. Rigo Ramirez, A. F. Kairuz Jimenez, M. E. Olivera, R. H. Manzo and D. A. Allemandi, "Interaction between a cationic polymethacrylate," European Jornal of Pharmaceutical Science , vol. 33, pp. 72-79, 2008.

[90]   J. Eisele, G. Haynes and T. Rosamilla, "Charaterisation and toxicological behaviour of Basic Methacrylate Copolymer for GRAS Evaluation," Regulatory Toxicology and Pharmacology, vol. 61, pp. 32-43, 2011.

[91]   BASF SE - Nutrition & Health - Pharma Ingredients & Services, "Technical Information Kollicoat Smartseal 30 D," 02 06 2011.

[92]   BASF The chemical Company, "Information on toxicological data," BASF, Ludwigshafen, 2014.

[93]   The Dow Chemical Company, "Dow (R)," 26 06 2010. [Online]. Available: http://www.dow.com/dowwolff/en/industrial_solutions/polymers/ethylcellulose/. [Accessed 02 08 2016].

[94]   R. Voigt, Pharmazeutische Technologie, 9 ed., Stuttgart: Deutscher Apotheker Verlag , 2000, p. 221.

[95]   K. H. Bauer, K.-H. Frömming and C. Führer, Lehrbuch der Pharmaceutischen Technologie, 7. ed., Stuttgart: Wissenschaftliche Verlagsgesellschaft mbH, 2002, p. 177.

[96]   K. Hughes and J. Walsh, "Survey on Paediatric Product Developmemt - Industry Position," Colorcon, Basel, 2016.

[97]   Colorcon, "Product specification - Surelease Ethylcellulose Dispersion Type B NF E-7-19040," pp. 1-3, 13 07 2016.

[98]   J. Crönlein, "Surelease - Aqueous Ethylcellulose Dispersion," Prasentation, p. p.16, 2007.

[99]   M. T. Am Ende and A. Berchielli, "A Thermodynamic Model for Organic and

Aqueous Tablet Film Coating," Pharmaceutical Development and Technology, vol. 10, no. 1, pp. 47 - 58, 2005.

[100]   H. Hiestand and D. Smith, "Indices of tableting performance," Powder Technology, vol. 38, pp. 145-159, 1984.

[101]   E. Hienstand, "Mechanical properties of compacts and particles that control tabliting success," J Pharm Sci, vol. 86, pp. 985-990, 1997.

[102]   H. Brittain, "Physical Characterization of Pharmaceutical Solids," 1995.

[103]   G. Amidon, Pharmaceutical Material Sciences and Product Development, 2010.

[104]   F. Basam, P. York, R. Rowe and R. Roberts, "Young's modulus of powders used as pharmaceutical excipients," International Jornal of Pharmaceutics, vol. 64, pp. 55-60, 1990.

[105]   S. Jain, "Mechanical properties of powders for compaction and tableting: an overview," Pharmaceutical Science & Technology Today, vol. 2, pp. 20-31, 1999.

[106]   G. Carlsonand and B. Hancock, "A comparison of Physical and Mechanical Properties of commom Tableting Diluents," Excipient Development for Pharmaceutical, Biotechnologiy and Drug Delivery Systems, pp. 127-153, 2006.

[107]   H. Hausner, "Friction conditions in a mass of metal powder," International Journal of Powder Metall, vol. 3, pp. 7 - 13, 1967.

[108]   R. L. Carr, "Evaluation flow properties of solids," Chem. Eng., pp. 69-72, 1965.

[109]   A. W. Jenike, "Storage and flow of solids," BULLETIN OF THE UNIVERSITY OF UTAH, no. 123, 1964.

[110]   European Pharmacopoia, "2.2.42. Density of Solids," vol. 5.0, pp. 64-65.

[111]   Gas Pycnometry Volume and Density. [Film]. Micromeritics, 2015.

[112]   K. G. Pitt and J. M. Newton, "Tensile fracture of doubly-convex cylindrical discs under diametral loading," Jornual of Materials Science, vol. 23, pp. 2723-2728, 1988.

[113]   H. Batchelor, T. Ernest, T. Flanagan, S. Klein, R. Turner, N. Fotaki and D. Storey, "Towards the development of a paediatric biopharmaceutics classification system: Results of a survey of experts," International Journal of Pharmaceutics, vol. 511, no. 2, pp. 1151 - 1157, 2016.

[114]   M. Preis, M. Pein and J. Breitkreutz, "Development of a Taste-Masked
         Orodispersible Film Containing Dimenhyrdrinate," Pharmaceutics, vol. 4, pp. 551-
         562, 2012.

[115]   D. Kirsanov, M. Khaydukova, M. Pein-Hackelbusch, I. L. Immohr, V. Gilemkhanova
         and A. Legin, "Critical view on drug dissolution in artificial saliva: a possible use of
         in-line e-tongue measurements," European Journal of Pharmaceutical Sciences, p.
         submitted, 2016.

[116]   J. L. Kaye, "Review of paediatric gastrointestinal physiology data relevant to oral
         drug delivery," International Clinical Pharmacy, vol. 33, pp. 20-24, 2011.

[117]   B. Albertini, C. Cavallari, N. Passerini and D. Voinovich, "Characterization and
         taste-masking evaluation of actaminophen granules: comparison between different
         preparation methods in a high-shear mixer," European Journal of Pharmaceutical
         Science, vol. 21, pp. 295 - 303, 2004.

[118]   G. E. Amidon, P. J. Secreast and D. Mudie, "Particle, Powder and Compact
         Charaterization," in Developing Soild Oral Dosage Forms, Oxford, Elsevier Inc.,
         2009, pp. 163 - 186.

[119]   DMV International bv., "Directly compressible lactose: general considerations,"
         [Online]. Available: http://www.phexcom.cn/uploadfiles/20130217102234_5017.pdf.
         [Accessed 08 03 2016].

[120]   Molkerei MEGGLE Wasserburg GmbH & Co. KG, "Meggle Excipients and
         Technology," [Online]. Available: http://www.meggle-pharma.de/de/lactose/10-
         flowlac-100.html. [Accessed 08 03 2016].

[121]   FMC Corporation, "FMC Health and Nutrition," 10 03 2016. [Online]. Available:
         http://www.fmcbiopolymer.com/Pharmaceutical/Products/Avicelforsoliddoseforms.as
         px.

[122]   C. F. Lerk and H. Sucker, "Interaction of lubricants and colloidal silica during mixing
         with excipients. I. Its effect on tabletting," Pharm Acta Helv, vol. 52, p. 39, 1977.

[123]   S. Leigh, J. E. Carless and B. W. Burt, "Compression characteristics of some
         pharmaceutical materials," Journal of Phamaceutical Science, vol. 56, pp. 888 -
         892, 1967.

[124]   G. Alderborn and C. Nyström, "Radial and axial tensile strenght and strenght
         variablility of paracetamol tablets," Acta Pharmacutica Suecica, vol. 21, pp. 1 - 8,

1984.

[125]   S. Malamataris, S. b. Baie and N. Pilpel, "Plasto-elasticity and tableting of
         paracetamol, avicel and other powders," Journal of Pharmacy and Pharmacology,
         vol. 36, pp. 616 - 617, 1984.

[126]   A. B. Bangadu and N. Pilpel, "Effects of composition, moisture and steric acid on
         the plasto-elasticity and tableting of paracetamol-micocrystalline celullose mixtures,"
         Journal of Pharmacy and Pharmacology, vol. 37, pp. 289 - 293, 1985.

[127]   M.-C. Lin and W. C. Duncan-Hewitt, "Deformation kinetics of acetaminophen
         crystals," International Journal of Pharmaceutics, vol. 106, pp. 187 - 200, 1993.

[128]   P. D. Martino, A. M. Guyot-Hermann, P. Conflant, M. Drache and J. C. Guyot, "A
         new pure paracetamol for direct compression: The orthorhombic form," International
         Journal of Pharmaceutics, vol. 128, no. 1-2, pp. 1 - 8, 1996.

[129]   P. Lennartz and J. Mielck, "Minitabletting: improving the compactability of
         paracetamol powder mixtures," Int. J. Pharm., no. 173, pp. 75 - 85, 1998.

[130]   Evonik Industries AG, "E-Lab Eudragit," Evonik Industries AG, [Online]. Available:
         https://e-lab.eudragit.com/application_guidelines/wiki/?v=43. [Accessed 03 10
         2016].

[131]   D. D. Douroumis, A. Grycke and S. Schminke, "Development and Evaluation of
         Cetirizine HCL Taste-Masked Oral Disintegrating Tablets," AAPS PharmSciTech,
         vol. 12, no. 1, 2010.

[132]   B. C. Hancock, J. T. Colvin, M. P. Mullarney and A. V. Zinchuck, "The relative
         densities of pharmaceutical powders, blends, dry granulations, and immediate-
         release tablets," Pharmaceutical Technology, vol. 27, no. 4, pp. 64 - 80, 2003.

[133]   P. D. Martino, A. Guyot-Hermann, P. Conflant, M. Drache and J. C. Guyot, "A new
         pure paracetamol for direct compression: the orthorhombic form," International
         Journal of Pharmaceutics, vol. 128, pp. 1 - 8, 1996.

[134]   K. E. Bürki , "Preparation of taste masked orally disintegration tablets by
         compression of coated pellets," Dissertation Freie Universität Berlin, Berlin, 2016.

[135]   Colorcon, "Colorcon," in The Influence of In Vitro Dissolution Method on
         Lansoprazole Release, Los Angeles, 2009.

[136]   Y. Hou, H. Wang, X. Zhang, M. Zou and G. Cheng, "Study of the mechanism of

cationic drug release increase coated with Surelease after curing," Asian Journal of Pharmaceutical Science, vol. 8, pp. 295 - 302, 2013.

[137]   A. Agresti , An introduction to categorical data analysis, New Jersey: John Wiley & Sons, 2007.

[138]   J. A. Mennella and G. K. Beauchamp, "Optimizing Oral Medications for Children," Clinical Therapeutics, vol. 30, no. 11, pp. 2120-2132, 2008.

[139]   J. Lutz, "Stability Testing of SM IMP: Accelerated Stability Approaches - PASTA (Internal Report)," Roche, Basel, 2015.

[140]   H. Batchelor, T. Ernest, T. Flanagan, S. Klein, R. Turner, N. Fotaki and D. Storey, "Towards the development of a paediatric biopharmaceutics," International Journal of Pharmaceutics, vol. 511, no. 2, pp. 1151 - 1157, 2016.

[141]   S. Potdar, B. Skalsky and S. Chakraborty, "Science Behind Effectice Coating with Eudragit Polymers," Pharma Times, vol. 45, no. 3, pp. 17-21, 2013.

[142]   A. Zajicek, M. J. Fossler, J. S. Barrett and J. H. Worthington, "A Report from the Pediatric Formulations Task Force: Perspectives on the State of Child-Friendly Oral Dosage Forms," AAPS Journal, vol. 15, no. 4, pp. 1072 - 1080, 2013.

[143]   H. Lou, M. Liu, L. Wang, S. R. Mishra, W. Qu, J. Johnson, E. Brunson and H. Almoazen, "Development of a Mini-Tablet of Co-Grinded Prednisone-Neusilin Complex for Pediatric Use," AAPS PharmSciTech, vol. 14, no. 3, pp. 950-958, 2013.

9. List of Figures

10. List of Tables

11. List of Equations

12. Curriculum Vitae

Date of birth   21.08.1990

Place of Birth   Bad Säckingen, Germany

Education

10/2014 – 12/2016	**University of Technology Graz,** Graz, Austria Degree: MSc in Chemical and Pharmaceutical Engineering
09/2011 – 07/2014	**University of Applied Sciences Northwestern Switzerland,** Muttenz, Switzerland Degree: BSc in Life Sciences Technologies
09/2010 – 07/2011	**Vocational Technical College,** Bad Säckingen, Germany Advanced technical college entrance qualification
09/2007 – 02/2010	**Apprenticeship for Pharmaceutical Technicians**, Novartis Pharma Produktion GmbH, Wehr, Germany

Professional Experience

Since 02/2016	**F. Hoffmann-La Roche Ltd,** Basel, Switzerland Internship in department of process development Master Thesis: Development and Evaluation of a taste-masked pediatric Minitablet Formulation with a bitter Model Drug
10/2015 – 01/2016	**Institute of Process and Particle Engineering TU Graz,** Graz, Austria: Student assistant
11/2014-08/2015	**Research Center Pharmaceutical Engineering GmbH,** Graz, Austria: Student research assistant
07/2014 – 09/2014	**Queen´s University,** Belfast, United Kingdom Internship in department for Pharmaceutical Technology

| 03/2013 – 02/2014 | **Engineering office Böttinger**, Wehr, Germany |
| | Working student at Novartis Pharma Produktions GmbH |

| 07/2011 – 09/2011 | **GP Grenzach Produktions GmbH**, Grenzach, Germany |
| | Pharmaceutical technician |

| 06/2010 – 09/2010 | **Novartis Pharma Produktions GmbH,** Wehr, Germany |
| | Pharmaceutical technician |

Awards

| 09/2016 | **PCCA Poster Award** |
| | 8th EuPHI Conference, Lisbon, Portugal |

| 09/2015 – 09-2016 | **Merit-based Scholarship** |
| | Dean's office of Faculty of Technical Chemistry, Chemical and Process Engineering, Biotechnology |

| 09/2014 | **Roche Award Life Science 2014** |
| | F. Hoffmann-La Roche Ltd. |

| 07/2011 | **Best high-school graduate in chemistry** |
| | GDCh - Gesellschaft Deutscher Chemiker |

13. Appendix

I.   Compositions artificial saliva

	PhEur	Guhmann 2013		Khaydukova 2015				Lennon 2006		Abdelbary 2005		Marques 2011	
	pH 6.8 buffer	SSF1 [g/l]	SSF2 [g/l]	AS1 [g/l]	AS2 [g/l]	AS3 [g/l]	[g/l]	[g/l]	SS1 [g/L]	SS2 [g/L]	SS3 [g/L]	SS4 [g/L]	SS5 [g/L]
Sodium dihydrogenphosphate			2.38					0.78			0.273		
Disodium hydrogenphosphate							0.34		0.866	0.866	0.204		2.38
Potassium dihdydrogenphosphate	1.000	1.63	0.19	3.402	3.402	3.402	0.33		0.68	0.68			0.19
Di potassium hydrogen phosphate	2.000												
Sodium chloride	8.500	2.34	8		0.402	0.402	0.17	0.4	0.6	0.6	1.017	0.117	8
Calcium chloride dihydrogen		0.17			0.209	0.209	0.16	0.8	0.22	0.22	0.228		
Potassiom chloride					0.712	0.712	1.27	0.4	0.72	0.72		0.149	
Sodium azide						0.005							
porcine gastric mucin						1.8						1	
submaxillary mucin											1		
alpha amylase						1					2	2	
Potassium bicarbonate									1.5	1.5			
Potassium thiocyanate									0.06	0.06			
Citric acid									0.03	0.03			
Magnesium chloride hexahydrate											0.061		
Potassium carbonate hemihydrate											0.603		
Sodium bicarbonate											0.273	2.1	
Ascorbic acid						0.002							
Ammonium chloride						0.16							
Sodium thiocyanate						0.16							
Sodium sulfide								0.005					
Urea								1					
Xanthan gum 200 mesh				0.75	0.75	0.75							
pH		6.2-7.4	6.75	7.2	7.2	7.2	6.4	5.8	6.5	7.4			6.8

II.   List of materials

Compound	Type	Supplier/Manufacturer	Article no.	Lot no.
Acetaminophen	powder	Sigma Aldrich	A5000-1KG	MKBV3323V
Acetic Acid	puriss. P.a. , ACS reagent, reag ISO. ; reag. Ph.Eur., >= 99.8%	Sigma Aldrich	33209-1L	SZBE0420V
Acetonitirl	Supra Gradient	Biosolve Chimie SARL	#0001203502RC	1087371
Aerosil	200	Sisseln	10018879	SIS02187
Alpha-amylase from porcine pancreas	Type VI-B >= 10 units /mg solid	Sigma Aldrich	A3176-1MU	SLBP401V
Avicel	PH 101	Hinderling	10013859	SIS02119
Avicel	PH 102	Fuchs Y.-A.	10018872	SIS01901
Calcium chloride dihydrate	BioUltra, for molecular biology, >= 99,5% (T)	Sigma Aldrich	21097-250G	BCBP0893V
Cetirizine dihydrochloride		SAFC	89126-1KGF	BCBR8731V
Croscarmellose Sodium	Ac-Di-Sol , SD 711	P. Schwerdt		SIS01933
Eudragit E PO®	Powder	Evonik		G150731543
Flowlac	100	Meggle	-	L1537 A4950
Iron oxide		Mimox (Schweiz)		13RM0040
Isomalt	galenIQ 721	beneo palatinit		L1214940U2
Kollicoat® Smartseal	30 D	BASF	50138478	12313802
Magnesiumstearat		Hinderling	10018948	SIS02018
Methanol	LiChrosolv (R)	Merck	1.06007.2500	I778407517
Mucin from porcine stomach	Type II	Sigma Aldrich	M2378-100G	SLBP5089V
Opadry® II	clear	Colorcon	85F190000	DT623570

Paraffin oil	Puriss., meets analytical specification of Ph.Eur., BP, viscous liquid	Sigma Aldrich	18512-1L	SZBC3380V
Parteck	M100	Merck	10068610	M691794120
Phosphoric acid	puriss. P.a., ACS reagent	Fluka Analytical	79620-500ml	BCBF6119
Polyethylenglycol	6000	Sisseln	10084043	SIS02243
Potassium chloride	99+% for analysis	Acros organics	196770010	A0360862
Potassium dihydrogenphosphate	Surapur (R), anhdyrous	Merck	1051080500	B0405508923
Potassium hydroxid	pro analysi	Merck	1056371A	-
Sodium azide	BioUltra, >= 99,5% (T)	Sigma Aldrich	71289-5G	STBG1259V
Sodium chloride	pro analysi	Merck	1064041000	K39486504849
Sodium lauryl sulfate	100	Produktion		SIS02289
Sodium stearyl fumarate		Hinderling	07648904	SIS01886
Stearic acid	fine	Sisseln		SIS01776
Surelease®	Type B NF	Colorcon	E-7-19040	IN530762
Talc		Hinderling		SIS01405
Triethylcitrate	Ph.Eur, JPE, NF	Merck	8.17059.1000	K46898559606
Wasser	LiChrosolv (R)	Merck	1.15333.2500	Z0379133614
Xanthan gum	180	CP Kelco	Xantural 180	3J0242K

III.   List of equipment

| Apparatus	Manufacturer	Type	Serial number
3D Microscope	Schott AG (Germany)	BX 51 M 1500	
Analytic balance	Mettler Toledo AG (Switzerland)	XP205	1123373550
Climatic chamber	Memmert GmbH & Co. KG (Germany)	HPP 108	5672D
Digital caliper	Tesa Technology SA (Switzerland)	TESA ShopCAL 150mm	6C0076301
Digital microscope	Keyrence Deutschland GmbH (Germany)	VHX-S550E	4B410186
Ultra Turax	Kinematica AG (Switzerland)	Polytron PT 10 - 35 GT	PF-809-0010-01-12
Dissolution apparatus	PION Inc. (USA)	µDiss, Rainbow	01137
Fuidized Bed Granulator	Glatt GmbH Process Technology (Germany)	Mini-Glatt	
Halogen Misture Analyzer	Mettler Toledo AG (Switzerland)	HR83-P	11233115
Hardness tester	Sotax AG (Switzerland)	Sotax HT-1	8700
Helium pycnometer	Micromeritics Instrument Corporation (USA)	AccuPyc 1330	4002
HPLC	Waters Corporation (USA)	Seperatrion Module 2795, Photodiode Array Detector 2996	K02SM9379M
HPLC waters 1690	Waters Corporation (USA)	Separation Module 2690, Dual lamda Absorbance Detector 2487	K97SM4776M
Hydraulic Press	Carver Inc. (USA)	Carver Press	260-563-7577 X5237
Infrared pistol	Testo AG (Switzerland)	830-T2	05608312
Lab balance	Sartorius AG (Germany)	ED4202S	24306869
Laboratory stirrer	IKA Werke GmbH & Co. KG (Germany)	Eurostar power b	IP42
Laser diffractometer	Malvern Instruments Ltd. (UK)	Mastersizer 3000	MAL1062527
Laboratory mill	IKA Werke GmbH & Co. KG (Germany)	M20	

Microscope	Zeiss (Germany)	Imager Z1	3512001787
Obital shaker	OmniLab (Switzerland)	GFL 3025	10384608F
Overhead stirrer	Heidolph Instruments GmbH & Co.KG (Germany)	RzR2041	02083370
Pendulum Impact Device	Pharmsci (USA)	PID II	PID II
Peristaltic pump	Flocon Products Inc. (USA)	Flocon 1B.1003-R/65	05033
Peristaltic pump	Watson-Marlow Ltd. (UK)	Sci 323	H010968
pH Meter	Mettler Toledo AG (Switzerland)	FiveEasy	1230195514
Quadro cone mill	Quadro Engineering Inc. (Canada)		U3-0031
Ring shear tester	Schulze (Germany)	RST XS	
Rotary Press	Korsch AG (Germany)	XL100	1510085
SEM	Zeiss (Germany)	∑igma VP	01-25
Sorting apperatus	CI Precision (UK)	SP 40	
Side vented pan	Glatt GmbH Process Technology (Germany)	GMPC1	102231
Tablet press	Korsch AG (Germany)	XL-100	1510085
Tablet testing device	Pharmatron (Switzerland)	Multitest 50	300.06400
Tap density meter STAV2003	J. Engelsmann AG (Germany)		65-543
Temperature sensor	Rational Technische Lösungen GmbH (Germany)	DTM-Nr.2	3190-2
Temperature/moisture sensor	Testo AG (Schwitzerland)	Testo 625	02416853
Turbula mixer T2C	Willy A. Bachofen AG Maschinenfabrik (Switzerland)		930252
Vortex mixer	Scientific Industries Inc. (USA)	Vortex Genie	PF-809001001-12
X-ray µCT	Bruker microCT (Belgium)	Skyscan 1172	08E01109

IV. List of Software

Name	Version	Company
Au PRO	5.1.6.0	PION Inc., USA
CTVox	2.4	
DataViewer	1.4	
Empower3	3471	Waters
Excel	2010	Microsoft
JMP	12	SAS Institute, NC, USA
NRecon		
R Core Team	2016	The R Fundation
RStudio	3.3.1.	RStudio®

V. Method development particle size development measurement
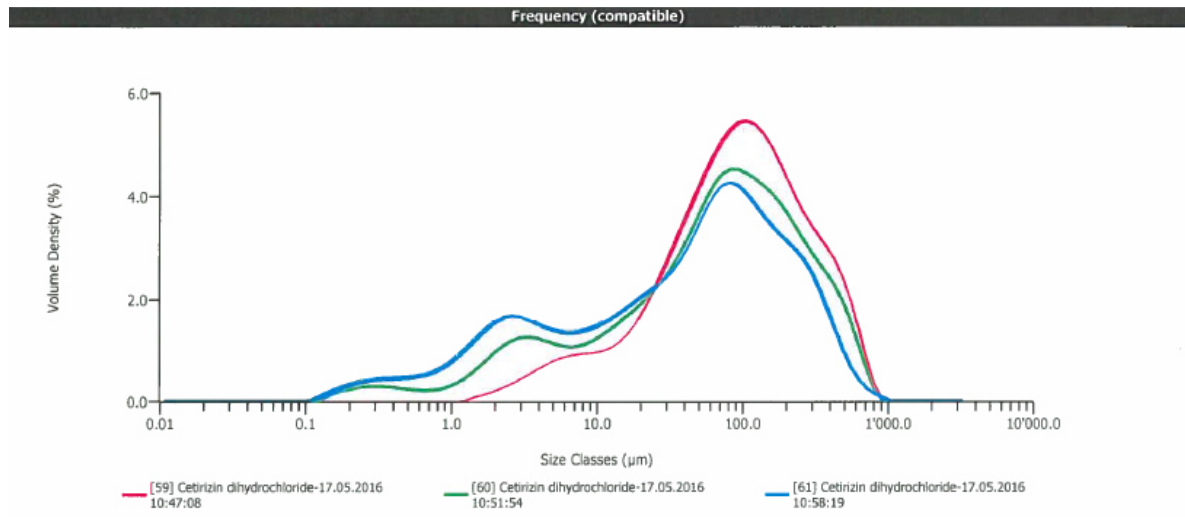
(red: 0bar; green: 0.5bar; blue: 1 bar)

VI.   QRA

Master Thesis Stefanie Keser	Version :01	Date : 10.03.2016	pCQA (potential Critical Quality Attribute)											
Development and Evaluation of a taste-masked pediatric Minitablet Formulation with a bitter Model Drug			Appearance			Efficient taste masked			Content Uniformity			Dissolution, SGF		
Potential factors influencing processes and / or quality attributes	Potential effect on process Y/N	Potential effect on quality attribute(s) Y/N	Severity	Probability	Primary risk number	Severity	Probability	Primary risk number	Severity	Probability	Primary risk number	Severity	Probability	Primary risk number
Raw materials														
Physical, Chem properties API														
Particle size , - distribution	Y	Y	1	1	(green)	2	1	(yellow)	2	1	(yellow)	1	1	(green)
Interaction with polymer (Cetirizine dihydrochloride)	N	Y	2	1	(yellow)	3	3	(red)	1	1	(green)	1	1	(green)
Polymorph (Orthorhombisc Polymorph Paracetamol)	Y	Y	2	2	(yellow)	1	1	(green)	1	1	(green)	1	1	(green)
Excipient properties in formulation														
Plasticizer concentration (Triethylcitrate)	Y	Y	3	1	(yellow)	3	2	(red)	1	1	(green)	2	2	(yellow)
Talc concentration	Y	Y	3	2	(red)	3	2	(red)	1	1	(green)	1	1	(green)
Talc quality (PSD)			2	1	(yellow)	2	1	(yellow)	1	1	(green)	1	2	(yellow)
Choice of polymer			1	1	(yellow)	3	2	(red)	1	1	(green)	3	2	(red)
Antioxidance (Butylhydroxytoluene) - Kollicoat Smartseal			2	1	(yellow)	3	2	(red)	1	1	(green)	3	2	(red)
Stearic acid			2	1	(yellow)	2	1	(yellow)	1	1	(green)	2	1	(yellow)
Sodium lauryl sulfate			2	1	(yellow)	2	1	(yellow)	1	1	(green)	2	1	(yellow)
Ratio Surelease: Pore Former (Opadry)			2	1	(yellow)	3	2	(red)	1	1	(green)	3	2	(red)
Coating (Fluidized Bed, Mini Glatt)														
Inlet air temperature	Y	Y	3	1	(yellow)	3	1	(yellow)	1	1	(green)	1	1	(green)
Volumetric flow rate	Y	Y	3	2	(red)	3	2	(red)	1	1	(green)	3	2	(red)
Outlet air temperature			2	2	(yellow)	2	2	(yellow)	1	1	(green)	2	2	(yellow)
Product temperature			3	1	(yellow)	3	2	(red)	1	1	(green)	3	2	(red)
Atomization pressure			1	2	(yellow)	2	1	(yellow)	1	1	(green)	2	1	(yellow)
Distance bottom plate to Wurster column			2	1	(yellow)	2	1	(yellow)	1	1	(green)	2	1	(yellow)
exhaust air temperatur, - humidity			3	1	(yellow)	3	1	(yellow)	1	1	(green)	1	1	(green)
spraying amount (coating time, spray rate)			2	1	(yellow)	3	2	(red)	1	1	(green)	3	2	(red)

VII.   Overview coating results acetaminophen minitablets

Batch	Para2.2.I	Para2.2.II	Para2.2.III	Para2.2.IV	Para2.2.V	Para2.2.VI	Para2.2.VII	Para2.3.I	Para2.3.II	Para2.3.III
Polymer	Eudragit EPO	Eudragit EPO	Eudragit EPO	Smartseal	Smartseal	Surelease (85:15), 2%WG	Surelease (85:15); 4%WG	Surelease (80:20), 2%WG	Surelease (80:20), 4%WG	Surelease (80:20), 6%WG
Description			0.5mm Nozzle		reduced Batch size	Filter 500µm	Filter 500µm			
Process evaluation										
LOD before [%]	2.04	2.04	2.04	2.04	2.04	2.04	2.04	1.99	1.99	1.99
LOD after [%]	1.33	1.01	1.83	1.28	1.78	2.19	2.08	2.2	2.05	1.99
Initial MT weight [mg]	14.37	14.37	14.37	14.37	14.37	14.37	14.37	14.30	14.22	14.22
Final MT weight [mg]	17.33	17.45	17.11	16.20	17.46	14.54	15.07	14.69	15.11	15.15
Srel Weight[%]			5.14		5.60	5.18	11.42	5.19	5.02	5.63
Weight gain [%]	21.49	22.72	19.32	13.59	21.85	1.03	4.79	2.45	6.25	6.59
Polymer applied [mg/cm²]	7.02	7.42	6.31	3.92	6.92	1.33	2.30	1.86	2.84	3.20
Coating Uniformity	2.071	1.93	0.86	1.97	0.961	0.736	1.685	0.745	0.743	0.836
Coating Process Efficiency[%]	87.76	92.76	78.90	49.01	86.49	51.40	109.84	112.43	146.29	99.85
Problems	Layering of wurster	Layering of wurster even bigger	Blockage of Filter	Blockage of Filter	Blockage of Filter	-	-	-	-	-
IPC coated MT										
Appearance	peeling due to adhesion	Less peeling	good	broken MT , capped	small amount of broken MT	some MT rough surface and broken	some MT rough surface	some MT rough surface	good	good
Hardness [N]	45.50	39.30	53.10	47.50	53.30	27.70	28.30	30.00	30.10	31.30
Height [mm]	2.88	2.90	2.88	2.83	2.91	2.75	2.75	2.76	2.77	2.78
Coating Thickness [µm] µCT (n>600)	-	-	80.6±1.2	-	78.3±2.2	-	-	-	-	-
Coating Thickness [µm] SEM (n=4)	-	-	79.25±5.3	-	85.8±5.7	-	-	-	-	-
Dissolution SGF immediate release [mm:ss]	-	-	02:15	-	03:37	-	-	-	-	-

Batch	Para2.3.IV		Para2.3.V		Para2.3.VI			
Polymer	SMA; 1mg/cm^2	SMA; 1.5mg/cm^2	SMA; 2mg/cm^2	SMA; 4mg/cm^2	EPO; 2mg/cm^2	EPO; 4mg/cm^2	EPO; 6mg/cm^2	EPO; 8mg/cm^2
Description								
Process evaluation								
LOD before [%]	2.06	2.06	2.03	2.03	2.02	2.02	2.02	2.02
LOD after [%]	1.76	1.95	1.93	1.94	2.07	1.98	1.86	1.92
Initial MT weight [mg]	14.22	14.22	14.22	14.22	14.22	14.22	14.22	14.22
Final MT weight [mg]	14.703	14.907	15.021	16.246	15.192	15.912	16.899	17.869
Srel Weight [%]	5.74	5.50	5.39	14.66	6.05	6.58	7.46	7.04
Weight gain [%]	3.74	4.98	5.74	14.35	6.78	11.94	19.03	25.79
Polymer applied [mg/cm²]	1.70	1.97	1.97	4.23	2.22	3.90	6.22	8.42
Coating Uniformity	0.829	0.804	0.794	0.473	0.9	1.027	1.237	0.984
Coating Process Efficiency [%]	160.34	121.51	88.63	95.79	100.7542	87.54525	93.6272	95.3054
Problems								
IPC coated MT								
Appearance	rough surface, broken MT, inhomogen in color	rough surface, broken MT, inhomogen in color	rough surface, broken MT	-	inhomogenious in color	-	-	-
Hardness [N]	29	33.3	36.6	42.2	44.8	39.4	50.2	52
Height [mm]	2.73	2.79	2.89	2.83	2.77	2.8	2.88	2.92
Coating Thickness [µm] µCT (n>1000)	13.3±0.3	18.7±0.4	22.8±0.3	37.1±0.7		-	-	-
Coating Thickness [µm] SEM (n=4)	10±0.8	20.3±3.3	23±1.4	39±4.2	-	-	-	-

VIII. Overview coating results cetirizine minitablets

Batch	CET1.2.I		CET1.2.II		Technology comparison		
	CET1.2.I-1	CET1.2.I-2	CET1.2.II-1	CET1.2.II-2	CET1.2.XIII	CET1.2.XIV	CET1.2.XV
Description	Sur91.7:Opa8.3; 5.965%WG	Sur91.7:Opa8.3; 12.448%WG	Sur85:Opa15; run7; 2.25%WG	Sur85:Opa15; run3; 4.75%WG	Sur80:Opa20, 6.5%WG	Sur80:Opa20, 6.5%WG	Sur80:Opa20, 6.5%WG
Process evaluation							
LOD before [%]	1.84	1.84	1.84	1.84	1.84	1.84	1.84
LOD after [%]	0.69	1.29	1.14	0.75	1.21	1.28	1.26
Initial MT weight [mg]	16.670	16.670	16.670	16.670	16.67	16.67	16.67
Final MT weight [mg] MT50	17.433	18.567	16.9	17.205	17.51	17.53	17.53
Srel weight [%]	0.71	0.81	1.25	1.28	1.416	1.743	1.349
Weight gain [%]	5.80	12.00	2.10	4.36	5.73	5.78	5.79
Polymer applied [mg/cm²]	2.534	5.242	0.893	1.801	2.37	2.39	2.39
Coating Uniformity	0.122	0.293	0.208	0.218	0.25	0.30	0.23
Coating Process Efficiency [%]	97.272	96.432	93.453	91.693	88.08	88.97	89.02
Problems							
IPC coated MT							
Appearance	Glossy, no coating defects, homogenous	Glossy, no coating defects, homogenous	good	good	less glossy, not homogenious coloring	less glossy, not homogenious coloring, twinning	less glossy
Hardness [N]	34.8	43	32.9	35.5	40.1	38.1	38.6
Height [mm]	2.97	3.01	2.95	2.96	2.95	2.96	2.95
Dissolution SGF immediate release [hh:mm:ss]	01:10:58; 00:17:36	no release within 05:17:36	00:02:41	00:06:04	00:03:58	00:04:16	00:05:17
Taste masking [µg/ml]: 60s; 180s; 300s	0; 0; 0	0; 0; 0	0; 2.067; 65.534	0; 0; 14.861			

IX.   Raw data DoE

Run	Polymer.Ratio [%]	Spraying.Rate [g/min]	Spraying.Time [min]	Theoretical Weigth gain [%]	Taste masking 60s [µg/ml]	Taste masking180s [µg/ml]	Taste masking 300s [µg/ml]	Dissolution t 85% [s]	Coating Uniformity []	Coating Process Efficiency [%]	Hardness [N]	Height [mm]
1	85	1	45	2.25	0.174	29.151	119.376	161	0.208	93.453	32.9	2.95
2	80	2	70	6.5	0.000	0.000	0.000	463	0.203	98.154	34.2	2.95
3	85	3	45	5.75	0.000	0.000	1.765	535	0.240	97.736	37.5	2.94
4	85	1	95	4.75	0.000	0.000	14.861	389	0.226	98.113	32.6	2.95
5	85	3	95	13.25	0.000	0.000	0.000	1860	0.238	93.884	39.3	3.06
6	80	2	70	6.5	0.000	0.000	0.000	498	0.244	94.856	36.3	3.04
7	75	1	95	4.75	0.000	2.696	44.386	186	0.212	92.791	33.7	2.97
8	75	1	45	2.25	1.410	49.029	143.112	182	0.184	93.049	30.6	2.94
9	75	3	95	13.25	0.000	0.000	0.000	1358	0.216	90.621	41.7	3.01
10	75	3	45	5.75	0.000	0.000	0.258	417	0.234	90.475	37.0	2.95
11	80	2	70	6.5	0.000	0.000	0.000	434	0.208	84.257	37.0	2.96

X.   In vitro taste assessment in AS DoE
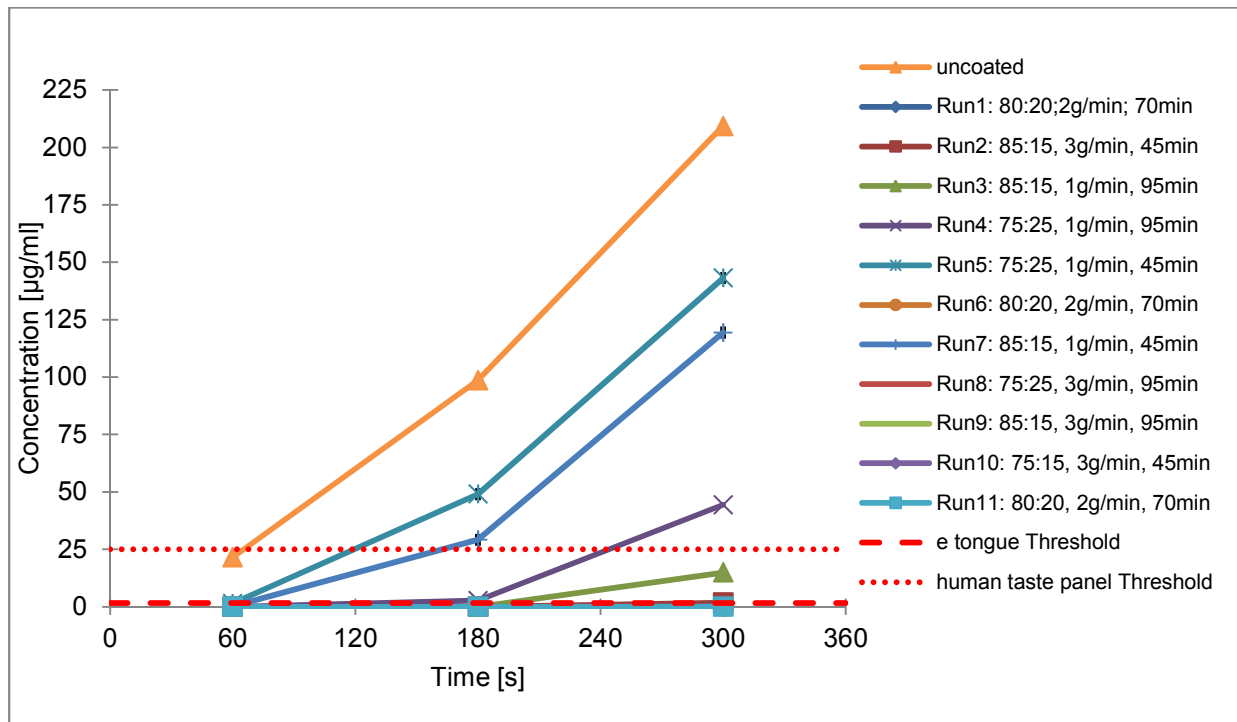
XI.   Dissolution in SGF DoE
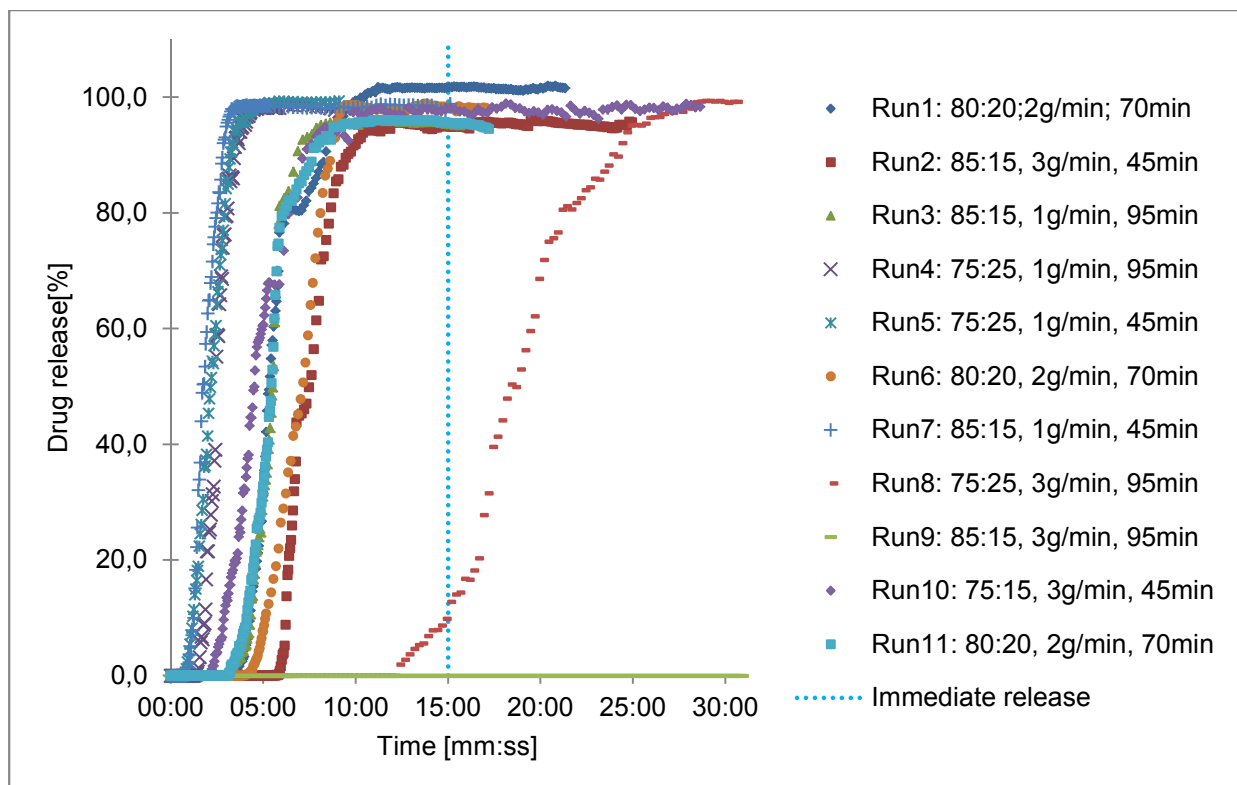
XII.   R code – statistical analysis DoE

```r
rm(list=ls())

install.packages("ggplot2")
install.packages("dplyr")
install.packages("knitr")
install.packages("lmerTest")
install.packages("reshape2")
install.packages("pander")
install.packages("xtable")
install.packages("pastecs")
install.packages("scales")


library(ggplot2)
library(dplyr)
library(knitr)
library(lmerTest)
library(reshape2)
library(pander)
library(xtable)
library(pastecs)
library(scales)


### General graphical functions
multiplot <- function(..., plotlist=NULL, file, cols=1, layout=NULL) {
  library(grid)

  # Make a list from the ... arguments and plotlist
  plots <- c(list(...), plotlist)

  numPlots = length(plots)

  # If layout is NULL, then use 'cols' to determine layout
  if (is.null(layout)) {
    # Make the panel
```

```r
    # ncol: Number of columns of plots
    # nrow: Number of rows needed, calculated from # of cols
    layout <- matrix(seq(1, cols * ceiling(numPlots/cols)),
                ncol = cols, nrow = ceiling(numPlots/cols))
  }

  if (numPlots==1) {
    print(plots[[1]])

  } else {
    # Set up the page
    grid.newpage()
    pushViewport(viewport(layout = grid.layout(nrow(layout), ncol(layout))))

    # Make each plot, in the correct location
    for (i in 1:numPlots) {
      # Get the i,j matrix positions of the regions that contain this subplot
      matchidx <- as.data.frame(which(layout == i, arr.ind = TRUE))

      print(plots[[i]], vp = viewport(layout.pos.row = matchidx$row,
                          layout.pos.col = matchidx$col))
    }
  }
}

cbPalette <- c("#0072B2", "#D55E00", "#E69F00", "#56B4E9", "#009E73", "#F0E442",
"#CC79A7")
cbPalette2 <- c("grey20", "#237F23")
cbPalette3 <- c("#0072B2","#237F23", "#D55E00")
cbPalette4 <- c("grey20", "#237F23", "grey20")


### Creating data set
### Reading data table
d <- read.table("DoE_TM_COAT.csv", header=TRUE, sep=";", quote="", comment.char="",
as.is=TRUE)


any(sapply(d, is.factor))
```

```
names(d)


### Creating new variable names
dat <- with(d, data.frame(
  Run=Run_real.Order,
  Run_old,
  Polymer.Ratio,
  Spraying.Rate,
  Spraying.Time,
  Taste.masking.60s=Taste.masking.60s..µg.ml.,
  Taste.masking.180s=Taste.masking.180s..µg.ml.,
  Taste.masking.300s=Taste.masking.300s..µg.ml.,
  Dissolution=Dissolution..hh.mm.ss.,
  Coating.Uniformity=Coating.Uniformity...,
  Coating.Process.Efficiency=Coating.Process.Efficiency....,
  Hardness=Hardness..N.,
  Height=Height.mm.,
  stringsAsFactors=FALSE
))


rm(d)


dat$Dissolution <- ifelse(dat$Dissolution==">30:00", "00:31:00", dat$Dissolution)


dat$Dissolution                                                            <-
as.numeric(substr(dat$Dissolution,4,5))*60+as.numeric(substr(dat$Dissolution,7,8))


dat$Weight.Gain      <-      (dat$Spraying.Rate*dat$Spraying.Time-10*(dat$Spraying.Rate-
1))*0.15*(100/300)


names(dat)
dim(dat)


FactorIndices <- 3:5
ResponseIndices <- 6:13


factors <- names(dat)[FactorIndices]
factors
```

```
responses <- names(dat)[ResponseIndices]
responses

### Creating responses
resp_exp <- data.frame(cbind(
  Name=c("Taste Masking at 60 seconds",
      "Taste Masking at 180 seconds",
      "Taste Masking at 300 seconds",
      "Time to 85% Dissolved",
      "Coating Uniformity",
      "Coating Process Efficiency",
      "Hardness",
      "Height"),
  Label=responses,
  Unit=c("micro g/mL",
      "micro g/mL",
      "micro g/mL",
      "sec",
      "unitless",
      "%",
      "N",
      "mm"
  )),
  stringsAsFactors=FALSE)

tab_responses <- resp_exp
tab_responses

### Computing coded factor levels
c_factor_val <- sapply(factors, FUN=function(f) {
  x <- dat[,f]
  H <- max(x, na.rm = TRUE)
  L <- min(x, na.rm = TRUE)
  (x-(H+L)/2)/((H-L)/2)
})
```

```r
### checking design orthogonality
sum_c_factor_val <- sapply(factors, FUN=function(f) {
  sum(c_factor_val[,f])
})


sum_c_factor_val


### Naming coded factors
factors_c <- c("Pol.Ratio", "Spray.Rate", "Spray.Time")


colnames(c_factor_val) <- factors_c


### Adding coded factors to data frame
dat <- as.data.frame(cbind(dat, c_factor_val))


names(dat)


### Creating factors
factors_exp <- data.frame(
  Name=c("Polymer Ratio", "Spraying rate", "Spraying Time"),
  Label=factors,
  Unit=c("% w/w", "g/min", "min"),
  CodedName=factors_c,
  Low=sapply(factors, FUN=function(f){min(dat[,f])}),
  Target=sapply(factors, FUN=function(f){dat[dat$Pol.Ratio==0,f][1]}),
  High=sapply(factors, FUN=function(f){max(dat[,f])}),
  stringsAsFactors=FALSE)


tab_factors <- factors_exp


rownames(tab_factors) <- NULL


tab_factors


### Creating table with factor levels and run order
table_runs1 <- with(dat, data.frame(Run,
                    dat[,factors],
```

```
                              stringsAsFactors = FALSE))
table_runs <- table_runs1


### Creating table with summary statistics
## Getting summary statistics
resp_stats <- as.data.frame(t(stat.desc(dat[,responses])))


tab_stats <- with(resp_stats, data.frame(
  Response=row.names(resp_stats),
  N=nbr.val,
  Min= min,
  Max=max,
  Range=range,
  Median=median,
  Mean=mean,
  Std.Dev=std.dev,
  CV=coef.var*100
))


tab_stats


## Fitting lm models for responses


responses_m <- responses[3:8]


models <- sapply(responses_m, FUN=function(response) {
  lm(formula(paste(response,    "~    Pol.Ratio    +    Spray.Rate    +    Spray.Time    +
Pol.Ratio*Spray.Rate + Pol.Ratio*Spray.Time + Spray.Rate*Spray.Time")), data=dat)
}, simplify=FALSE)


## Extracting information from lm models
model.summary <- sapply(models, FUN=function(model){
  summary(model)$coefficients[-1,]
}, simplify=FALSE)


model.summary_2 <- lapply(model.summary, FUN=function(data){
  Effect <- data.frame(Effect=rownames(data), stringsAsFactors=FALSE)
  rownames(data) <- NULL
```

```r
  data.frame(cbind(Effect, data))
})


model.summary_2  <-   lapply(model.summary_2,   function(x)   x[order(abs(x$Estimate),
decreasing = TRUE),])


summary_collapsed <- do.call(rbind.data.frame, model.summary_2)


colnames(summary_collapsed)


Response <- as.data.frame(rownames(summary_collapsed), stringsAsFactors=FALSE)


Response_2 <- substr(Response[,1], 1, nchar(Response[,1])-2)


rownames(summary_collapsed) <- NULL


summary_collapsed_new <- data.frame(Response=Response_2,
                    Effect=gsub("1", "", summary_collapsed$Effect),
                    Eff.Size=round(2*summary_collapsed$Estimate,3),
                    Estimate=round(summary_collapsed$Estimate,3),
                    Std.error=round(summary_collapsed$Std..Error,3),
                    p.value=round(summary_collapsed$Pr...t..,3),
                    stringsAsFactors=FALSE)
summary_collapsed_new

### Creating main effects plots
# First set of responses
responses_p <- responses[1:4]


combns <- as.matrix(expand.grid(responses_p, factors, stringsAsFactors = FALSE))
colnames(combns) <- c("Response", "Factor")


ps_ME1 <- apply(combns, 1, FUN=function(vars) {
  xvar <- vars[2]
  yvar <- vars[1]
  x <- dat[,xvar]
  y <- dat[,yvar]
```

```
  p <- qplot(x=x, y=y, xlab=xvar, ylab=yvar, size = I(3), alpha = I(0.5), colour=factor(x)) +
    geom_smooth(method='lm',      se=FALSE,      size=1.5,      col="#F8766D")      +
scale_x_continuous(breaks=range(x))   +   scale_colour_manual(values=cbPalette4)   +
theme(legend.position="none")


  p
})


multiplot(plotlist = ps_ME1, cols = 3)


# Second set of responses
responses_p <- responses[5:8]


combns <- as.matrix(expand.grid(responses_p, factors, stringsAsFactors = FALSE))
colnames(combns) <- c("Response", "Factor")


ps_ME2 <- apply(combns, 1, FUN=function(vars) {
  xvar <- vars[2]
  yvar <- vars[1]
  x <- dat[,xvar]
  y <- dat[,yvar]


  p <- qplot(x=x, y=y, xlab=xvar, ylab=yvar, size = I(3), alpha = I(0.5), colour=factor(x)) +
    geom_smooth(method='lm',      se=FALSE,      size=1.5,      col="#F8766D")      +
scale_x_continuous(breaks=range(x))   +   scale_colour_manual(values=cbPalette4)   +
theme(legend.position="none")


  p
})


multiplot(plotlist = ps_ME2, cols = 3)


### Creating interaction plots for GRA responses


a <- c("Taste.masking.300s",  "Spraying.Rate" , "Spraying.Time")


b <- c("Dissolution",  "Spraying.Rate" , "Spraying.Time")


c <- c("Coating.Uniformity",  "Spraying.Rate" , "Spraying.Time")
```

```
d <- c("Height",  "Spraying.Time" , "Spraying.Rate")

resp_factor_int <- as.matrix(data.frame(rbind(a, b, c, d)))

ps_int <- apply(resp_factor_int, 1, FUN=function(vars) {
  yvar <- vars[1]
  x1var <- vars[2]
  x2var <- vars[3]
  x1 <- dat[,x1var]
  x2 <- dat[,x2var]
  x2_f <- as.factor(dat[,x2var])
  y <- dat[,yvar]

  data.sel1 <- dat[dat[,x2var]==min(dat[,x2var]),]
  model_sel1 <- lm(formula(paste(yvar, '~', x1var)), data = data.sel1)

  data.sel2 <- dat[dat[,x2var]==max(dat[,x2var]),]
  model_sel2 <- lm(formula(paste(yvar, '~', x1var)), data = data.sel2)

  qplot(x1, y, col=x2_f) +
    geom_point(size=3, alpha=0.5) +
    scale_x_continuous(breaks=range(x1)) +
    geom_abline(intercept=coef(model_sel1)[1],
          slope=coef(model_sel1)[2],
          col="#0072B2", lwd=2)+
    geom_abline(intercept=coef(model_sel2)[1],
          slope=coef(model_sel2)[2],
          col="#D55E00", lwd=2)+
    guides(color = guide_legend(title=x2var, keywidth = 1, keyheight = 1))+
    xlab(x1var) +
    ylab(yvar) +
    scale_colour_manual(values=cbPalette3)
})

multiplot(plotlist = ps_int, cols = 2)
```

Dissolution vs. Taste.Masking.300 by Weight gain

```
p_diss_taste_weight    <-    ggplot(dat,    aes(x=Taste.masking.300s,    y=Dissolution,
color=Weight.Gain)) +

geom_point(size=3, alpha=0.7) +

ggtitle("Dissolution vs. Taste Masking at 300s") +

theme(plot.title = element_text(lineheight=1, face="bold", size = 11)) +

scale_colour_gradient2(high = "red", mid = "yellow" , low = muted("green", l=50), midpoint =
7.75) +

geom_hline(aes(yintercept=15*60), color="#56B4E9", lwd=1.5, linetype="dotted")


p_diss_taste_weight
```

Contour plots

```
grid    <-    list(x=seq(from=min(dat$Spraying.Rate)-0.3,    to=max(dat$Spraying.Rate)+0.3,
by=(max(dat$Spraying.Rate)-min(dat$Spraying.Rate)+0.6)/100),
y=seq(from=min(dat$Spraying.Time)-5,                              to=max(dat$Spraying.Time)+5,
by=(max(dat$Spraying.Time)-min(dat$Spraying.Time)+10)/100))


f_w <- function(x,y){
(x*y-10*(x-1))*0.15*(100/300)}


grid$z <- outer(grid$x,grid$y, f_w)


plot(grid$x, grid$y, xlab='Spraying Rate', ylab='Spraying Time', type='n')
title("Weight Gain (%)", cex.main=1.2, line=0.5)
pal <- brewer_pal(type="seq", palette="RdYlGn")
image(grid, col=rev(colorRampPalette(pal(8))(200)), add=TRUE)
contour(grid, add=TRUE)


points(1, 45, pch=19, col=1, cex=1)
text(1, 45+3 , f_w(1,45), cex=0.8)


points(1, 95, pch=19, col=1, cex=1)
text(1, 95+3 , f_w(1,95), cex=0.8)


points(3, 45, pch=19, col=1, cex=1)
text(3, 45+3 , f_w(3,45), cex=0.8)


points(3, 95, pch=19, col=1, cex=1)
```

```
text(3, 95+3 , f_w(3,95), cex=0.8)


points(2, 70, pch=19, col=1, cex=1)
text(2, 70+3 , f_w(2,70), cex=0.8)


## Printing table all data
tab_data <- data.frame(cbind(Run=dat$Run,
dat[, factors],
dat[, responses]))


tab_data
```

XIII. Evaluation Sheet Human Taste Panel

Human Taste Panel – Master Thesis - Stefanie Keser 〈Roche〉

Number: _____

Age: _____

Gender: ○ male   ○ female

Smoker: ○ yes   ○ no

Please don't drink, eat or smoke 30 min before the taste evaluation.

1.   Detection of the bitterness Threshold

Procedure:

- Take 5 ml of the solutions in the mouth for 10s
- Spit the solutions out and rinse the mouth at least 3 times
- Score the taste according the following evaluation table
- Feel free to drink water before the next taste assessment

	1	2	3	4	5
	No taste	Perception	Slightly bitter	Moderate bitter	Strongly bitter
	„ I can not detect a difference to water"	"I detect some difference but was not able to be specific about taste"	"I detect a bitter taste, but I is fairly okay"	"I detect a bitter taste and it is unpleasant"	"It is awful"
Solution A	○	○	○	○	○
Solution B	○	○	○	○	○
Solution C	○	○	○	○	○
Solution D	○	○	○	○	○
Solution E	○	○	○	○	○
Solution F	○	○	○	○	○

Human Taste Panel – Master Thesis - Stefanie Keser 〈Roche〉

2.   Evaluation of the taste masking efficiency

Procedure:

- Place the prepared minitablets (n=3) on the tongue
- Measure the time until you detect a bitter taste and spit it out (max. 5 min)
- Rinse the mouth at least 3 times
- Write down the time
- Feel free to drink water before the next taste assessment

	Time [min:ss]
Sample A	
Sample B	

Thank you very much !!! ☺

XIV.   Raw data human taste panel

Panelist No.	1	2	3	4	5	6	7	8	9	10	11	12
Concentration [µg/ml]						Bitterness scores						
0.24975	1	2	1	2	1	3	3	1	1	1	1	2
0.98	1	1	1	2	2	2	1	1	2	1	1	1
9.94	1	1	2	1	2	3	3	2	1	2	2	2
50	1	2	1	1	2	2	2	1	2	2	1	2
99.9	3	1	3	3	1	4	4	3	3	2	2	1
199.92	4	4	4	4	3	5	5	3	4	3	4	3
Age	26	24	26	25	25	36	32	23	32	30	37	31
Sex [f/m]	f	m	f	f	m	f	f	m	f	m	m	m
Smoker [y/n]	y	n	n	n	n	n	n	n	n	n	n	n

XV.   SEM Coating Thicknesses

Coating (cross section measurements)			Pellet 1		Pellet 2	
			1	2	1	2
Eudragit EPO Coating level 6.31 mg/cm²	Para2.2.III	PTL16/1579	72.00	79.00	84.00	82.00
Kollicoat Smartseal Coating level 6.92 mg/cm²	Para2.2.V	PTL16/1580	91.00	85.00	89.00	78.00
Kollicoat Smartseal Coating level 1 mg/cm²	Para2.3.IV-1	PTL16/1581	11.00	10.00	10.00	9.00
Kollicoat Smartseal Coating level mg/cm²	Para2.3.IV-2	PTL16/1582	20.00	25.00	18.00	18.00
Kollicoat Smartseal Coating level 2 mg/cm²	Para2.3.V-1	PTL16/1583	23.00	21.00	24.00	24.00
Kollicoat Smartseal Coating level 4 mg/cm²	Para2.3.V-2	PTL16/1584	34.00	37.00	43.00	42.00

XVI.   X-ray µCT Coating Thicknesses

Coating (cross section measurements)			Pellet 1 Average	Pellet 2 Average
Eudragit EPO/Coating level 7.29 mg/cm2	Para2.2.III	PTL16/1579	84 µm	77 µm
Eudragit EPO, Drum Coating 8mg/cm²	Para2.3.VI-4	PTL16/1979	101 µm	100 µm
Kollicoat Smartseal/Coating level 6.92 mg/cm2	Para2.2.V	PTL16/1580	81 µm	75 µm
Kollicoat Smartseal/Coating level 1 mg/cm2	Para2.3.IV-1	PTL16/1581	12 µm	14 µm
Kollicoat Smartseal/Coating level 1.5 mg/cm2	Para2.3.IV-2	PTL16/1582	19 µm	19 µm
Kollicoat Smartseal/Coating level 2 mg/cm2	Para2.3.V-1	PTL16/1583	24 µm	21 µm
Kollicoat Smartseal/Coating level 4 mg/cm2	Para2.3.V-2	PTL16/1584	37 µm	38 µm
Run5: Sur75:Opa25, 1g/min, 45min	CET1.2.IX,	PTL16/1977	22 µm	19 µm
Run9: Sur85:Opa15, 3g/min, 90min	CET1.2.VI,	PTL16/1978	54 µm	57 µm
Run1 (CP): Sur80:Opa20, 2g/min, 70min	CET1.2.III:	PTL16/1980	19 µm	22 µm